INFORMATION TO USERS

This manuscript has been reproduced from the microfilm master. UMI films the text directly from the original or copy submitted. Thus, some thesis and dissertation copies are in typewriter face, while others may be from any type of computer printer.

The quality of this reproduction is dependent upon the quality of the copy submitted. Broken or indistinct print, colored or poor quality illustrations and photographs, print bleedthrough, substandard margins, and improper alignment can adversely affect reproduction.

In the unlikely event that the author did not send UMI a complete manuscript and there are missing pages, these will be noted. Also, if unauthorized copyright material had to be removed, a note will indicate the deletion.

Oversize materials (e.g., maps, drawings, charts) are reproduced by sectioning the original, beginning at the upper left-hand corner and continuing from left to right in equal sections with small overlaps.

ProQuest Information and Learning
300 North Zeeb Road, Ann Arbor, MI 48106-1346 USA
800-521-0600

University of Alberta

CHARACTERIZATION OF ALIEN NEAR-END CROSSTALK IN HIGH-SPEED COMMUNICATION SYSTEMS

by

Pranavi Anand 

A thesis submitted to the Faculty of Graduate Studies and Research in partial fulfillment of the requirements for the degree of **Master of Science.**

Department of Electrical and Computer Engineering

Edmonton, Alberta
Fall 2005

Dedicated to my parents

Abstract

Ethernet is the most widely used local area network protocol in the world today. 10GBASE-T is a proposed Ethernet standard, which aims to achieve a data rate of 10 Gbps. The high frequencies involved in its operation give rise to a new type of crosstalk in data cables, termed Alien Near-End Crosstalk (ANEXT). ANEXT is predicted to be one of the major impairments for 10GBASE-T systems and it is necessary to measure and analyze ANEXT.

An innovative technique to measure ANEXT in 10GBASE-T systems and a model for ANEXT are proposed in this thesis. The model is developed on the basis of measurement data obtained from experiments performed in a laboratory environment. The experiments were conducted using a wireline testbed consisting of CAT5E and CAT6 UTP cables.

Digital Signal Processing techniques are used to design the ANEXT model. Investigations have also been made in the thesis to find a technique to mitigate the impact of ANEXT in 10GBASE-T systems.

Acknowledgements

First of all, I would like to thank my supervisor, Dr. Stephen Bates for his valuable guidance, patience and continuous support during research and writing of this thesis. My thanks go also to Gary Block for his help in the development of the Software Interface. I would also like to thank Lee Cameron for his suggestions in setting up the laboratory environment.

My sincere thanks to Dr. Dmitry Trukhachev, Marco Castellon, Łukasz Krzymień, Christian Giasson, Ram Swamy and Nikolaj Larionov for their suggestions and feedback in the writing of the thesis. I would also like to thank Sheryl Howard, Robert Hang and Paul Goud for discussions on different aspects of communication systems.

In the end, I would like to express my gratitude to my parents for their love and encouragement.

Table of Contents

1 Introduction **1**
- 1.1 Origin of Ethernet . . . 1
  - 1.1.1 Timeline of Ethernet . . . 2
- 1.2 10GBASE-T . . . 2
  - 1.2.1 Criteria for the feasibility of 10GBASE-T . . . 3
  - 1.2.2 Objectives of 10GBASE-T . . . 4
  - 1.2.3 Channel Impairments . . . 4
- 1.3 ANEXT- Alien Near-End Crosstalk . . . 8
- 1.4 Contributions of 10GBASE-T Taskforce . . . 12
- 1.5 Thesis Organization . . . 14

2 Experimental Configuration for ANEXT **15**
- 2.1 HCDC Wireline Testbed . . . 15
  - 2.1.1 Cabling Standards . . . 16
  - 2.1.2 Cable Categories and Connectors . . . 16
  - 2.1.3 Balun for Impedance Matching . . . 19
- 2.2 Experimental Setup Apparatus . . . 21
  - 2.2.1 UTP Cable Setup . . . 21
  - 2.2.2 Patch Panel Setup . . . 24
- 2.3 Experimental Procedure . . . 25
- 2.4 Conclusion . . . 28

3 Calibration Measurements **29**
- 3.1 Interference from PCBs . . . 29
- 3.2 Methodology for Calibration Measurement . . . 30
- 3.3 Calibration Measurements using UTP cable . . . 30
  - 3.3.1 Results of Calibration Measurements with UTP cables . . . 31
- 3.4 Calibration Measurements with Patch Panels . . . 32
  - 3.4.1 Results of Calibration Measurements with Patch panels . . . 33
- 3.5 RF Shielding and Faraday Cage . . . 33
  - 3.5.1 Copper and Lead Faraday Cages . . . 38
  - 3.5.2 Grounding . . . 40
- 3.6 Conclusion . . . 42

4 ANEXT Measurements **43**
4.1 ANEXT Measurement Data From the UTP Cable Setup 43
4.2 ANEXT Measurement Data using Patch Panel Setup 45
4.3 Further Results 46
4.3.1 ANEXT as a function of Cable length 46
4.3.2 ANEXT as a function of cable separation 47
4.3.3 ANEXT as a function of Patch Panel Port Separation 50
4.3.4 Effect of bundling on ANEXT 51
4.4 Comparison between 10GBASE-T Task Force measurements and thesis research results 51
4.4.1 Comparison for CAT5E UTP 52
4.4.2 CAT 6 UTP Measurements 54
4.5 Conclusion 55

5 ANEXT Modeling **57**
5.1 ANEXT Modeling 57
5.1.1 Filter Design Techniques 57
5.2 Generation of an ANEXT Modeling Filter 59
5.2.1 Filter design using a bank of Notch Filters 60
5.3 Conclusion 65

6 Issues Relevant to ANEXT Mitigation **66**
6.1 Cyclostationary nature of ANEXT 66
6.2 Modeling the 10GBASE-T System 67
6.2.1 Tomlinson-Harashima Precoding 69
6.3 Proposed ANEXT Cancellation Circuit 71
6.3.1 Timing Recovery 72
6.3.2 ANEXT Symbol Detection 74
6.3.3 Impact of Clock Jitter on ANEXT Cancellation 75
6.4 Conclusion 76

7 Conclusions and Future Work **77**
7.1 Conclusions 77
7.2 Possible Future Work 79

Bibliography **81**

A Experimental Configuration **84**
A.1 Apparatus 84
A.2 RJ45 Pin configuration 85

B MATLAB Code **86**
B.1 Code for ANEXT Filter 86
B.2 Code for 10GBASE-T System Model 89

List of Tables

3.1 Calibration Measurement with UTP cables 31
3.2 Calibration Measurement with Patch Panels 35

A.1 RJ45 Pin Configuration 85

List of Figures

1.1 An early drawing of an Ethernet network [3]. 1
1.2 Timeline of XBASE-Y Ethernet 3
1.3 Attenuation, NEXT and ELFEXT for 100 m of Augmented Category 6 UTP cable 6
1.4 10GBASE-T Architecture and Channel Impairments 7
1.5 Power Spectral Density of PAM-12 8
1.6 Alien Near-End Crosstalk 9
1.7 Alien NEXT in 10GBASE-T Systems 11
1.8 Bundled and unbundled cables in typical installations [1]. 12

2.1 Horizontal and Work Area Cabling [4] 17
2.2 RJ45 Connector 18
2.3 RJ45 Jack 19
2.4 Inline Coupler 20
2.5 Balun 20
2.6 UTP Cable Setup 22
2.7 SMA Connector Board 23
2.8 100 Ω Termination Board 23
2.9 Rack housing the patch panels 25
2.10 Setup for Patch Panel 26
2.11 Splash Screen of the Software Interface 27
2.12 Software Interface showing the Measurements 27

3.1 Calibration Measurement setup for UTP cables with whole Cable assembly 32
3.2 Calibration Measurement Setup for UTP cables with SMA Connector Board removed 33
3.3 Calibration Result for UTP cable setup with whole Cable assembly . 34
3.4 Calibration Result for UTP cable setup with SMA connector PCB removed 34
3.5 Calibration Result for UTP cable setup with whole Cable assembly removed 35
3.6 Calibration Measurement for Patch Panel Setup with entire cable assembly 36

3.7 Calibration Measurement Results for Patch Panel Setup with entire cable assembly 37
3.8 Calibration Measurement Results for Patch Panel Setup without SMA connector PCB 37
3.9 Aperture Attenuation vs. Frequency 38
3.10 Copper Faraday Cage 39
3.11 Lead Faraday Cage 40
3.12 SMA connector PCB in copper cage 41
3.13 SMA connector PCB in lead cage 41

4.1 ANEXT Data (in log scale) obtained using UTP Cable Setup 44
4.2 ANEXT Data (in linear scale) obtained using UTP Cable Setup . . . 44
4.3 ANEXT Data (in log scale) obtained using Patch Panel Setup 45
4.4 ANEXT Data (in linear scale) obtained using Patch Panel Setup . . 46
4.5 ANEXT as a function of cable length 47
4.6 ANEXT as a function of cable separation using Patch Panel Setup . 48
4.7 ANEXT Power as a function of cable separation using Patch Panel Setup 49
4.8 ANEXT as a function of cable separation using UTP Cable Setup . 50
4.9 ANEXT Power as a function of cable separation using UTP Cable Setup 51
4.10 Power vs Patch Panel Port Separation 52
4.11 Effect of bundling and unbundling 53
4.12 Model Comparison for 40 m CAT5E UTP 54
4.13 Model Comparison for CAT5E 55
4.14 Model Comparison for CAT6 56

5.1 Design of Notch Filter 61
5.2 ANEXT Filter 62
5.3 Impulse Response of ANEXT Filter 62
5.4 ANEXT Signal obtained using model for Data Set I 63
5.5 ANEXT Data Set I obtained from measurements 64
5.6 ANEXT Signal obtained using model for Data Set II 64
5.7 ANEXT Data Set II obtained from measurements 65

6.1 Tomlinson-Harashima Precoding [13] 70
6.2 A simple model of 10GBASE-T system 71
6.3 Proposed ANEXT Cancellation Circuit 72
6.4 Timing Error Detector Characteristics for Received PAM Signal with ANEXT 74
6.5 Error due to Clock jitter 76

Acronyms

IEEE Institute for Electrical and Electronics Engineers

10GBASE-T Ten Gigabit Ethernet

802.3an Proposed IEEE standard for 10 Gigabit Ethernet

ISO International Organization for Standardization

IEC International Engineering Consortium

UTP Unshielded Twisted Pair

Gbps Gigabits per second or billions bits per second

Mbps Megabits per second or million bits per second

LAN Local Area Network

PC Personal Computer

PHY Physical layer device

ANEXT Alien Near-End Crosstalk

NEXT Near-End Crosstalk

FEXT Far-End Crosstalk

BASE-T Baseband T refers to copper

PAM Pulse Amplitude Modulation

CS Cyclostationary

TED Timing Error Detector

THP Tomlinson-Harashima Precoder

QoS Quality of Service

CoS Class of Service

Chapter 1

Introduction

1.1 Origin of Ethernet

In 1973, researchers at Xerox's Palo Alto Research Center (PARC) pioneered a technology for interconnecting personal computers and started work on developing the local area network (LAN) topology [3]. Bob Metcalfe, an employee at PARC termed the technology "Ethernet". He chose the word "Ether" to describe the physical medium - a cable - that carries bits to all nodes in the network. Figure 1.1 shows an early sketch of an Ethernet network by Metcalfe [3].

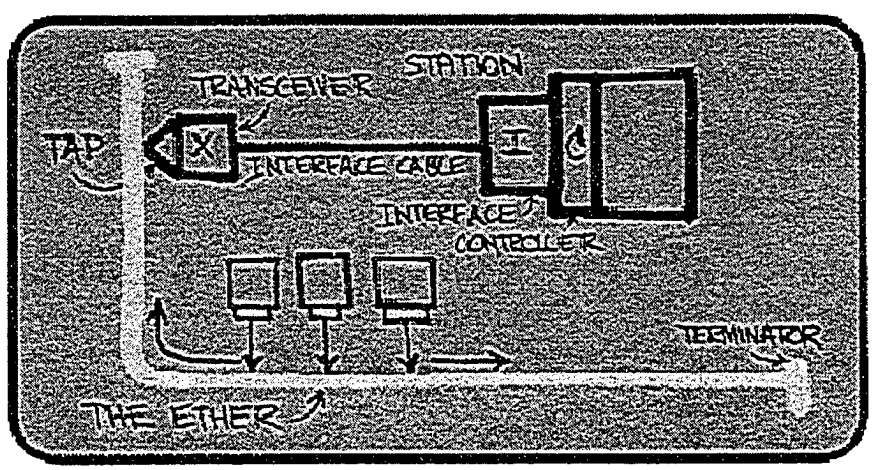

Figure 1.1: An early drawing of an Ethernet network [3].

The requirements for higher data rates and bandwidth have resulted in the evo-

lution of a family of Ethernet standards [17, 26]. This has been facilitated by the advancement of semiconductor technology giving way to higher processing speeds and larger storage capacities.

1.1.1 Timeline of Ethernet

The first Ethernet-based LAN network was developed in 1976, by Xerox to connect more than 100 personal computers (PCs) together. Four years later Digital Equipment, Intel and Xerox released the first Ethernet standard for 10 Mbps data transmission. The first internationally recognized standard for Ethernet, 802.3 was approved by the Institute of Electrical and Electronics Engineers (IEEE) in 1983.

The IEEE naming conventions for Ethernet standards can be categorized as "XBASEY". The first number X stands for the data rate in Mbps. The second term indicates the transmission type i.e. "BASE" stands for "baseband". Finally, Y indicates the segment length (e.g. 500 m for 10BASE-5). In newer standards, the numbers in Y have been replaced by letters indicating the type of medium, for instance T for unshielded twisted pair (UTP) copper cable (e.g. 10BASE-T) and T4 for four such pairs.

The evolution of the Ethernet has seen an increase in the data transmission rates and an improvement in the quality of the medium. Figure 1.2 shows the timeline of Ethernet standards. The very first Ethernet standard, approved by IEEE in 1983, was 10BASE-5 or "thick" Ethernet for coaxial cable. In 1986, 10BASE-2 or "thin" Ethernet for a thinner and more flexible coaxial cable was approved. 10BASE-T Ethernet, using ordinary telephone twisted-pair wire, was ratified in 1991 while 100BASE-T or "Fast Ethernet" came into existence in 1995. In 1998, IEEE802.3 standard for Gigabit Ethernet over fiber was approved while its counterpart, 1000BASE-T or Gigabit Ethernet over copper was approved in 1999 [8].

1.2 10GBASE-T

10GBASE-T is a proposed Ethernet standard with an objective to provide a data rate of 10 Gigabits per second (Gbps) over a copper cable. It is an upgrade for

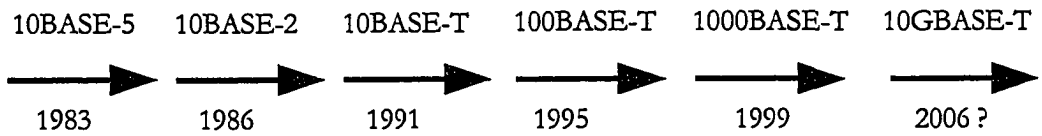

Figure 1.2: Timeline of XBASE-Y Ethernet

the existing 1000BASE-T and a competitor to 10 Gigabit Ethernet over fiber [15]. Being a full-duplex only technology, it does not need the Carrier Sense Multiple Access Collision Detect (CSMA-CD) protocol that is a part of the slower, half-duplex Ethernet technologies.

The physical medium for data transmission in 10 Gigabit Ethernet systems can be copper cable or optical fiber. 10GBASE-T over copper is considered to be more practical primarily because of its cost effectiveness. Another major factor favoring its adoption is that it will run over copper cable. This would lead to cost efficiencies as compared to the optical version of 10 Gigabit Ethernet standard.

A Task Force of the IEEE is presently working on the details and specifications for the standardization of the proposed 10GBASE-T over copper. The latest proposed standard is a 10GBASE-T PHY upgrade for 802.3 using its cabling definitions in present or future editions of international cabling standard ISO/IEC 11801 [1].

1.2.1 Criteria for the feasibility of 10GBASE-T

The broad market potential for 10GBASE-T technology justifies the introduction of this new Ethernet standard. There is a broad set of applications, which would use 10GBASE-T such as horizontal cabling in buildings, data centers and backplanes [1]. The presence of multiple vendors and multiple users on the IEEE Task Force also indicates that this technology will be widely adopted. The price of computers is coming down with the advancement in silicon technologies. The cost of networking different workstations is better balanced if copper is used as the medium.

Presentations by several cable manufacturers have demonstrated the technical

feasibility of 10GBASE-T standard over copper cable. The design of the transceivers for 10GBASE-T would depend on the specifications in the standard when it is ratified and thus, they are not available yet. But other connecting hardware such as connectors and couplers is already available in the market. The 10GBASE-T PHY device is projected to meet the 3 times higher cost versus 10 times better performance guidelines applied to previous advanced Ethernet standards [1].

1.2.2 Objectives of 10GBASE-T

Information in Ethernet systems is transmitted in frames. One of the main objectives of 10GBASE-T is to preserve the 802.3 Ethernet frame format. It will additionally preserve the minimum and maximum frame size of current 802.3 standards. It will support star-wired local-area networks using point-to-point links and structured cabling topologies. It will also support full-duplex operation with speed of 10 Gbps.

1.2.3 Channel Impairments

UTP copper cable is the medium for 10GBASE-T data transmission. Despite the numerous advantages of this standard, there are several impairments that adversely affect performance. The data signal traveling through the channel is degraded due to various channel impairments such as insertion loss, Near-End cross Talk (NEXT), Far-End cross Talk (FEXT) and echo. Figure 1.4 illustrates the architecture of 10GBASE-T and the channel impairments associated with it. Each of the pairs of the UTP cable acts as transmitter and receiver which are connected to the hybrid. Below is a detailed description of the impairments.

- *Insertion Loss or Attenuation*: This is the loss of signal power between two points of a cable. It is expressed as the reciprocal of the ratio of the signal power delivered to one point to the signal power delivered to the other point. The expression for insertion loss for Augmented Category 6

UTP cables in dB is given as below [1]:

$$IL_{channel} \leq 1.05 * (1.8 * \sqrt{f} + 0.0227f + \frac{0.2}{\sqrt{(f)}}. + 4 * 0.02 * \sqrt{f}) \quad (1.1)$$

The worst case attenuation for 100 m of Augmented Category 6 UTP cable is plotted against frequency in Figure 1.3.

- *Interference*: This is any form of energy that interferes with the received signal.
  - *Echo (Near + Far)*: Echo is caused by an impedance mismatch and is dominated in 10GBASE-T systems by the mismatch introduced by the hybrid. Hybrid combines send-path and receive-path signals from the PHY for full duplex data transmission.
  - *Crosstalk* : This is the signal coupling from one pair of UTP cable to another pair and this effect occurs on all four pairs. Crosstalk can occur at the near end of the transmitter (NEXT), the farther end of the transmitter (FEXT), or from a remote transmitter (ANEXT). The expressions for NEXT for a frequency range of 1 MHz to 330 MHz and from 330 MHz to 500 MHz and FEXT for the frequency range of 1 MHz to 500 MHz for Augmented Category 6 UTP cable in dB are as given below [1]:

$$NEXT_{channel}(f) \geq -20\log(10^{-\frac{44.3-15\log\frac{f}{100}}{20}} + 2.10^{\frac{-54-20\log\frac{f}{100}}{20}}) \quad (1.2)$$

$$NEXT_{channel}(f) \geq 31.0 - 27.15 * \log\frac{f}{330} \quad (1.3)$$

$$ELFEXT_{channel}(f) \geq -20\log(10^{\frac{-ELFEXT_{cable}}{20}} + 4 * 10\frac{-FEXT_{conn}}{20}) \quad (1.4)$$

where

$$ELFEXT_{cable} \geq 27.8 - 20\log\frac{f}{100} \quad (1.5)$$

and

$$FEXT_{conn} \geq 43.1 - 20\log\frac{f}{100} \qquad (1.6)$$

Figure 1.3 shows the NEXT and ELFEXT loss limit curves for 100 m of Augmented Category 6 UTP cable channel.

- *Noise*: This includes thermal noise, impulse noise and quantization noise.

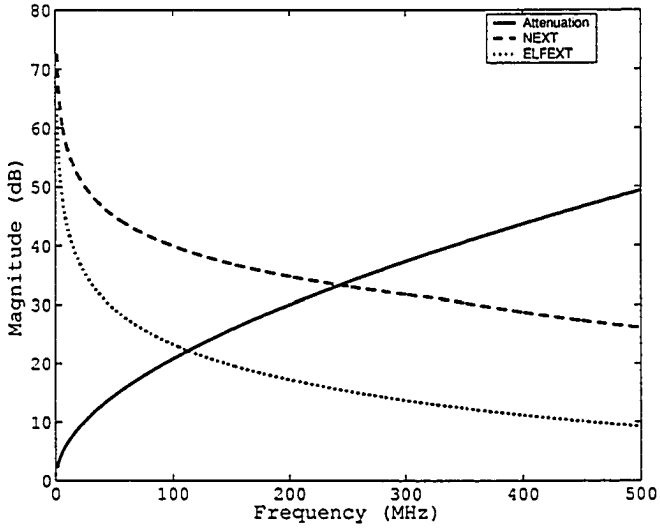

Figure 1.3: Attenuation, NEXT and ELFEXT for 100 m of Augmented Category 6 UTP cable

The channel impairments described above are not common to all XBASE-T Ethernet standards. For example, 10BASE-T and 100BASE-T have no echo impairment. The effect of all of them is more significant in 10GBASE-T systems than in previous XBASE-T Ethernet standards and one is unique to 10GBASE-T and is discussed further in Section 1.3.

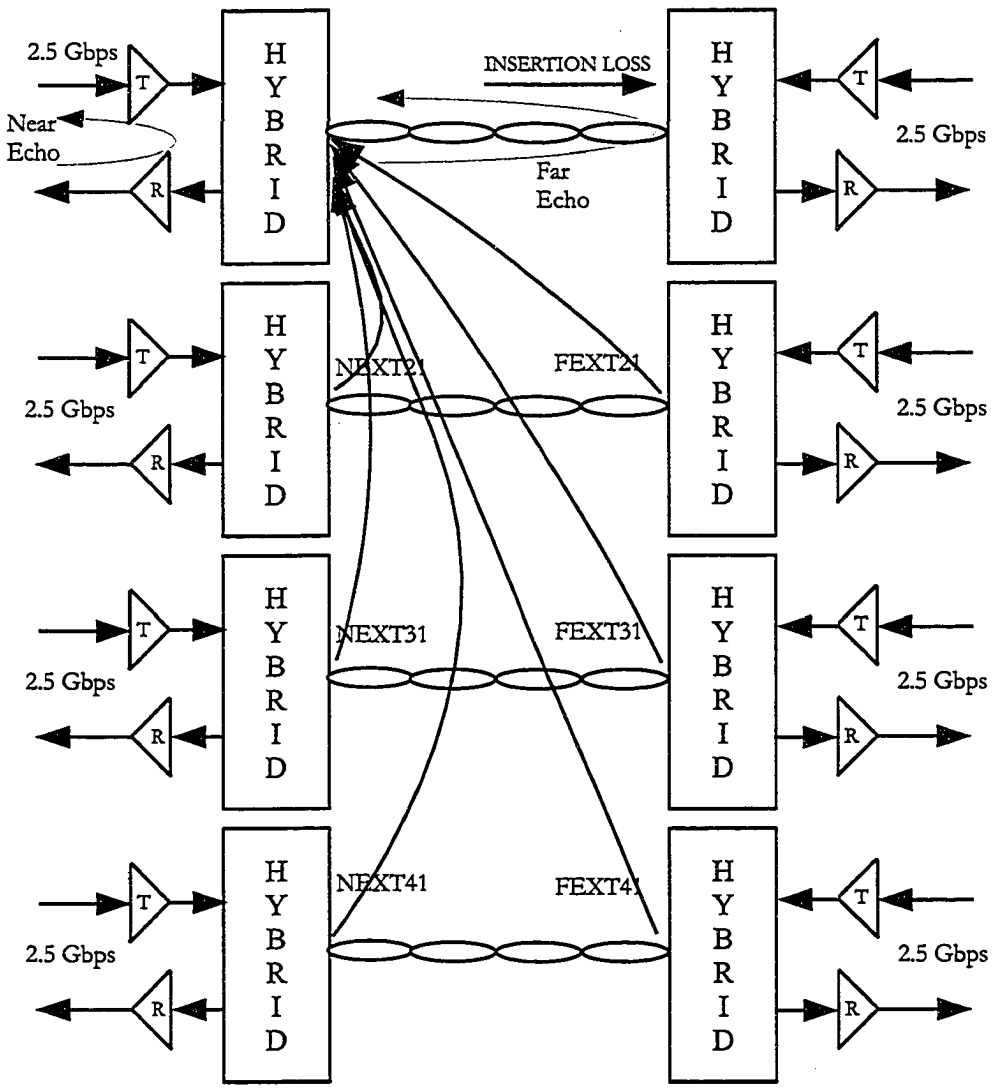

Figure 1.4: 10GBASE-T Architecture and Channel Impairments

1.3 ANEXT- Alien Near-End Crosstalk

In 10GBASE-T, the data rate of the signal traveling on one of the four pairs of UTP cable is 2.5 Gbps. The modulation scheme proposed is 12-level Pulse Amplitude Modulation (PAM) with the baud rate of approximately 800 MBauds per second having 3 information bits per symbol [1]. The total number of levels required are $2^3 = 8$ [14]. The extra 4 levels in PAM-12 scheme are used for coding and control purposes. Thus, a data rate of 2.5 Gbps is achieved and this gives an overall rate of 2.5 x 4 = 10 Gbps for the four pairs. However, when generating PAM-12 symbols at a rate of 800 MBauds per second, a considerable amount of high frequency energy is produced. The power spectral density (PSD) of PAM-12 pulses at 825 MHz is plotted in Figure 1.5. Note that significant energies are present up to around 550 MHz. This was not a problem in the earlier lower data rate version of Ethernet, 1000BASE-T where the modulation scheme used is PAM-5 with a signalling rate of 125 MBauds. The PSD of PAM-5 at 125 MHz is also shown in Figure 1.5 to illustrate this difference.

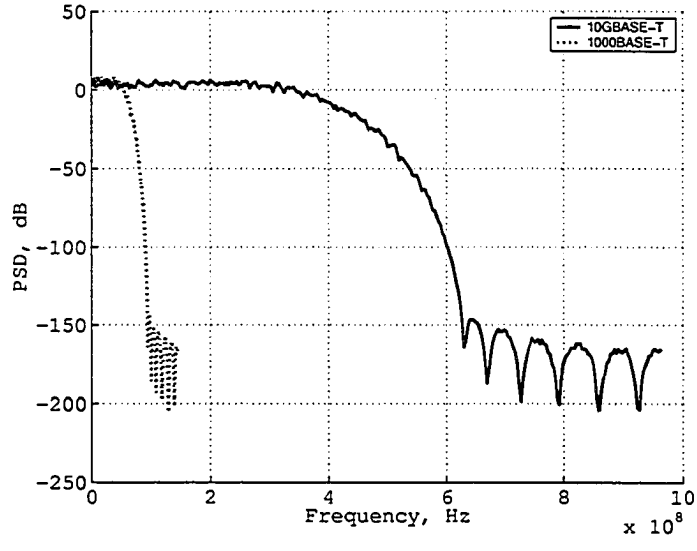

Figure 1.5: Power Spectral Density of PAM-12

At such high frequencies of operation, a UTP cable starts to behave like an antenna, radiating and picking up energy from the surroundings [9]. Crosstalk orig-

inates due to inductive effects when current flows on two adjacent metallic conductors represented by two neighboring cables. As a result of current flowing in the two conductors, electromagnetic fields are formed that produce signal distortions in the adjoining cable. Crosstalk is thus, the crossing over of a signal from one cable to the other.

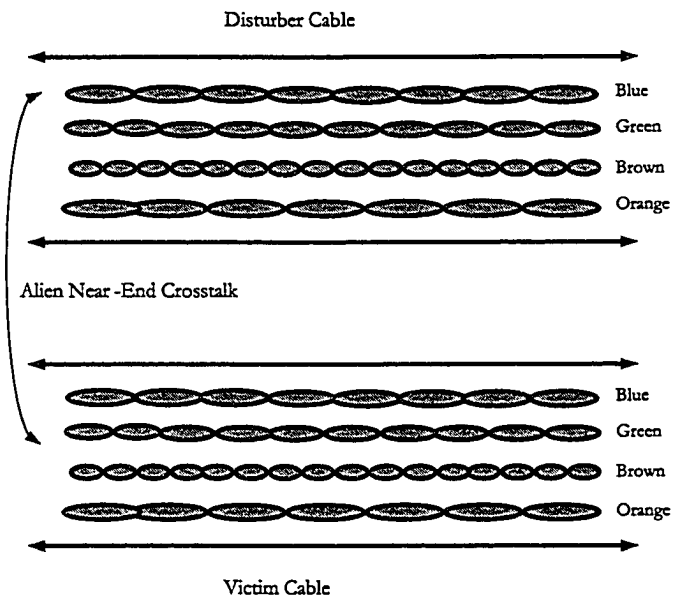

Figure 1.6: Alien Near-End Crosstalk

Signal energy coupling from one 4-pair UTP cable to another 4-pair UTP cable is termed Alien Near-End Crosstalk (ANEXT). ANEXT between two neighboring UTP cables is illustrated in Figure 1.6. Each pair of the UTP is color coded for identification, which is shown by labels beside the pairs in the figure. The twisting for each pair is different to reduce crosstalk levels by canceling the out of phase signals.

The cable over which the information or desired data signal travels is termed as the "victim" cable. All the neighboring cables contributing to the ANEXT are termed the "disturber" cables. Thus, ANEXT for a given "victim" can be defined as the signals coupled from all neighboring "disturber" cables. The phenomena of ANEXT in 10GBASE-T systems is illustrated in Figure 1.7. The "disturbers" are

adjacent data cables carrying 10GBASE-T signals.

ANEXT is also predicted to be installation-dependent. UTP cables can be installed as unbundled or bundled as shown in Figure 1.8. Bundled cable is an assembly of two or more cables continuously bound together to form a single unit. It is the usual way to lay cables in installations especially in data centers and conduits. A conduit is a hollow pipe-like structure used to lay down bundled cables. Besides cable bundling, ANEXT is also affected by cable type (category of UTP cable), patch panel coupling and cable separation. Higher categories of cable give better performance than the lower ones in terms of ANEXT levels.

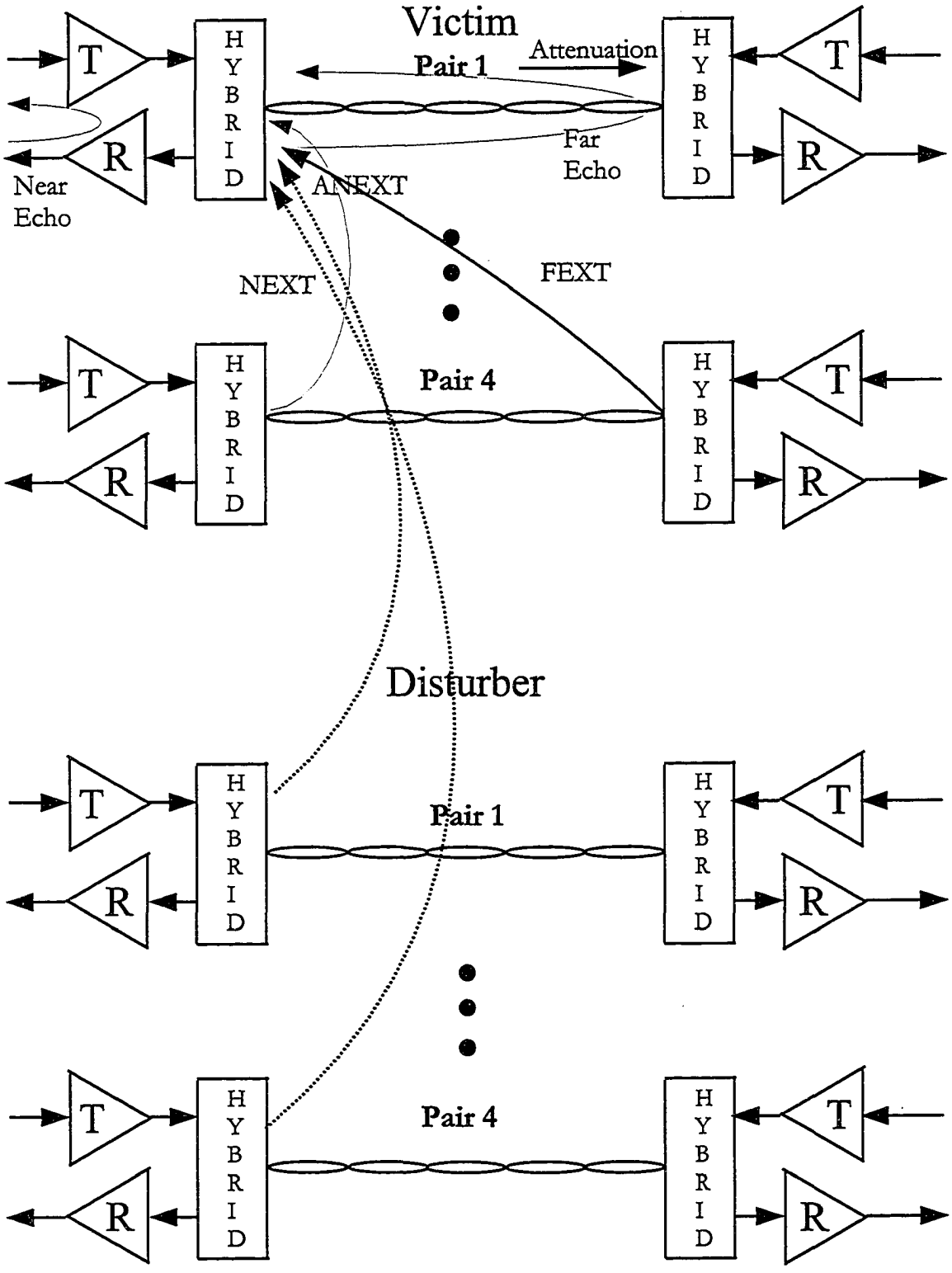

Figure 1.7: Alien NEXT in 10GBASE-T Systems

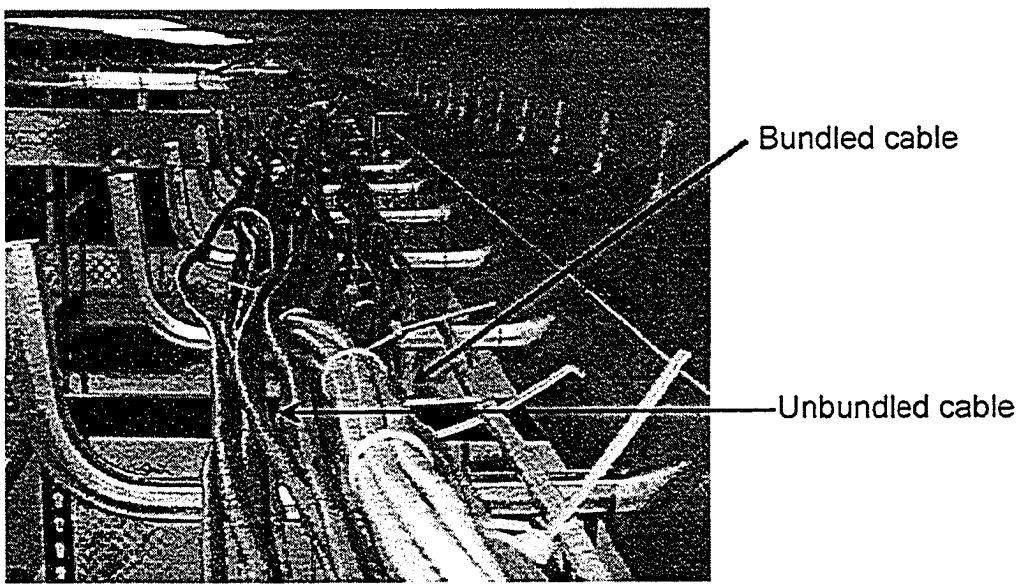

Figure 1.8: Bundled and unbundled cables in typical installations [1].

One of the main difficulties in the characterization of ANEXT is the absence of suitable field measurement instruments. Therefore, measurement of ANEXT is a challenge. The absence of any research at an academic level on characterization and mitigation of ANEXT has motivated this thesis research. An innovative technique to measure ANEXT in laboratory environment is proposed in this thesis. It is important to accurately measure ANEXT and develop a model in order to find suitable techniques to accommodate ANEXT and achieve reliable data transmission. This would prove useful in the design of transceivers for 10GBASE-T systems. We use our measurement data to construct a model of ANEXT and investigate the impact of this model on simulation of 10GABSE-T performance.

1.4 Contributions of 10GBASE-T Taskforce

In order to standardize 10GBASE-T, an IEEE Study Group was formed in November 2002. In January 2003, the Study Group became the 10GBASE-T Task Force. The Task Force has identified ANEXT to be one of the fundamental limits to the operation of 10GBASE-T [1]. This section discusses the contributions to the char-

acterization of ANEXT made by the 10GBASE-T Task Force.

ANEXT is measured at the near-end of the transmitter and thus, is called "Alien Near-end Crosstalk". ANEXT loss is defined by the Task Force as "the measure of the unwanted signal coupling between pairs in adjacent cabling from transmitters at the near-end into a pair measured at the near-end" [1]. Since each single wire pair can be disturbed by more than one "disturber" wire pair, another term, Power Sum Alien Near-end Crosstalk (PS ANEXT) loss, is coined by the IEEE Task Force. "PS ANEXT is the cumulative sum of ANEXT from one or more adjacent cables coupling into the "victim"" [1].

As mentioned in Section 1.3, ANEXT was not a problem in the lower data rate versions of XBASE-T Ethernet. Therefore, until now there has been no need to characterize ANEXT. The IEEE Task Force is currently working on measurement methodology, modeling and suitable mitigation techniques for ANEXT. It has been suggested that the maximum operating channel length will be less than 100 m for the targeted cable category if proper compensation for ANEXT is not provided. Cable vendors are now working on better quality cabling with respect to ANEXT.

The complete characterization and mitigation of ANEXT continues to be a challenge for 10GBASE-T Task Force. It is known that ANEXT depends greatly on installation practices [1]. Measurements for ANEXT were done by IEEE Task Force under different installation configurations using different cables. These include horizontal cable bundles in data centers, cable connectors in patch panels and cables in conduits.

The 10GBASE-T Task Force in their meeting in January, 2005 presented ANEXT results regarding measurement, modeling and mitigation. The standard measurement procedure for ANEXT used by the Task Force employs seven UTP cables and the frequency range of 1 MHz to 500 MHz. The equipment for conducting the measurements includes Network Analyzer, baluns, 100 Ω pair terminations, tie wraps or other cable binding devices and seven 100 meter lengths of four pair UTP cables. A reference test procedure to measure ANEXT in conduits has also been presented. Besides those mentioned above, several other measurement configurations are also

under discussion. These include two cables in conduit, two cables bound together, six cables around one cable bound together, drum accumulator, two cables side by side with fixed spacing, connecting hardware ANEXT measurement procedures and channel ANEXT measurement procedures.

It has been proposed that ANEXT could either be compensated through shielding or by digital signal processing techniques. With regard to cabling, suitable installation practices such as unbundling cable could reduce ANEXT. Foiled twisted pair (FTP) or shielded twisted pair (STP) could be used as a method to reduce ANEXT. In FTP, the individual twisted pairs are shielded with foil that reduce ANEXT due to Faraday shielding effect [25]. Enhanced quality patch cords could also help in reducing ANEXT. The absence of any research at an academic level on characterization and mitigation of ANEXT has motivated the research presented in this thesis.

1.5 Thesis Organization

Following this introduction chapter, the rest of the thesis is organized as follows. Chapter 2 describes the laboratory setup for the measurement of ANEXT. Calibration measurements are discussed in Chapter 3. Chapter 4 presents the results of experiments and comparison with measurements made by the IEEE Task Force. The modeling of ANEXT on the basis of the measurement data is explained in Chapter 5. In Chapter 6, possible mitigation techniques for ANEXT are discussed. Finally, the conclusions are given in Chapter 7.

Chapter 2

Experimental Configuration for ANEXT

Ten Gigabit Ethernet (10GBASE-T), as introduced in the previous chapter, is proposed to run over unshielded twisted pair (UTP) copper cable [1]. ANEXT is predicted to be one of the major challenges for the practical implementation of this standard. The main objective of the research presented in this thesis is to characterize ANEXT in high-speed communication systems such as 10GBASE-T. Several experiments using different categories and lengths of UTP cables were performed in order to model the behavior of ANEXT. This chapter presents a detailed description of the experimental setup used throughout this thesis.

2.1 HCDC Wireline Testbed

A model of ANEXT is obtained in this thesis using the measurement data collected from experiments conducted in a laboratory environment. In order to perform the experiments to measure ANEXT, a wireline testbed was setup in the High Capacity Digital Communications (HCDC) laboratory at the University of Alberta. The setup can be categorized into two sections : (i) the measurement instruments and (ii) the experimental cable assembly. The main objective was to make the laboratory measuring system as close to real-world Ethernet installations as possible.

2.1.1 Cabling Standards

The medium of transmission for Ethernet systems was originally coaxial cable. This has been gradually replaced by UTP copper cable to alleviate installation complexity and achieve higher throughput. The installation of cables for Ethernet systems is done on the basis of the recommendations of the EIA/TIA 568-B standards [7]. The EIA/TIA 568-B standard was developed by the Electronic Industries Association in 1991 for telecommunications building cabling systems. The experimental setup arranged for this thesis research was done following the EIA/TIA 568-B standard.

According to EIA/TIA 568-B, a structured cabling system comprises of six subsystems. These are termed Building Entrance, Equipment Room, Backbone Cabling, Telecommunication Closet, Horizontal Cabling and Work Area [7]. The channel considered in this thesis comprises the Horizontal Cabling and the Work Area. Horizontal Cabling system extends from the work area telecommunications (information) outlet to the telecommunications closet and consists of horizontal cabling, telecommunications outlet, cable terminations and cross-connections. A typical Horizontal and Work Area cabling is illustrated in Figure 2.1. In the new Ethernet standards using UTP cable, the specified topology for Horizontal Cabling is a star where all the workstations are connected to a central node represented by a switch.

According to the EIA/TIA 568-B standard, a maximum of 90 m of UTP cable can be used for Horizontal Cabling. In addition, two patch cords of a total length of 10 m can be used for Work Area and Telecommunications Closet patch and jumper cables [8]. The patch cords are connected to the cable using inline couplers. These are important parameters, which had to be considered while setting up the testbed and during the experiments.

2.1.2 Cable Categories and Connectors

UTP cables have four twisted pairs of high performance cable. The twisting of the four pairs provides a degree of noise immunity [27]. By twisting two wires over small distances, the electromagnetic energy coupling over a small segment of

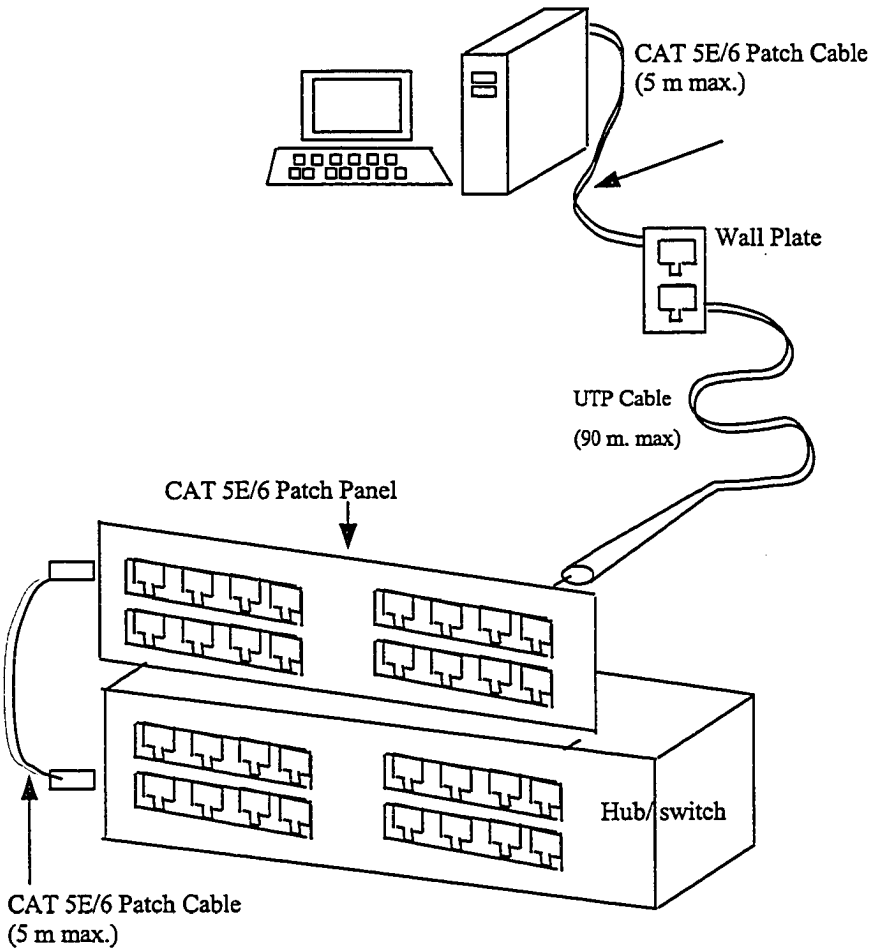

Figure 2.1: Horizontal and Work Area Cabling [4]

wire is canceled by the out of phase energy coupled on the next segment of wire. The UTP cables used for the measurements of ANEXT are classified into different categories that are discussed in this section.

According to the 10GBASE-T Task Force [1], UTP cable of Category 5E (CAT5E), Category 6 (CAT6), Category 6A (CAT6A) and possibly Category 7 (CAT7) are proposed to be used as 10GBASE-T medium. The most common cable categories in use today are CAT5E and CAT6. CAT6A and CAT7 cables are still under development. Therefore, the research experiments were conducted using CAT5E and CAT6 UTP cable and patch cords. The following is a description of the different categories of UTP cable and the basis on which this classification is made.

Category 5E, also called Enhanced Category 5, is characterized up to 100 MHz and is suitable for data applications up to 1000 Mbps. *Category 6* cable is characterized up to 250 MHz and can be used for 10,000 Mbps or 10 Gbps data rates [1]. Augmented *Category 6* or CAT6A is a new type of cable that will be characterized up to 500 MHz. The term characterization refers to the transmission parameters or the channel impairments described in Chapter 1 that are defined up to these frequencies. The upper frequency range of 10GBASE-T is 500 MHz, which is higher than for its earlier counterpart, 1000BASE-T. Since the power of ANEXT increases with frequency, ANEXT will become a fundamental limit to the operation of 10GBASE-T [1]. There is no characterization for ANEXT in this range of frequencies.

The UTP cables are terminated at either end with RJ45 connectors. RJ45 is a modular 8-pin connector similar to a telephone connector in appearance. It is an 8 conductor female jack that is used to terminate the CAT5E/CAT6 cable at the user location. The term RJ stands for *Registered Jack* and 45 designation specifies the pin numbering system. The RJ45 pin configuration is presented in Table A.1 of Appendix A. The connector is attached to the cable and the jack is the device that can be plugged into either the wall outlet, the network interface card in the computer or the patch panel. The RJ45 plug is inserted into the cable using the EIA/TIA 568-B scheme taking care of the color sequence.

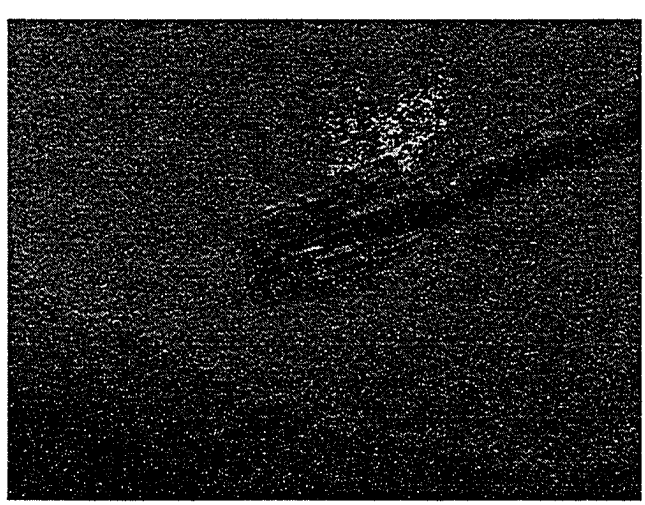

Figure 2.2: RJ45 Connector

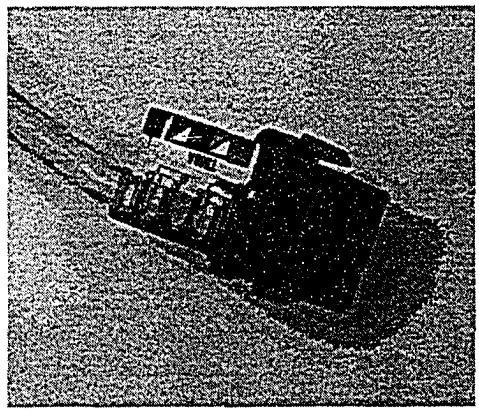

Figure 2.3: RJ45 Jack

Patch cords are also an important component of the cable assembly for which ANEXT has been measured. These are stranded cables of varying lengths with CAT5E/CAT6 jacks crimped at either ends. These provide connectivity between any two female outlets (jacks). The two most common places where they are used are from hub to the patch panel and work area outlet (jack) to the computer. The maximum length of patch cords to be used for horizontal cabling is 5 m at each end making a total of 10 m. An inline coupler is used to connect two patch cords or patch cord with UTP cable or two UTP cables together. A RJ45 connector, a RJ45 jack and an inline coupler are shown in Figure 2.2, Figure 2.3 and Figure 2.4 respectively.

The RG58U coaxial cable forms the output point of the measurement instruments. It is terminated in a SubMiniature version A (SMA) connector that is threaded and has an impedance of 50 Ω.

2.1.3 Balun for Impedance Matching

A balun is an impedance matching transformer that converts unbalanced coaxial signals to balanced signals in the UTP cable. The word balun is made from two words *bal*anced and *un*balanced. The impedance of the coaxial cable connected to the measurement instruments (eg. spectrum analyzer and signal generator) is 50 Ω. The intrinsic impedance of the UTP cable is 100 Ω. Due to this impedance

Figure 2.4: Inline Coupler

mismatch, the voltages at the termination points are not balanced. As a consequence of this impedance mismatch, reflections of the signal will occur. Therefore, the measurements for ANEXT would not be accurate.

A balun, which is illustrated in Figure 2.5 was used to resolve this problem. The specifications of the balun can be downloaded from the website of BH Electronics [6]. The balun has two SMA connector ports C1 and C2, one at the top and other in the side. There are four termination ports on the side opposite to the C1 port, A, B, C and D. A and B are used to connect a pair of UTP cable while C and D are for grounding purposes. During the measurements, coaxial cable from spectrum analyzer was connected to port C1 while port C2 was terminated in a 50 Ω load. Ports C and D were not connected.

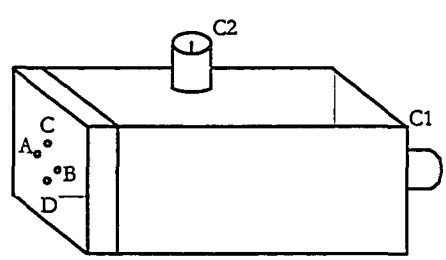

Figure 2.5: Balun

2.2 Experimental Setup Apparatus

The measurements for ANEXT were performed using two different configurations. One of the setups was used to measure ANEXT in adjacent cable sections while the other was used to measure ANEXT at the connectors. In the second experiment, patch panels were used. Thus, two different setups were designed and implemented.

The measurement instruments used were an Agilent E4438C ESG Vector Signal Generator and an Agilent E4402B ESA-E Series Spectrum Analyzer [2]. The cable setup for the measurements included patch cords and UTP copper cables of CAT5E and CAT6 categories. SMA connectors and RG58U coaxial cable were used to connect the measurement instruments with the experimental cable assembly. Apart from these, PCBs such as SMA connector board and 100 Ω termination board were designed and used as interfaces. A crimping tool, punch-down tool and continuity tester were used to connect the RJ45 jacks at either ends of the UTP cable and check the proper sequence of the wires. PCBs tend to radiate electromagnetic energy that interferes with the ANEXT signal. In order to eliminate this interference, shielding in the form of Faraday Cages made up of copper and lead were used. The detailed list of the measurement equipment and tools used for the experiments is included in Appendix A.

2.2.1 UTP Cable Setup

As has been previously mentioned, ANEXT is the signal coupling from the "disturber" cable to the "victim" cable. In the setup for UTP cable, ANEXT between two adjacent cables was measured. The measurements involved taking two sections of UTP cables of arbitrary lengths and connecting them to the measurement instruments.

The "disturber" cable is connected to the vector signal generator that produces sinusoidal signals of frequency range 1 MHz to 1 GHz. The signal coupling from this cable to the adjacent "victim" cable was measured with the help of the spectrum analyzer. Different typical lengths of UTP cables such as 5 m, 10 m and 20 m and

40 m were used for these measurements.

The setup is illustrated in Figure 2.6.

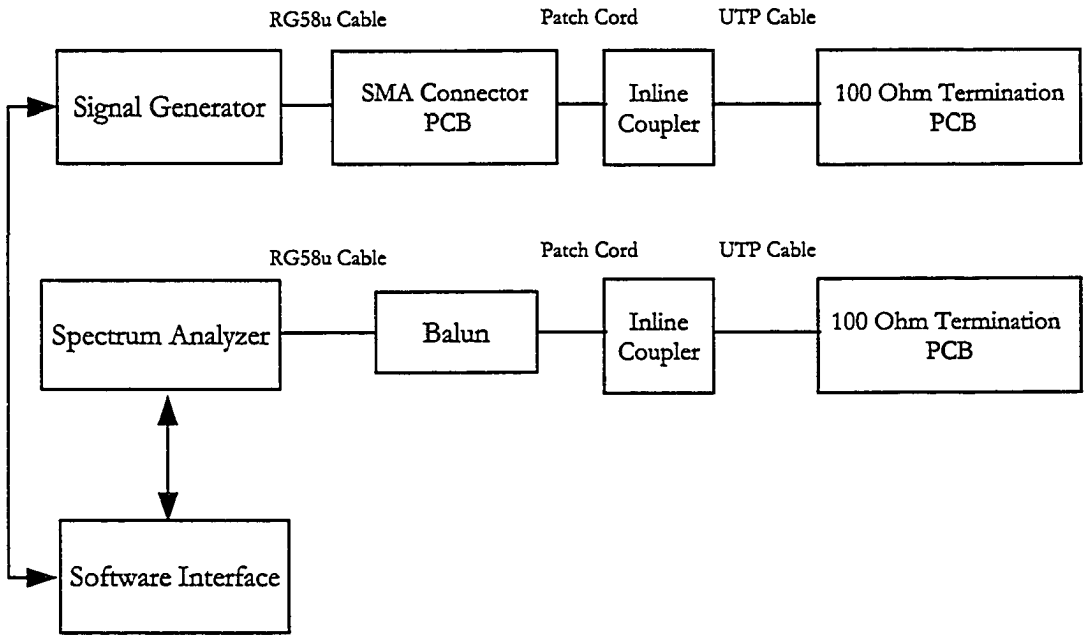

Figure 2.6: UTP Cable Setup

The top part of Figure 2.6 shows the assembly for the "disturber" cable. The vector signal generator has at its output a coaxial cable RG58U terminated in SMA connector while the UTP cable is terminated in a RJ45 jack. Therefore, in order to send the generated signal from the signal generator to the UTP cable, a PCB, called an "SMA Connector Board", was designed to connect them. It contains a SMA connector mounted on one side of the PCB and a RJ45 jack mounted on the other side. The SMA Connector PCB is illustrated in Figure 2.7.

The RJ45 jack mounted on the PCB is connected to the patch cord following the EIA/TIA 568-B cabling standard. The patch cord is connected to the "disturber" UTP cable with an inline coupler, which is popularly called a female-to-female RJ45 connector. The impedance of the UTP cable is 100 Ω , therefore, to avoid any undesirable reflections of the transmitted signal, the UTP cable was terminated with 100 Ω resistors using a terminator circuit. As there are four twisted pairs, four 100 Ω resistors were used. They were mounted on a termination PCB designed for

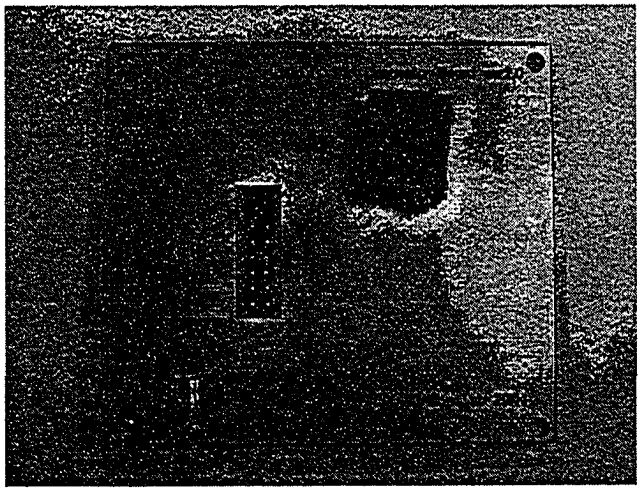

Figure 2.7: SMA Connector Board

this purpose. The 100 Ω Termination PCB is shown in Figure 2.8.

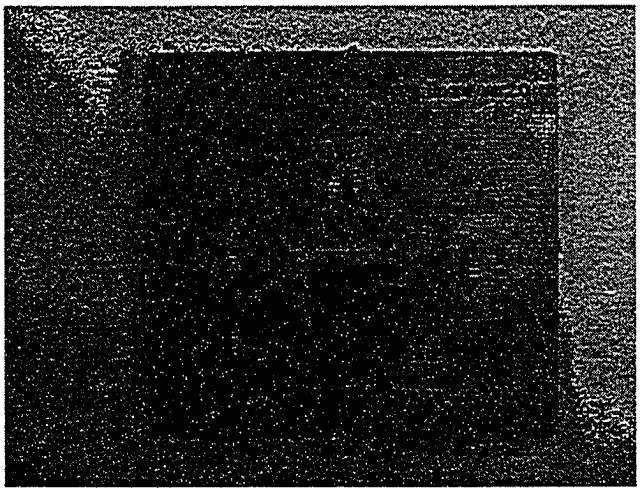

Figure 2.8: 100 Ω Termination Board

Similar connections were made for the "victim" cable assembly except that the signal generator was replaced with the spectrum analyzer that analyzes the magnitude of the coupled signal in the desired frequency range. The SMA connector PCB was replaced by a balun for impedance matching as was mentioned earlier. As shown in Figure 2.6, the signals are generated from the signal generator into the "disturber". Due to the phenomenon of ANEXT, the noise signal couples from the

"disturber" into the "victim" cable. The Software Interface analyzes the generated and coupled signals and stores the magnitude of the coupled ANEXT signal for further modeling and mitigation purposes. The detailed procedure of the experiments is explained in Section 2.3.

2.2.2 Patch Panel Setup

ANEXT is predicted to occur not only in the UTP cables but also at the cable connectors [1]. Therefore, motivation for this setup was to measure ANEXT at the connectors. The connectors are RJ45 jacks, which are terminated using patch panels. The later are used at the places where all the horizontal cable sections meet, and connect the segments to the network hub. A common number of connectors on a patch panel is 24, 36 or 48.

In this setup, 24-port patch panels housed in a 7 ft rack were used. The rack loaded with jacks on the patch panel ports is illustrated in Figure 2.9. One of the panels was loaded with Category 6 jacks and the other with Category 5E jacks in order to perform experiments for different cable categories. CAT5E/CAT6 cables were terminated with CAT5E/CAT6 jacks respectively with the help of a punch-down tool. The other end of the cables was connected to RJ45 connectors with the crimping tool. The connections were done using the EIA/TIA 568-B configuration type and tested using the continuity tester.

The Patch Panel Setup is illustrated in Figure 2.10. The signal generator was connected to the SMA connector PCB with RG58U coaxial cable similar to the setup in Figure 2.6. The RJ45 jack mount on the SMA connector board was connected to the patch cord. Unlike the UTP cable setup, the patch cord is not connected to the inline coupler but instead connected directly to the patch panel port. The patch cord is terminated in the RJ45 jack on port 1 of the patch panel. The UTP cable to be measured was connected to the other side of the patch panel port and terminated into a 100 Ω termination PCB at the other end. Similar connections were done for the "victim" cable assembly. The signal generator was replaced with spectrum analyzer and "victim" cable was inserted in port 2 of the patch panel. A

Figure 2.9: Rack housing the patch panels

balun was used instead of the SMA connector PCB. The detailed procedure of the experiments is given in Section 2.3.

2.3 Experimental Procedure

In the experiments, we wish to measure the signal coupling from the "disturber" UTP cable to the adjacent "victim" UTP cable.

The methodology for these experiments was to inject sinusoids of different frequencies in the range 1 MHz to 1 GHz and with a power of 0 dBm, into the "disturber" cable. The signals were generated by the signal generator and transmitted into one of the pairs of a four-pair UTP "disturber" cable. The magnitude of the sinusoids received at the near end of the transmitter, which is actually the signal coupling to the "victim", was measured using the spectrum analyzer. The desired frequency range was input through the graphical user interface (GUI) designed for the experiment. The resulting measurement data was stored on a PC connected to the spectrum analyzer.

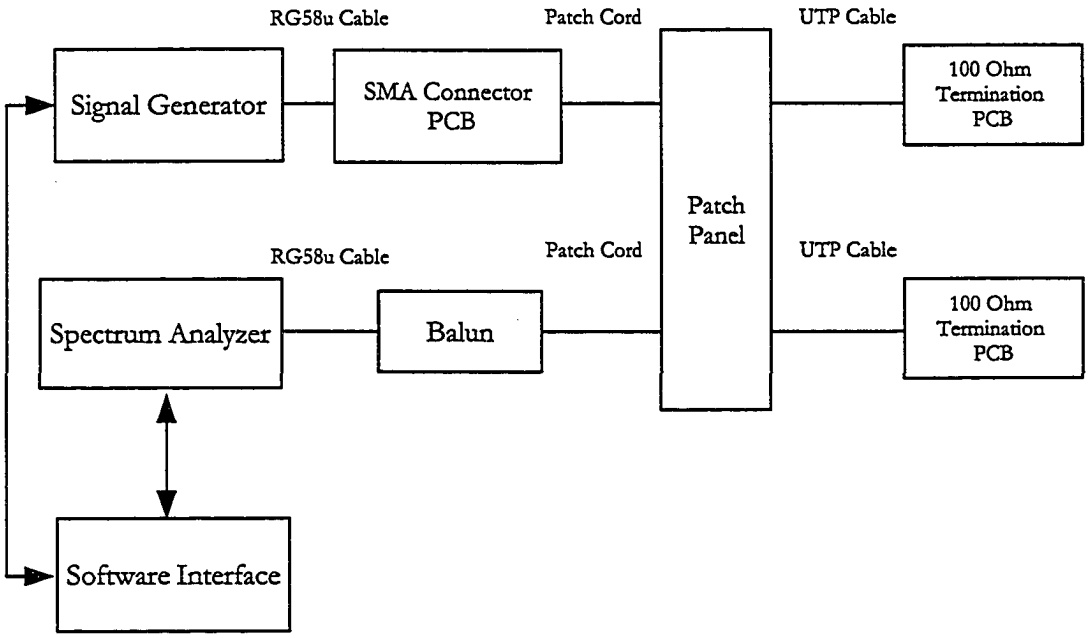

Figure 2.10: Setup for Patch Panel

In order to facilitate the measurement procedure, a software package was developed. It serves as a software interface between the signal generator and spectrum analyzer. The software interface automates the measurement process and greatly reduces the measurement time. A screen image of the software interface is shown in Figure 2.11 and Figure 2.12. It also imparts attributes like repeatability and reliability to the measurement process.

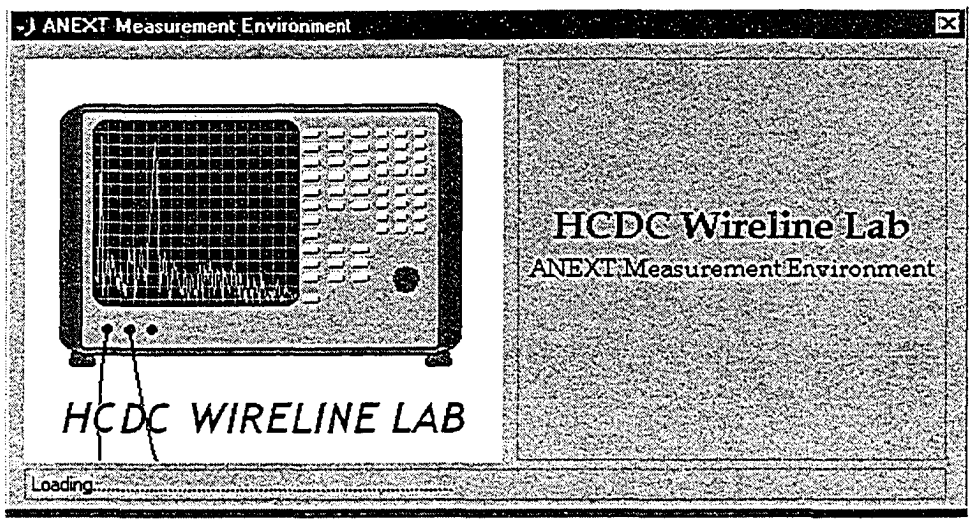

Figure 2.11: Splash Screen of the Software Interface

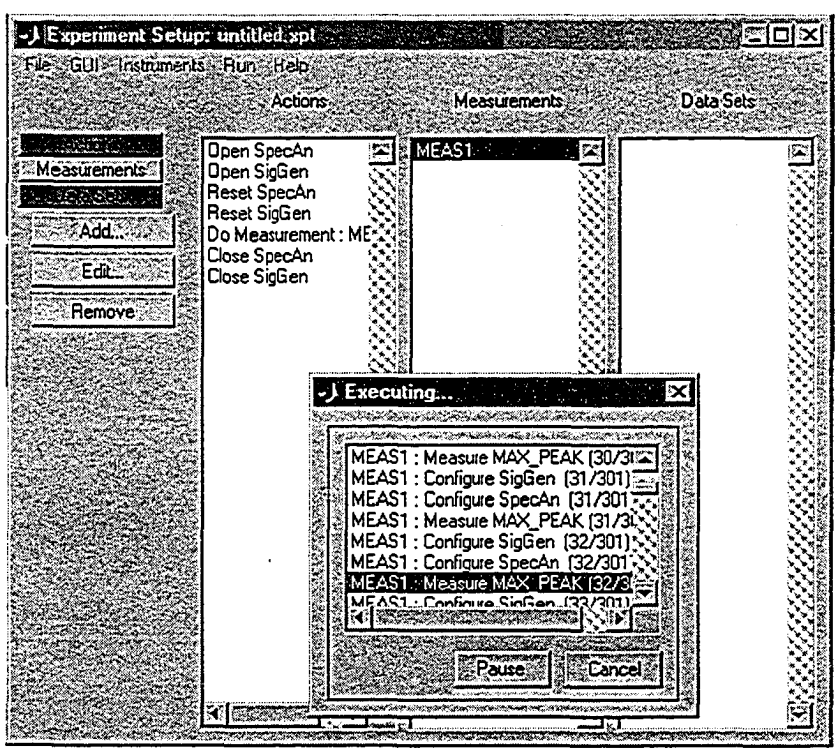

Figure 2.12: Software Interface showing the Measurements

2.4 Conclusion

This chapter gives a detailed description of the laboratory setup. This consisted of two setups designed to measure ANEXT in two possible real-world scenarios. Several PCBs were created for interfacing the different parts of the measurement system. Baluns were used to ensure impedance matching between the SMA connector and UTP cable.

Chapter 3

Calibration Measurements

The preceding chapter presented a description of the experimental setup and the steps involved in the measurement of ANEXT. Interfaces in the form of PCBs were built and used to connect the signal generator and spectrum analyzer with the UTP cable. However, during the experiments, these PCBs tend to contribute to the ANEXT data and thus, the measured data did not portray the true behavior of ANEXT in 10GBASE-T systems. Calibration measurements were performed to eliminate these unwanted contributions and obtain reliable ANEXT data. This chapter describes the procedure and result of these calibration measurements.

3.1 Interference from PCBs

As was mentioned in the previous chapter, PCBs were designed to interface the measurement instruments and the UTP cable. PCBs consist of a fiber glass base and multiple copper layers. The components namely the RJ45 jack mount, SMA connector, jumpers and resistors were mounted, soldered and interconnected by traces on the PCBs. The problem of electromagnetic interference and unwanted contribution to ANEXT from the components arises due to the high frequencies involved in the experiments. This interference can happen in the frequency range from a few MHz to several GHz depending on the design. PCBs affect the circuit operation by radiating electromagnetic waves in the following ways. The traces on the PCBs start to behave like transmission lines and produce radiation. There is also some

unpredictable effect from components. The interference produced from the PCBs additively interferes with the ANEXT signal. As a result, the measured value of ANEXT signal becomes more than the actual value. PCBs were designed and used for interfacing in the experiments and are not part of real-world Ethernet cabling setups. It is therefore important to determine the amount of electromagnetic interference from the PCBs and find a way to remove it for the accurate measurement of ANEXT.

3.2 Methodology for Calibration Measurement

The experimental setup was described in Chapter 2. The main objective of performing calibration measurements is to calibrate out the unwanted interference. In order to achieve this, several calibration experiments were performed. In each of these experiments, the contribution of the different parts of the cable assembly was determined. Different parts of the cable assembly described in Chapter 2 such as the SMA connector PCB and RG58U coaxial cable were removed one by one and experiments conducted to determine the exact contribution of each. A detailed description of the calibration experiments and results is presented in the following sections.

3.3 Calibration Measurements using UTP cable

In order to perform the experiments for calibration, the setup described in Chapter 2 was used. Each part of the cable assembly was removed one by one. In the first experiment, ANEXT data was obtained for the complete channel using the UTP cable. After this, the UTP cable along with the 100 Ω termination PCB was removed and measurements were conducted. In the next experiment, the inline coupler was removed and measurements performed. The patch cord was removed in the next experiment and measurements done. Then, the SMA connector PCB was removed and measurements were conducted. In the next experiment, the RG58U cable was removed and measurements were done. In the last experiment, the entire

cable assembly was removed and measurements done. The experimental setup is illustrated in Figure 3.1 and summarized in Table 3.3. The second column of the table shows the components used in the "disturber" and "victim" parts of the cable assembly.

From the results of the experiments, it was seen that the contribution of SMA connector PCB was the most significant to ANEXT measurement data.

Table 3.1: Calibration Measurement with UTP cables

Setup No.	Cable Assembly	Diagram of Setup	Results
1	• VSG • RG58U cable • SMA connector PCB • RJ45 jack • Patch cord • inline coupler • UTP cable • 100Ω termination PCB • SA • RG58U cable • SMA connector PCB • RJ45 jack • Patch cord • inline coupler • UTP cable • 100Ω termination PCB	Figure 3.1	Figure 3.3
2	• VSG • RG58U cable • SA • RG58U cable	Figure 3.2	Figure 3.4

3.3.1 Results of Calibration Measurements with UTP cables

The setups for the calibration measurements using UTP cables are illustrated in Figure 3.1 and Figure 3.2 and corresponding results are presented in Figure 3.3 and Figure 3.4. Figure 3.5 shows the result of the experiment for the case where no cable assembly was connected to the measurement instruments.

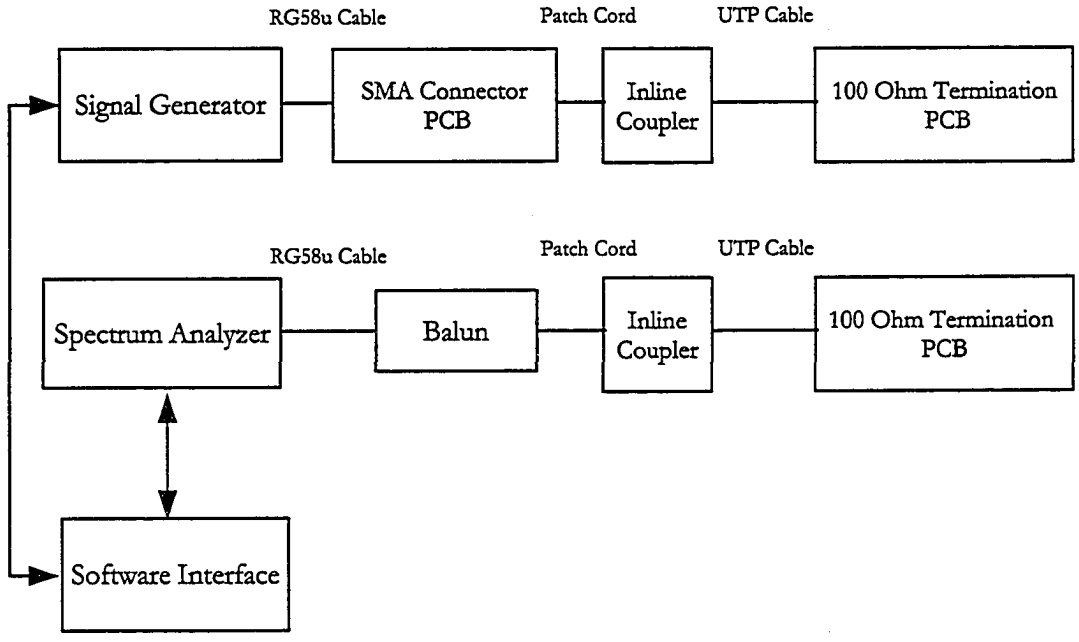

Figure 3.1: Calibration Measurement setup for UTP cables with whole Cable assembly

The measurement data for ANEXT contains the summation of ANEXT from UTP cable and electromagnetic coupling from the SMA connector PCB. From the plots in the Figure 3.3 and Figure 3.4, the contribution of the SMA connector PCB was found to be approximately 60 dBm. Figure 3.5 shows the background noise of -120 dBm that is present when the entire cable assembly was removed.

3.4 Calibration Measurements with Patch Panels

Using the same methodology as in the previous calibration measurements, a set of calibration measurements were also performed on the patch panel setup. During these experiments, the different parts of the setup were removed one after the other in a similar way as for the UTP cable setup. The results for each experiment was recorded using the software interface.

The experimental setup used for the calibration measurements with patch panels using the whole cables assembly is illustrated in Figure 3.6. The configuration where SMA Connector PCB is removed is same as Figure 3.2. Table 3.2 represents

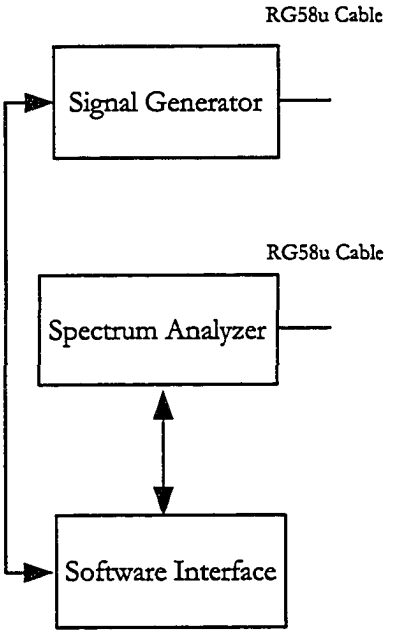

Figure 3.2: Calibration Measurement Setup for UTP cables with SMA Connector Board removed

the details of these calibration measurements.

3.4.1 Results of Calibration Measurements with Patch panels

Comparing the plots in the Figure 3.7 and Figure 3.8, it is evident that SMA Connector PCB interfered in the measured data to a great extent. The contribution of SMA Connector PCB is approximately 60 dBm.

3.5 RF Shielding and Faraday Cage

As was mentioned earlier, PCBs produce electromagnetic interference at the high frequencies used in ANEXT experiments. At high frequencies, the components of the PCBs start to affect the operation of the circuit by introducing electromagnetic interference. The results of the calibration measurements showed that the contribution from the SMA Connector PCB affected the ANEXT data greatly. A possible way to eliminate the interference was to employ some kind of shielding for this interface.

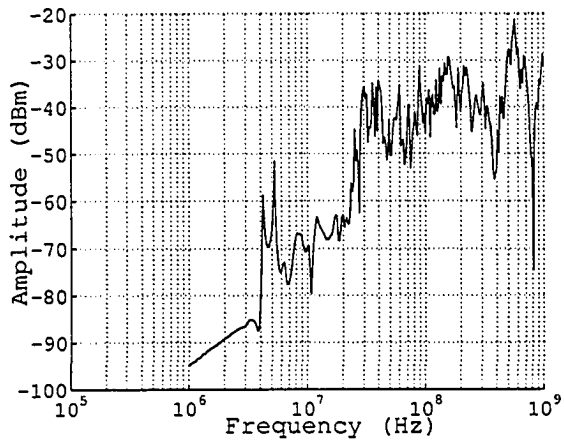

Figure 3.3: Calibration Result for UTP cable setup with whole Cable assembly

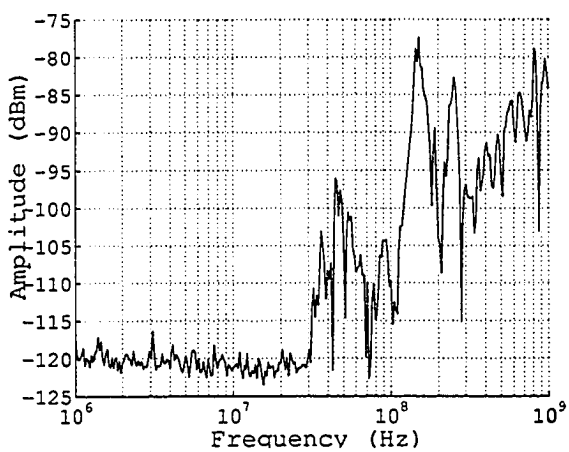

Figure 3.4: Calibration Result for UTP cable setup with SMA connector PCB removed

Radio Frequency (RF) shielding protects sensitive electrical equipment from external RF electromagnetic radiation by enclosing it in a conductive material and also prevents any charges from inside the enclosure to get out. It is based on the principle of the Faraday cage, which is an electrical apparatus discovered by the physicist Michael Faraday. According to Faraday, the charge on a hollow charged conductor remains only on the surface and not inside the conductor. Therefore, it has no influence on anything enclosed inside the hollow conductor. This shielding effect is employed to eliminate electrical fields within a volume.

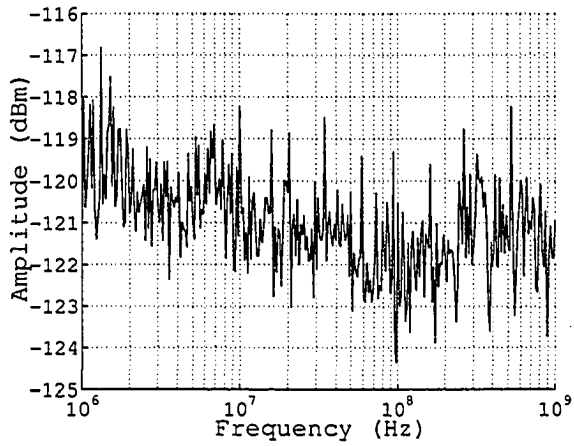

Figure 3.5: Calibration Result for UTP cable setup with whole Cable assembly removed

Table 3.2: Calibration Measurement with Patch Panels

Setup No.	Cable Assembly	Diagram of Setup	Results
1	• VSG • RG58U cable • SMA connector PCB • RJ45 jack • Patch cord • RJ45 jack in patch panel • UTP cable • 100Ω termination PCB • SA • RG58U cable • SMA connector PCB • RJ45 jack • Patch cord • RJ45 jack in patch panel • UTP cable • 100Ω termination PCB	Figure 3.6	Figure 3.7
2	• VSG • RG58U cable •SA • RG58U cable	Similar to Figure 3.2	Figure 3.8

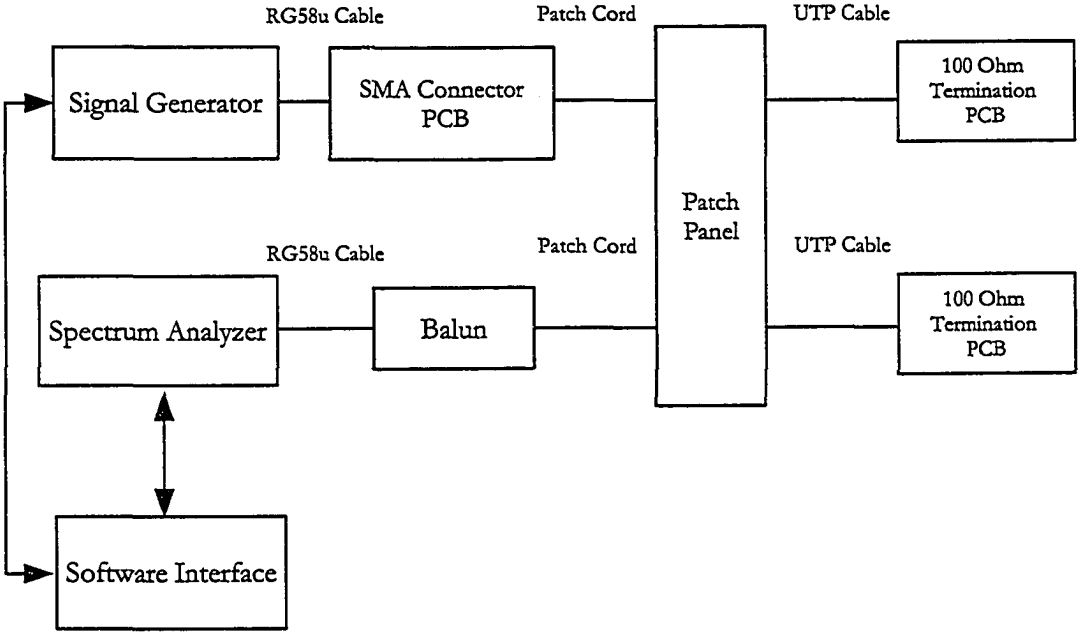

Figure 3.6: Calibration Measurement for Patch Panel Setup with entire cable assembly

Electromagnetic radiation consists of coupled electric and magnetic fields. The electric field produces forces on the charge carriers within the conductor. As soon as an electric field is applied to the surface of an ideal conductor, it generates an electric current that causes displacement of charge inside the conductor that cancels the applied electric field inside. The material used for the Faraday cage can be aluminium, copper or lead sheet or wire mesh.

In our experiments, the objective was to prevent the interference produced by the PCBs from affecting the coupled signals. Therefore, the PCBs were enclosed in Faraday cage boxes to prevent any electromagnetic signal from leaking out of the enclosure. Another way to use shielding could be to use some sort of shield for individual components on the PCB. There are however implementation difficulties due to the small size of the components. Therefore, in our case to get rid of the unwanted RF radiation from the SMA connector PCB, a Faraday cage of copper sheets was designed.

Although the Faraday cage should be of continuous material, it must have aper-

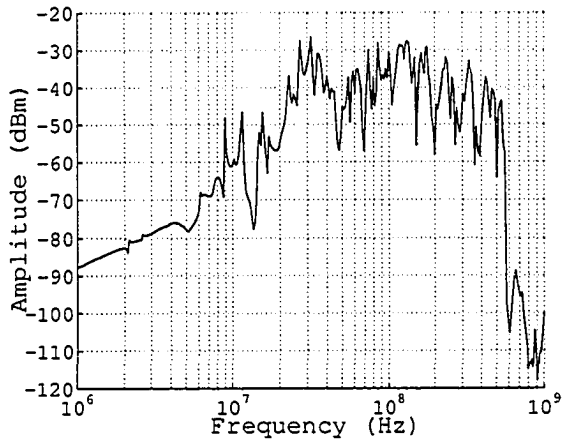

Figure 3.7: Calibration Measurement Results for Patch Panel Setup with entire cable assembly

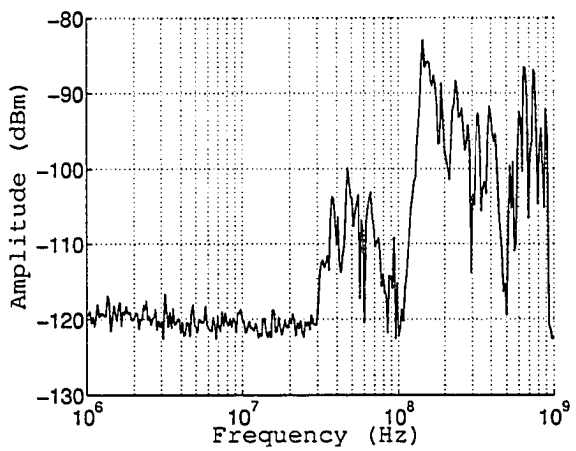

Figure 3.8: Calibration Measurement Results for Patch Panel Setup without SMA connector PCB

tures for interconnection. The size of the apertures is limited by the wavelength of the electromagnetic waves to be shielded. The attenuation for an aperture in dB is given by the following relationship:

$$A_{ap} = 20\log\frac{\lambda}{2L}, \tag{3.1}$$

where L is the longest aperture dimension and λ is the wavelength. The maximum frequency of measurements is 2.5 GHz and so the corresponding wavelength can

be calculated from the following expression

$$\lambda = \frac{c}{f}, \tag{3.2}$$

where c is the velocity of light and f is the frequency of electromagnetic wave. There are two apertures in the designed cages. An aperture for UTP cable is to insert RJ45 jack and has dimensions of 1.2 cm. x 1.0 cm. The other aperture is to connect the RG58U coaxial cable terminated in SMA connector with a diameter of 0.5 cm. The approximate attenuation for these apertures are plotted against frequency in Figure 3.9. It can be seen that the attenuation is around 20 dB and 28 dB for 1.2 cm and 0.5 cm aperture around 1 GHz.

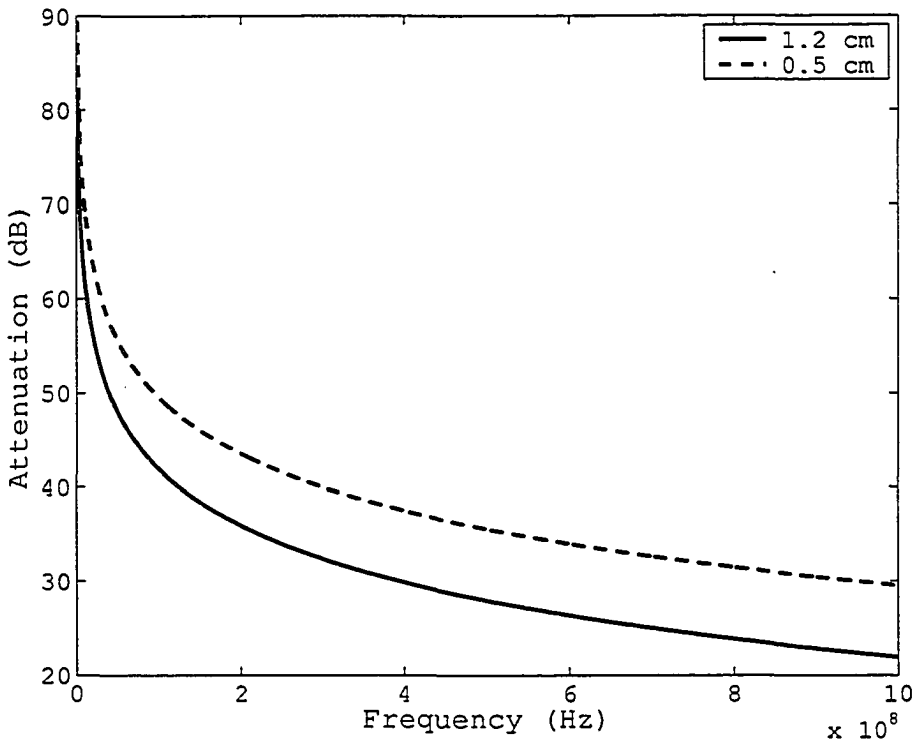

Figure 3.9: Aperture Attenuation vs. Frequency

3.5.1 Copper and Lead Faraday Cages

A Faraday cage was built from the copper sheets to eliminate the interference from the SMA connector PCB. Figure 3.10 shows a picture of the cage. Copper is gen-

erally used for such structures because it has high electrical resistance, provides shielding and is easier to work with.

The result of the measurements made with copper cages are presented in Figure 3.12. They show that the interference from the SMA PCBs was reduced but not completely eliminated. Similar structures were built using lead sheets, which are illustrated in Figure 3.11. The SMA connector PCBs were enclosed in them and properly grounded. The result of the experiment is shown in Figure 3.13. The results show that ANEXT magnitude reduces by approximately 30 dBm by using lead cages instead of copper ones. The interference from the SMA Connector PCB dropped by approximately -74 dBm around 10 MHz, around -60 dBm at MHz and approximately -75 dBm at 800 MHz. Although lead provides good shielding, it is not used commonly. Lead poisoning is one of the main problems. Another problem is that it is difficult to solder.

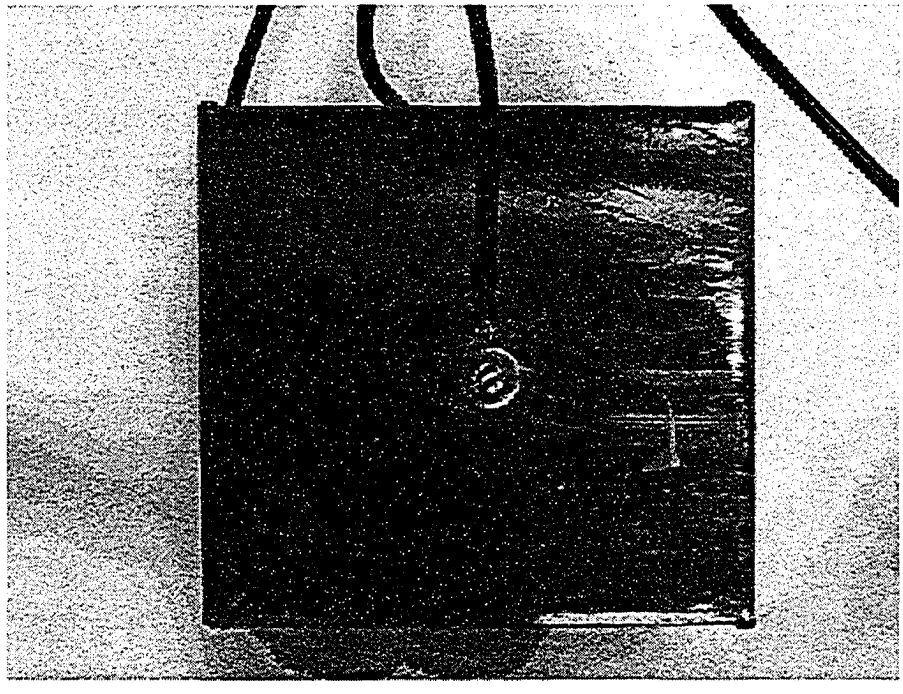

Figure 3.10: Copper Faraday Cage

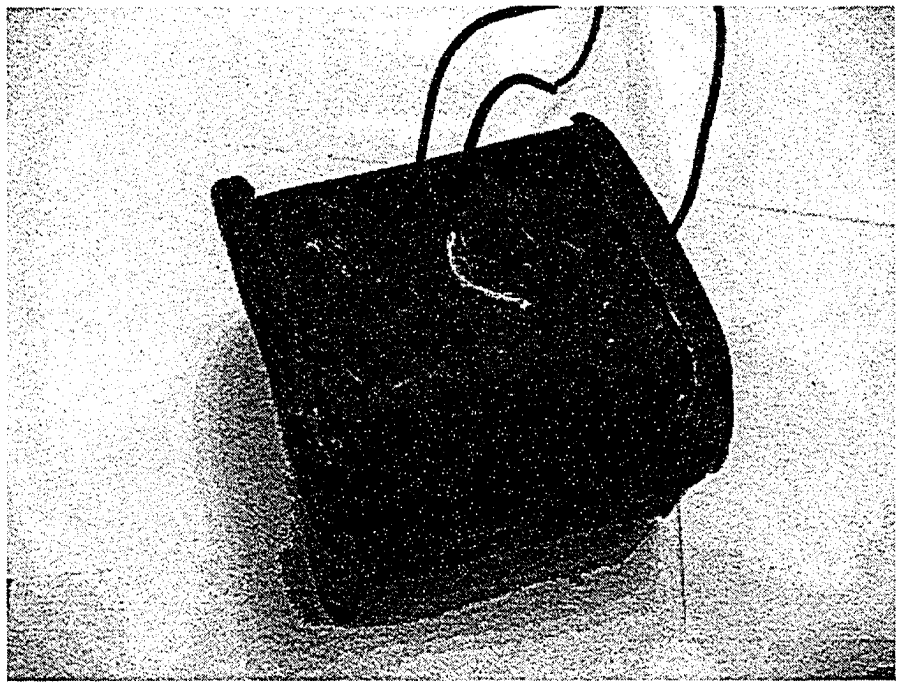

Figure 3.11: Lead Faraday Cage

3.5.2 Grounding

As discussed in the previous sections, the charges are concentrated on the surface of the enclosures i.e. Faraday cages. These collected charges need a sink that is provided by grounding them. For this purpose, stranded silver-plated copper cables were soldered to the body of the cages. The other end was connected to the ground connection of the workstation. These cages were connected to earth for grounding during measurements [20].

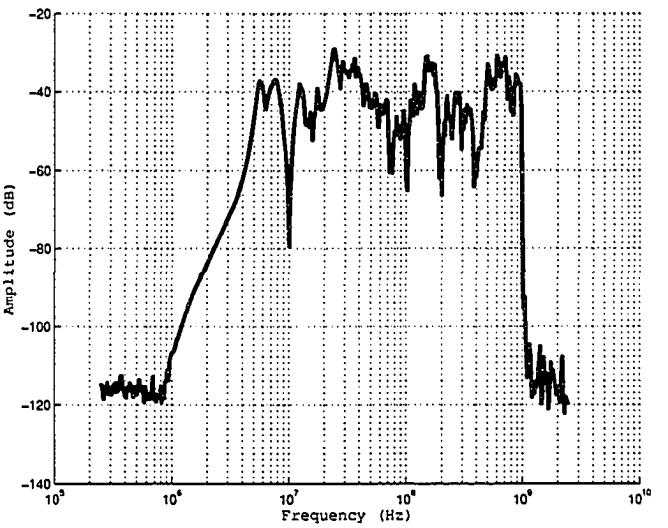

Figure 3.12: SMA connector PCB in copper cage

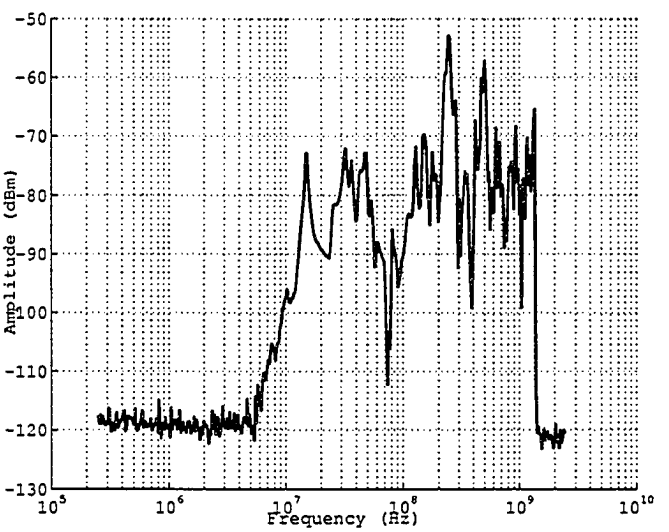

Figure 3.13: SMA connector PCB in lead cage

3.6 Conclusion

This chapter presented a detail of how calibration measurements were performed on the ANEXT experimental setup. A number of experiments were carried out to study the effect of these Faraday cages. The use of Faraday cage helped in the reduction of unwanted interference from the SMA Connector PCBs. The measurement results showed that a considerable amount of reduction in coupling was achieved by using the RF shielding. The magnitude of the ANEXT measured with shielding has dropped down by 15 dBm. However, the contribution due to the boards had not been completely eliminated by using copper cages. In order to get further improvement, Faraday cages were built from lead sheets. With the use of lead cages and proper grounding, a fairly accurate measurement of ANEXT was obtained.

Chapter 4

ANEXT Measurements

This chapter presents the results of the experiments performed in order to characterize ANEXT in 10GBASE-T systems. A comparison between the ANEXT measurements of IEEE802.3 Task Force for 10GBASE-T and measurement results of the thesis research is also discussed.

4.1 ANEXT Measurement Data From the UTP Cable Setup

As was mentioned in Chapter 2, experiments were performed for different lengths of UTP cable using the UTP cable setup. Different sets of data for ANEXT were obtained for CAT5E and CAT6 UTP cables from these experiments and stored in the PC with the help of software interface. Figure 4.1 and Figure 4.2 show the results for 20 m of UTP cable.

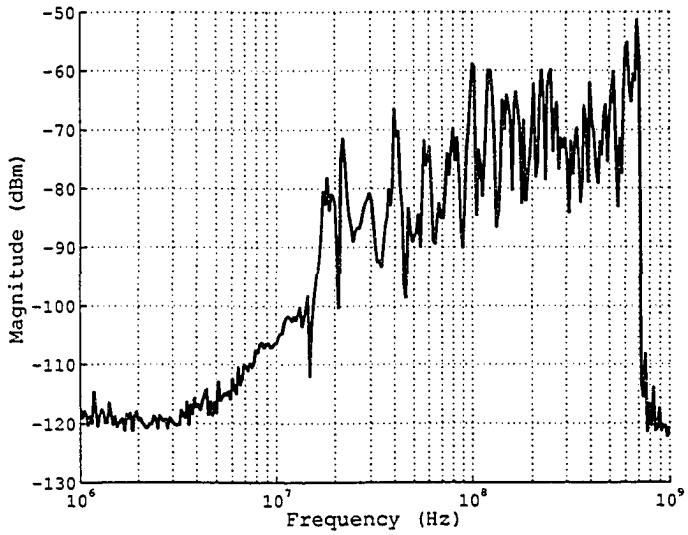

Figure 4.1: ANEXT Data (in log scale) obtained using UTP Cable Setup

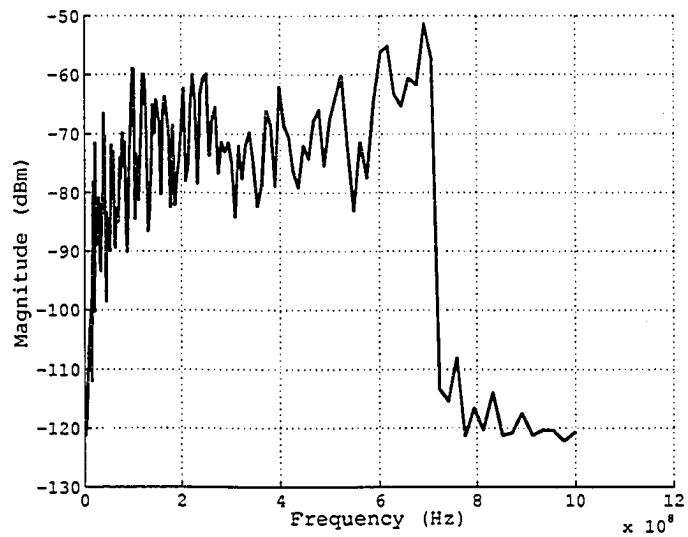

Figure 4.2: ANEXT Data (in linear scale) obtained using UTP Cable Setup

It is seen from the plots that the ANEXT signal increases over the frequency range of 1 MHz to up to around 650 MHz. At the lower frequency range, the magnitude of ANEXT is approximately -120 dBm and gradually rises to -50 dBm. There is a sharp cutoff at around 650 MHz where the ANEXT signal drops to -120 dBm. This is attributed to the cutoff frequency of 650 MHz of the balun being used for impedance matching. Therefore, our ANEXT measurement data is accurate up to around 650 MHz since measurements above this frequency are affected by the frequency range of the balun. The above results are significant since the Task Force has not presented any measurement results for UTP cables on their own.

4.2 ANEXT Measurement Data using Patch Panel Setup

The result of experiments using a patch panel with 24-ports are shown in Figure 4.3 and Figure 4.4.

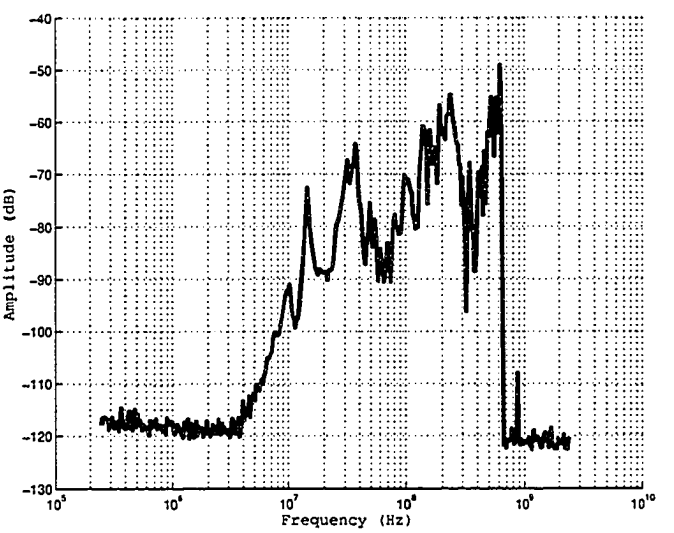

Figure 4.3: ANEXT Data (in log scale) obtained using Patch Panel Setup

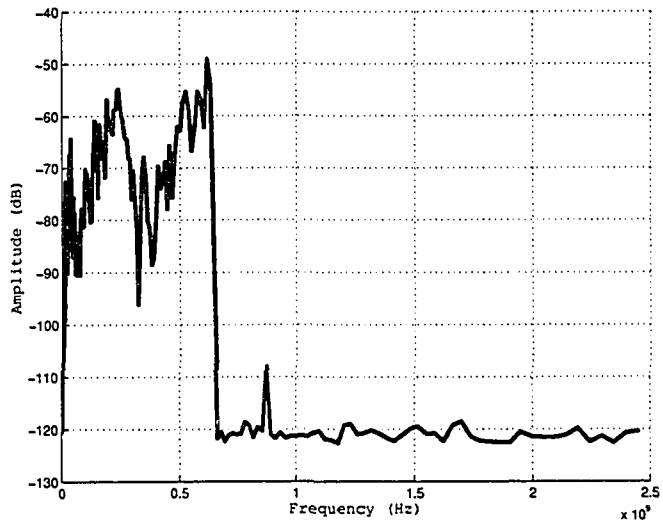

Figure 4.4: ANEXT Data (in linear scale) obtained using Patch Panel Setup

The nature of ANEXT data obtained for this setup is similar to that obtained using the UTP cable setup and ANEXT increases over the frequency range of 1 MHz up to around 650 MHz. It can be seen that the ANEXT signal is approximately 5 dBm higher than for UTP cables. We can therefore conclude that more ANEXT is introduced at the connectors. There is a sharp drop to -120 dBm at around 650 MHz, which represents the upper cutoff frequency of the balun as was seen in the UTP cable setup results.

4.3 Further Results

4.3.1 ANEXT as a function of Cable length

Several experiments were conducted using different length of UTP cable. The length of cable sections used were 5 m, 10 m, 20 m and 40 m . ANEXT power for different lengths was calculated and plotted against cable length and the results are illustrated in Figure 4.5. The plot shows the mean and standard deviation of six measurements taken for each length. It is seen from the results that ANEXT power is fairly constant for the different lengths of UTP cable. Therefore, it can be concluded that ANEXT is *independent* of the length of the cable. This also suggests

that most ANEXT couples from the "disturbers" to the "victims" at points which are close to the point of measurement.

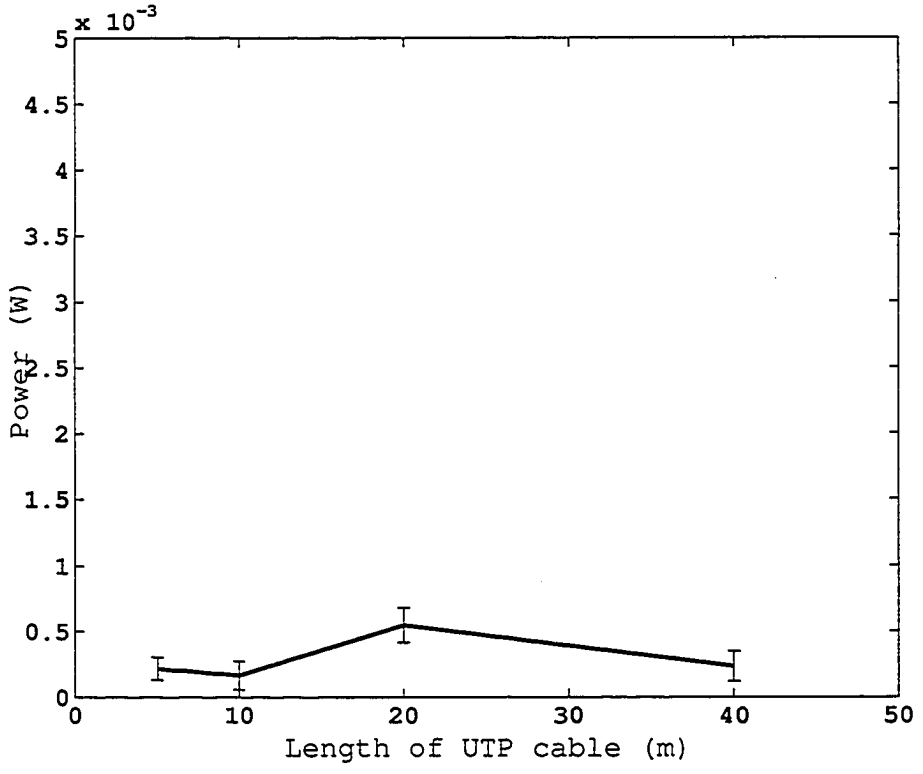

Figure 4.5: ANEXT as a function of cable length

4.3.2 ANEXT as a function of cable separation

We also conducted several experiments by varying the distance between the "victim" and "disturber" cables using both patch panel and UTP cable setups. The results of the experiments were used to find the relationship between ANEXT and adjacent cable separation.

In the experiment using patch panel setup, the cables were at first taped together and thus, there was no separation between them. The "victim" and "disturber" cables were terminated at adjacent patch panel ports. In the next experiment, the two cables were terminated at port 1 and port 19 such that there was a distance of 30 cm between them. More experiments were conducted by placing the cables at 150

cm and 300 cm apart. The "victim" and "disturber" cables were terminated in port 1 and port 24 i.e. the last one. The two cables could not be separated further at the patch panels. In the next experiment, the "disturber" cable was removed such that there was no signal source. The cables can be considered to be infinitely separated in this configuration. The results are illustrated in Figure 4.6 and Figure 4.7. These measurements show the mean and standard deviation of six measurements taken. The power for the position when cables are infinitely separate is plotted at 500 cm.

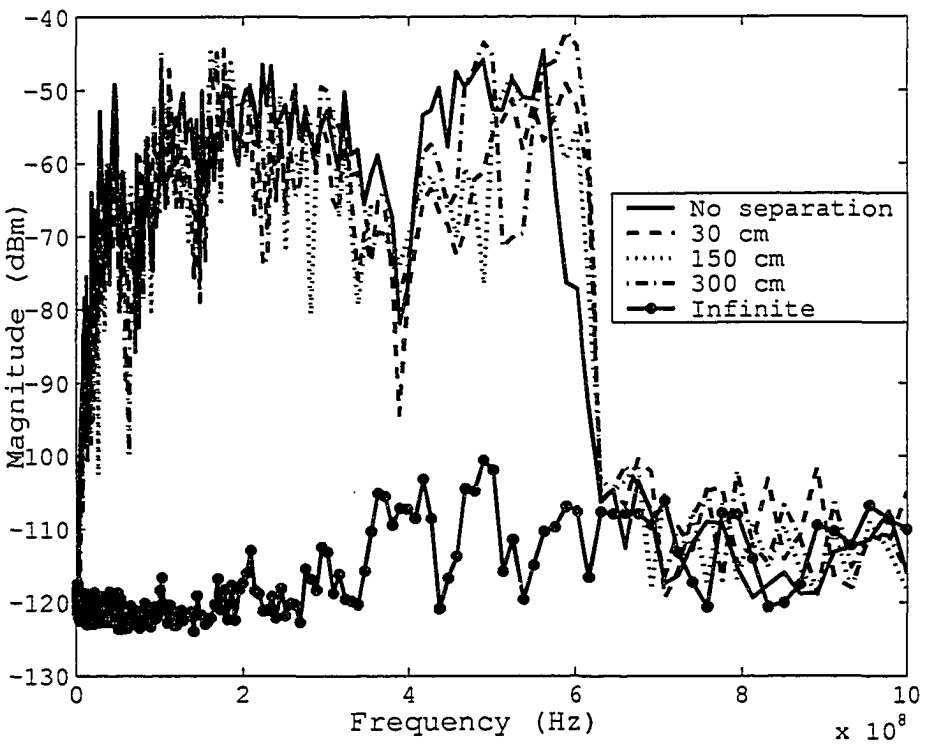

Figure 4.6: ANEXT as a function of cable separation using Patch Panel Setup

It is seen from the results that ANEXT power reduces by separating the "victim" and "disturber" cables by 30 cm, 150 cm and 300 cm. For the case when the cables are infinitely separated, ANEXT power is reduced greatly. Therefore, it can be concluded that the coupling at the connectors is so high in patch panels that even relatively large amount of cable separation results in only little reduction of ANEXT signal. The results suggest that to achieve any reduction in ANEXT power, the connectors need to be moved apart as well as the cables. This is difficult to achieve

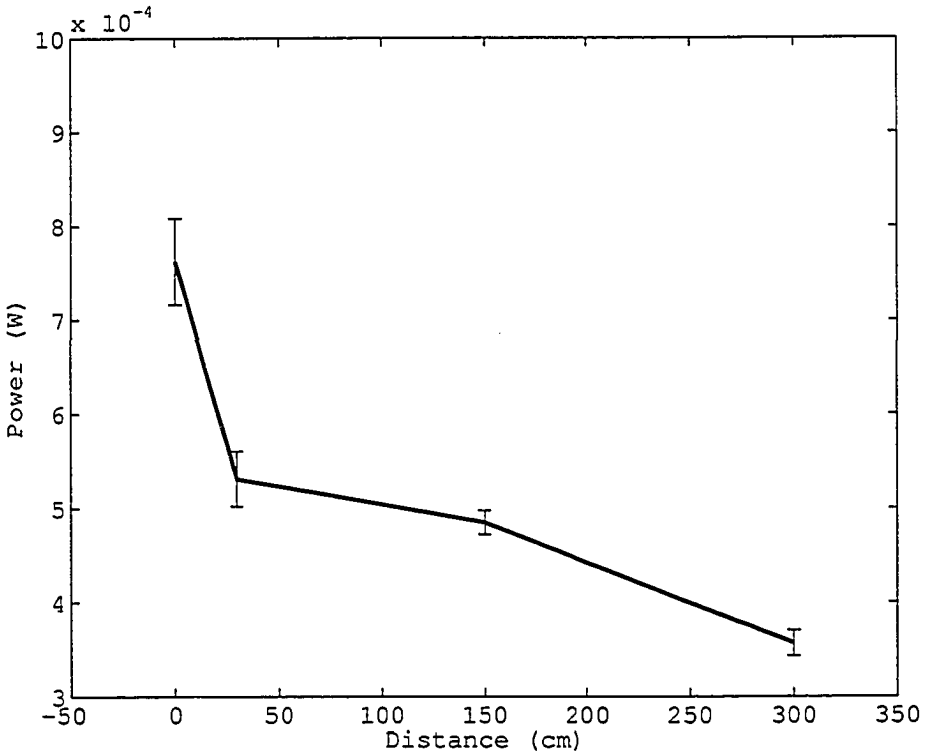

Figure 4.7: ANEXT Power as a function of cable separation using Patch Panel Setup

since the position of ports are fixed in a patch panel.

A set of experiments were also conducted using UTP cable setup. 'Victim" and "disturber" cables were taped together such that there was no distance between them. In these experiments, the UTP cables and inline couplers were separated by 30 cm, 120 cm and 200 cm. Another experiment in which the "disturber" cable was completely removed was also conducted. The results of the experiments are presented in Figure 4.8 and Figure 4.9. It is seen from the results that ANEXT power reduces by separating the inline couplers as well as the cables apart.

We therefore, conclude that ANEXT is dominant at the connectors and can be reduced by separating them. This effect is also seen in the UTP cable setup as the connectors could be moved and placed farther during the experiments. This is not possible in case of patch panel setup where the distance between the connectors is

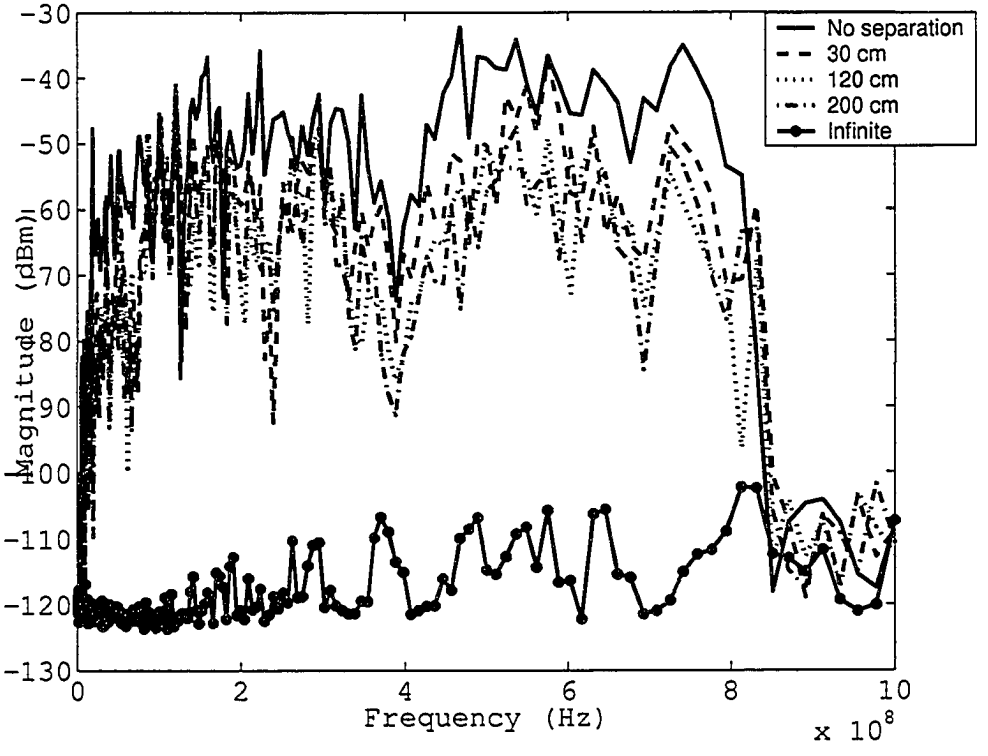

Figure 4.8: ANEXT as a function of cable separation using UTP Cable Setup

constant.

4.3.3 ANEXT as a function of Patch Panel Port Separation

Several experiments were conducted using the patch panel setup to determine the relation between ANEXT power and separation between consecutive patch panel ports. The "victim" cable was connected to port 1 of the patch panel. The "disturber" cable was connected to port 2 through port 24 and readings taken. The sum of total ANEXT power at each port was calculated and plotted against the distance between the ports in cm units. These results show the mean and standard deviation of four sets of measurement data.

It is obvious from the plot in Figure 4.10 that ANEXT power reduces across the ports. Therefore, it can be concluded that moving "disturber" away on the patch panel does result in reduction of ANEXT.

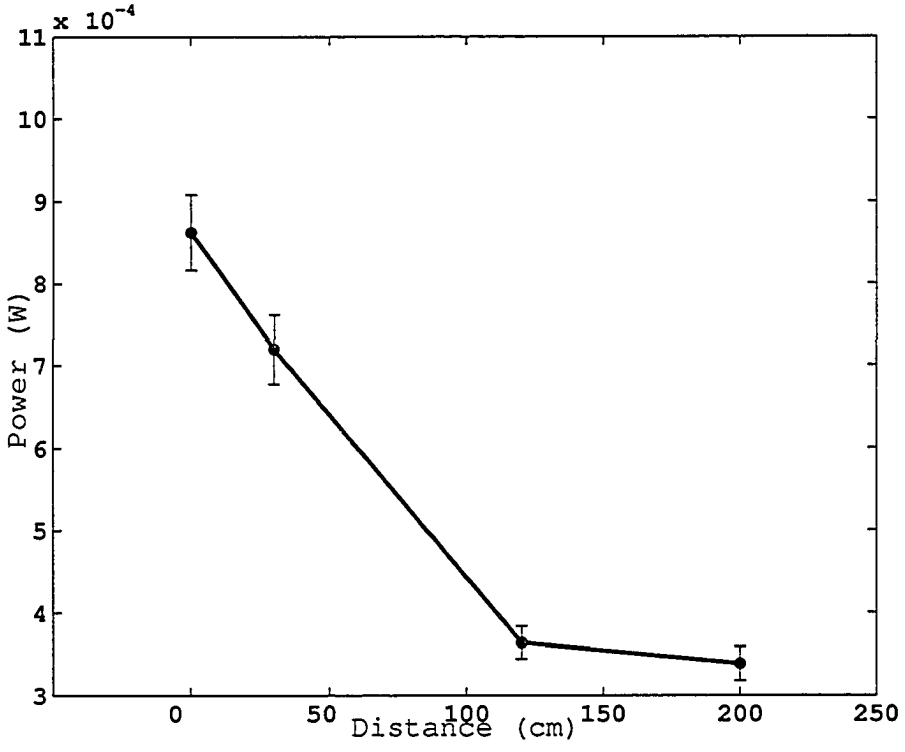

Figure 4.9: ANEXT Power as a function of cable separation using UTP Cable Setup

4.3.4 Effect of bundling on ANEXT

It has been suggested that bundling and coiling may play a part in ANEXT levels [1]. An experiment was conducted in which ANEXT was measured when "disturber" and "victim" cable were bundled together in both a coiled and uncoiled position. The results for these two are given in Figure 4.11. It can be seen that uncoiling the cables does appear to reduce the amount of ANEXT.

4.4 Comparison between 10GBASE-T Task Force measurements and thesis research results

The IEEE802.3 Task Force working on the 10GBASE-T standard has developed different models for ANEXT. These models are for CAT5E and CAT6 UTP cables using 36-port patch panels and channel lengths of 100 m and 55 m. We have an-

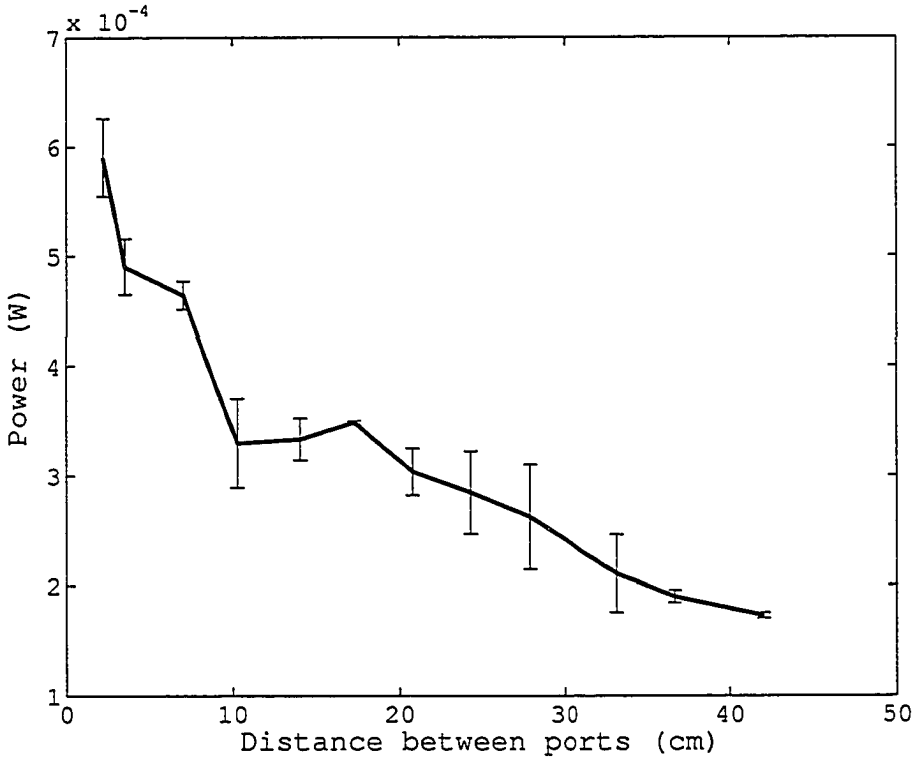

Figure 4.10: Power vs Patch Panel Port Separation

alyzed and compared our data under similar test configurations. In our case, as was mentioned in Chapter 2, 24-port patch panels were used. The measurement data used for the comparison was the one obtained for the case where the SMA Connector PCBs were enclosed in lead Faraday cages and properly grounded.

4.4.1 Comparison for CAT5E UTP

William Jones of Solarflare Communications presented measurement results on 40 m CAT5 UTP cable [1]. He used a single disturber cable and frequencies between 1 MHz to 500 MHz. We conducted several experiments using similar test configurations. The comparative plot is shown in Figure 4.12. It is clear from the plots that our measurement data follows the shape of the measurement data of Jones. An interesting observation is that our measurement data without baluns gives a better match than those with baluns. However, our results for the case when baluns were

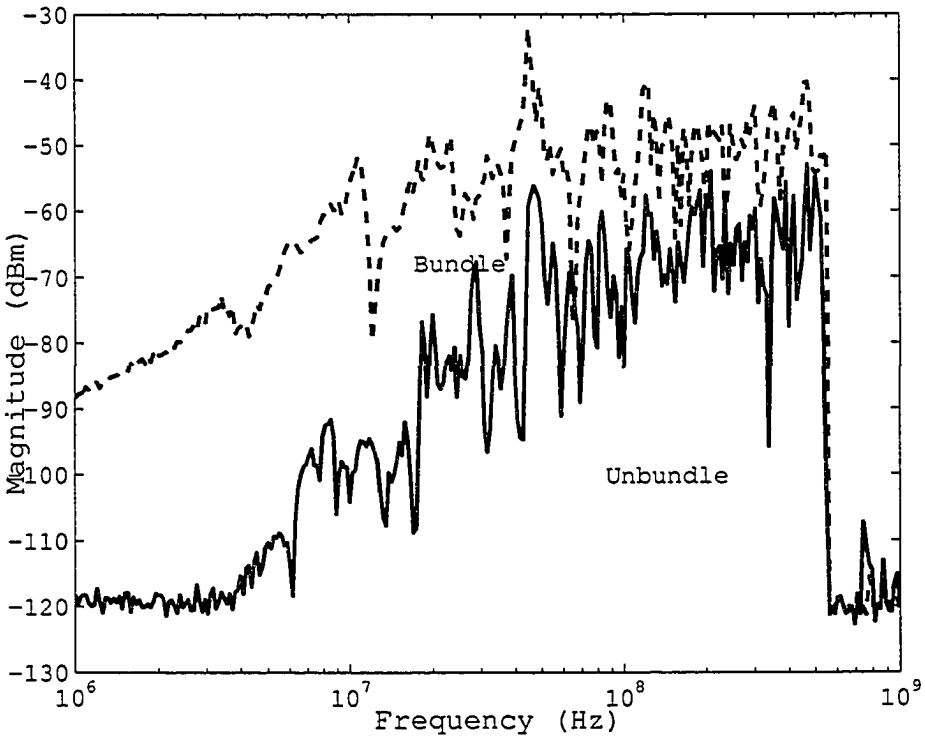

Figure 4.11: Effect of bundling and unbundling

used are much lower. It may be that our choice of balun is affecting our measurement results.

Several other measurements for CAT5E UTP cable have been presented by the Task Force. These include measurements done on sections of cable, patch panels and conduits. Another comparison between the Task Force data and our measurement results is shown in Figure 4.13.

It is seen from the plots that our experimental results follow the shape of IEEE Task Force measurement results closely. The main difference is in the magnitude difference of around 30 dBm and our data is lower than the Task Force data. This difference in values may be expected since the number of "disturbers" used is not the same. The values for ANEXT obtained by the 10GBASE-T Task Force are for Power-Sum (PS) ANEXT, which is the cumulative sum of ANEXT when six "disturbers" were used. Our experiments were conducted in a laboratory environment and we were limited by the number of "disturbers" that could be used. We

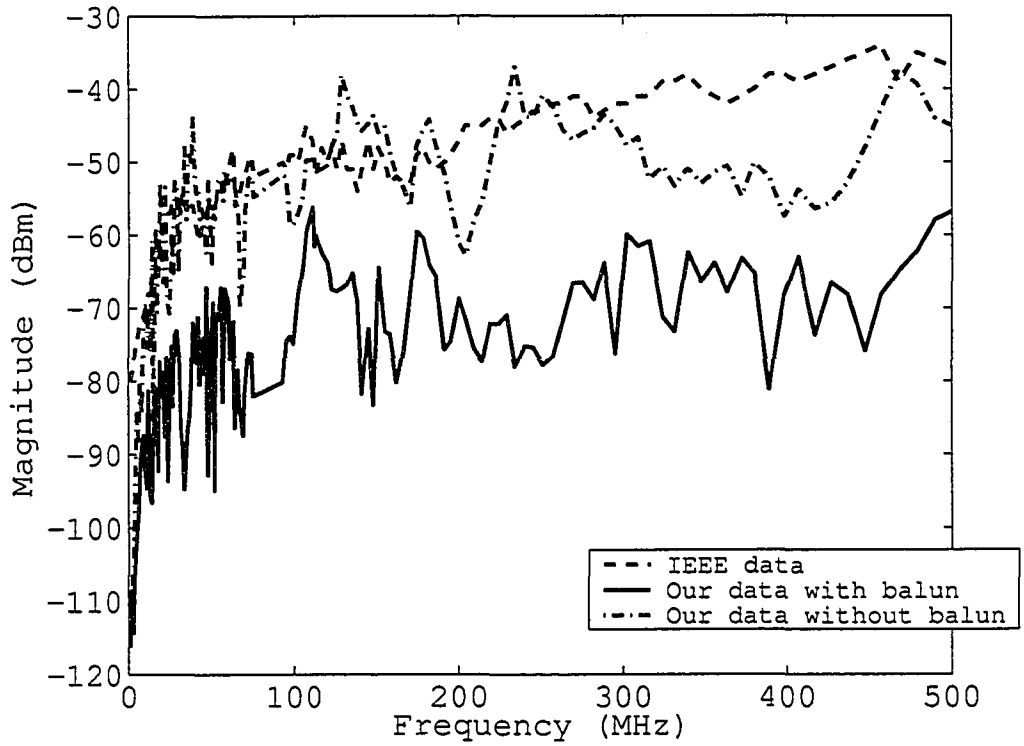

Figure 4.12: Model Comparison for 40 m CAT5E UTP

had access to only one signal generator and therefore, only one "disturber" could be used. Another possible difference may be the brand of the cable used during measurements.

4.4.2 CAT 6 UTP Measurements

We also compared our measurement results using CAT 6 cable. One of the measurements obtained by the IEEE802.3 Task Force is for a 100 m channel and six consecutive patch panel ports and "disturbers". Shielded CAT6 UTP cable was used for the measurements. Figure 4.14 shows the comparison between a Task Force measurements and our results. Their measurements were done using a 36 port patch panel and the "victim" cable was kept close to six "disturbers". As we have already discussed in Chapter 2 that in the thesis research, experiments were conducted with 24-port patch panels and there was only one "disturber" cable in close proximity of the "victim" UTP cable.

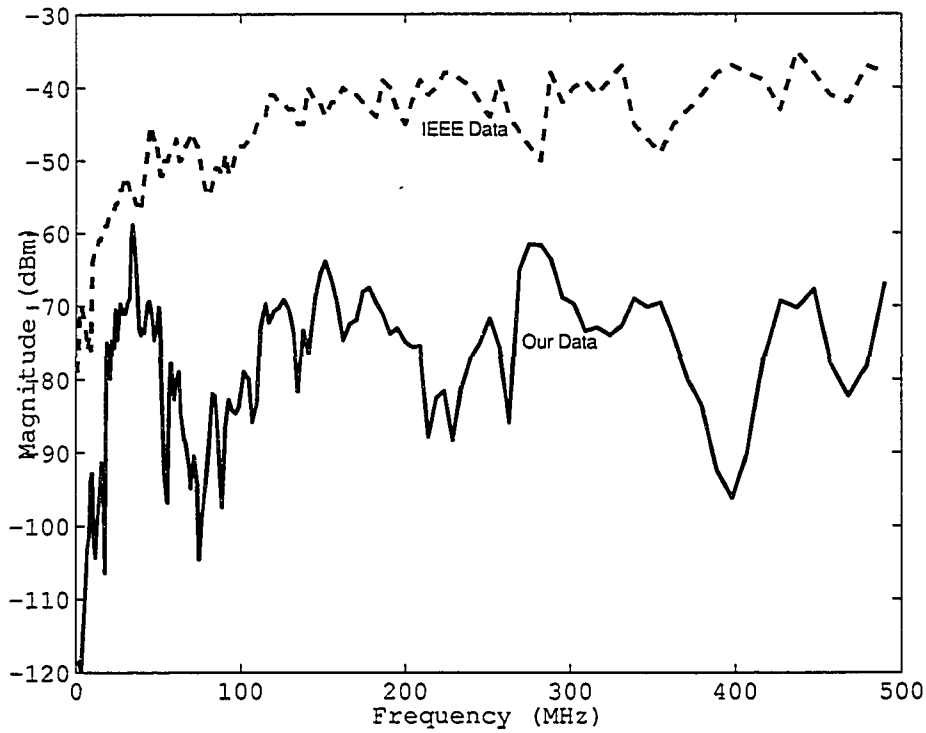

Figure 4.13: Model Comparison for CAT5E

It is seen from Figure 4.14 that although the Task Force data is lower than our measurement data, the shape of the measured ANEXT is similar. One of the main reasons for the difference is the type of UTP cable used. The Task Force measurements were conducted using shielded twisted pair, which reduces ANEXT to a certain extent using the Faraday cage principle [1]. It is obvious from Figure 4.14 that this shielded CAT 6 does significantly reduce the amount of ANEXT power. However, it can be seen that although this cable reduces ANEXT power, it does not completely eliminate it.

4.5 Conclusion

In this chapter, the results of the ANEXT experiments were presented. The variation of ANEXT with respect to cable length, patch panel port separation, cable separation and bundling/unbundling were also discussed. One of the most important conclusions is that ANEXT dominates at the connectors and more reduction

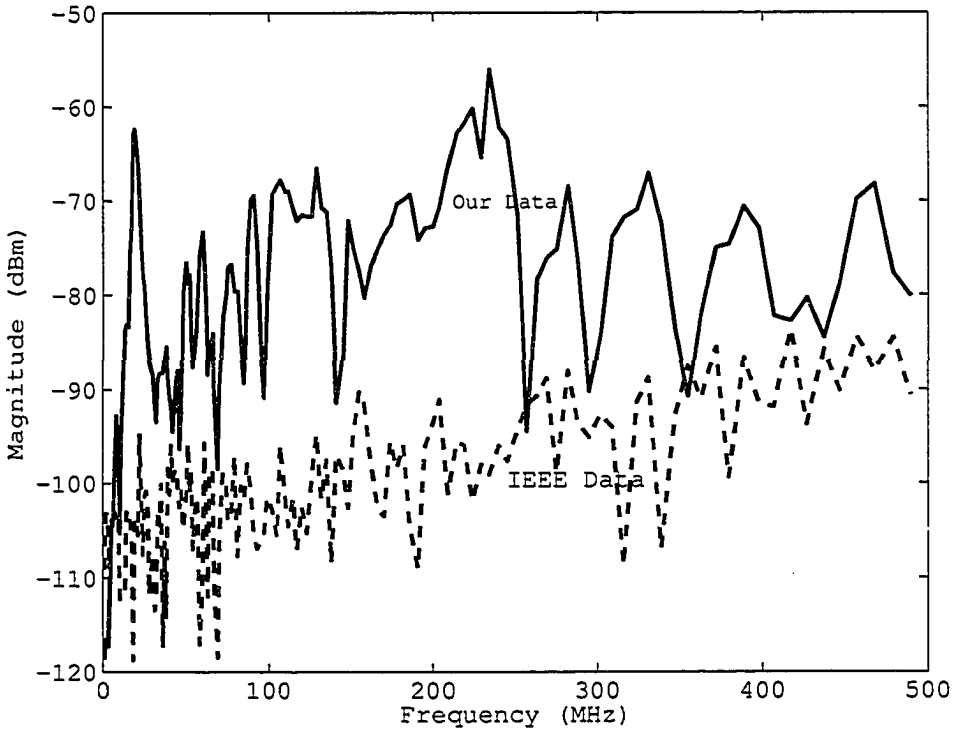

Figure 4.14: Model Comparison for CAT6

in ANEXT can be obtained by separating connectors than by separating cables. ANEXT power reduces across the ports of a patch panel, which depict real world installations. Since the patch panel ports are fixed, a large amount of reduction in ANEXT can not be achieved. It can therefore be concluded that ANEXT mitigation is very difficult to achieve by employing any kind of installation practices. However, based on a comparison with the 10GBASE-T measurements, we can conclude that shielding cables does significantly reduce the amount of ANEXT. Unbundling cables also appears to reduce the amount of ANEXT, at least in the single disturber case.

Chapter 5

ANEXT Modeling

In the previous chapters, we have described the experimental configuration for the measurement of ANEXT, the importance of calibration and discussed the measurement results. This chapter presents the methodology for the modeling and characterization of ANEXT. A filter model for ANEXT is developed using the data obtained from the measurements by applying digital filter design techniques.

5.1 ANEXT Modeling

One of the objectives of the work presented in this thesis is to attempt to find an accurate model of ANEXT. The modeling of ANEXT is done by using the measurement data obtained from the experiments in Chapter 4. The measurement data contains the magnitude of ANEXT in dBm for a range of frequencies in Hz. These can be considered as the design parameters of a digital filter. ANEXT can therefore be modeled by such a filter. Therefore, a digital filter was designed by using digital signal processing techniques and implemented in MATLAB. The filter design techniques involved and actual software implementation of the ANEXT filter are discussed in the following sections.

5.1.1 Filter Design Techniques

Digital filters process a time-domain signal resulting in some change in its original spectral content. The change is generally the filtering out of some unwanted input

spectral components. Filters, thus allow certain frequencies to pass while attenuating other frequencies. Digital filters are broadly of two types namely Finite-duration Impulse Response (FIR) filters and Infinite-duration Impulse Response (IIR) filters. IIR filters are different from FIR filters because of the presence of feedback that makes the duration of the impulse response infinitely long [22].

Due to the relative simplicity in the implementation of FIR filters, the ANEXT model is designed as a FIR filter. There are many techniques to design FIR filters but in this thesis, we focus on the *window* method and the so-called *optimum* method. The design of a filter using the *window method* begins with an ideal desired frequency response that can be represented as

$$H_d(e^{j\omega}) = \sum_{n=-\infty}^{\infty} h_d[n]e^{-j\omega n}, \tag{5.1}$$

where $h_d[n]$ is the impulse response sequence and ω is the normalized frequency in the range $0 \leq \omega \leq \pi$. The above expression can be expressed in terms of $H_d(e^{j\omega})$ in the frequency domain as

$$h_d[n] = \frac{1}{2\pi}\int_{-\pi}^{\pi} H_d(e^{j\omega})e^{j\omega n}d\omega. \tag{5.2}$$

The ideal frequency response as expressed above is infinitely long and not physically realizable. Therefore, in order to obtain a causal filter, the ideal frequency response is truncated. A simple way to obtain a causal FIR filter from $h_d[n]$ is to define a system with response $h[n]$ given by

$$h[n] = \begin{cases} h_d[n], & 0 \leq n \leq M \\ 0, & \text{otherwise.} \end{cases} \tag{5.3}$$

The duration or length of the impulse response of the filter is M+1. Generally $h[n]$ can be represented as the product of the desired impulse response and a finite-duration "window" $w[n]$ i.e.

$$h[n] = h_d[n]w[n], \tag{5.4}$$

where, for simple truncation, the window is the *rectangular window*. According to the windowing theorem, $H(e^{j\omega})$ is expressed as

$$H(e^{j\omega}) = \frac{1}{2\pi}\int_{-\pi}^{\pi} H_d(e^{j\omega})W(e^{j(\omega-\theta)})d\theta. \tag{5.5}$$

$H(e^{j\omega})$ is the periodic convolution of the desired frequency response with the Fourier transform of the window. There are several windows apart from the rectangular window that can be used in the design. The choice of a particular window is governed by the width of the main lobe and size of the side lobes. The main lobe is defined as the region between the first zero-crossings on either side of origin. It is desirable to have the width of the main lobe short as it is related to the implementation of the filter and actual number of taps. Commonly used windows are rectangular, Bartlett, Hanning, Hamming and Blackman [22]. The *FIR2* function in MATLAB uses the Hamming window by default. The function for a Hamming window is given as

$$w[n] = \begin{cases} 0.54 - 0.46\cos(\frac{2\pi n}{M}), & 0 \leq n \leq M \\ 0, & \text{otherwise.} \end{cases} \tag{5.6}$$

5.2 Generation of an ANEXT Modeling Filter

The so-called *Optimal* method for filter design uses the Parks-McClellan Optimal technique. This technique of filter design uses the *remez* function, which is implemented in MATLAB and designs a linear-phase FIR filter using the Remez Exchange Algorithm [24]. The filter design using the *remez* function minimizes the maximum error between the desired frequency response and the actual frequency response.

The filter design using the *remez* function is a two step procedure. The *remezord* function was used to estimate the order of the Optimal FIR filter to meet the design specifications. The output arguments of this function are frequency, amplitude and order to be used in *remez* function for *optimal* filter design. During the actual design of filters using *remez* function, the resulting output vectors are used instead of the original values of frequency and amplitude.

Implementation problems were encountered in the design of ANEXT filter due

to machine rounding errors and convergence failure. The function *remezord* underestimates the order of the filter in some cases with the result that the frequency response of the generated filter did not match the ANEXT data. The desired filter response was not obtained because of the inaccurate estimate of the order of the ANEXT filter.

The problem occurred due to the large number of points in the measurement data and wide frequency range of the input data. Therefore, it was determined that the so-called *optimal* method is not useful in designing ANEXT filter. In our case, the *window* method yielded the filter response that matched the ANEXT measured data reasonably well. The design of ANEXT filter by the *window* method is explained in the following section.

5.2.1 Filter design using a bank of Notch Filters

As seen above, the major problem in the ANEXT filter design is due to the wide frequency range of the measurement data. Therefore, for the practical implementation of ANEXT filter, a suitable number of points should be determined.

The measurement data for ANEXT represented by a number of frequency and amplitude points, is used to design a FIR filter model in the frequency range of 1 MHz to 1 GHz. During measurements, it was found that fewer points did not give proper representation of ANEXT. However, on increasing the number of measurement points, the measurement time increased considerably. Therefore, it was empirically established that approximately 300 points gave proper representation of ANEXT and resulted in less measurement time.

Although around 300 points gave a proper representation of ANEXT data spectrum, the impulse response of the filter had 10,000 taps, which is not suitable for practical implementations. We decided to divide the entire frequency range into suitable bands on the basis of the significant normalized amplitudes. The resulting bands were not equal to each other. From each selected band, 7 points were chosen where the amplitude of the first two points was unity. The middle two points were assigned the actual amplitude corresponding to those frequencies. The next

three points were assigned amplitude equal to unity. The frequency of the last point corresponded to the maximum frequency in the measurement data set. These parameters were used to design a notch filter that has unity gain in the stop band and desired gain in the pass band. Figure 5.1 illustrates the design of the one such notch filter and how the points were selected and assigned corresponding amplitudes.

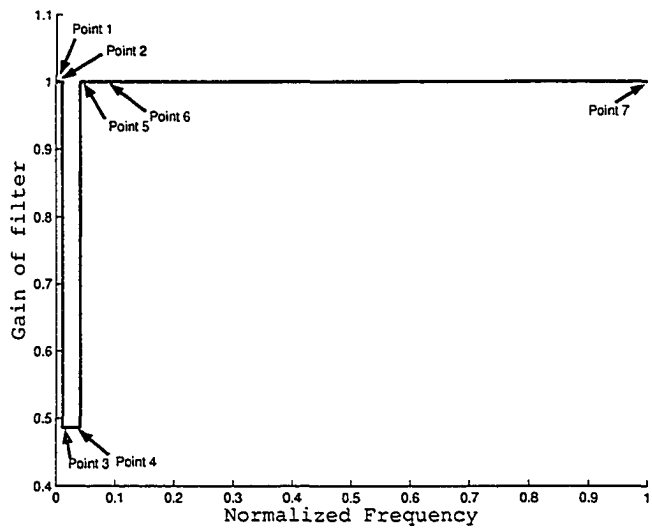

Figure 5.1: Design of Notch Filter

Several notch filters were designed using the measurement data and convolved together to obtain a single ANEXT filter. This filter is the model of the ANEXT obtained from the measurement data and is illustrated in Figure 5.2 for a specific ANEXT measurement. The corresponding impulse response of this ANEXT filter is illustrated in Figure 5.3. The ANEXT filter has approximately 2,500 taps that contain 99% of the energy. The MATLAB code for this implementation is included in Appendix B. It can be seen that the model matches the measurement data reasonably well.

The major advantage of designing several notch filters is that the number of taps in each filter is significantly lower than the resulting ANEXT filter. Therefore, these individual notch filters are physically realizable.

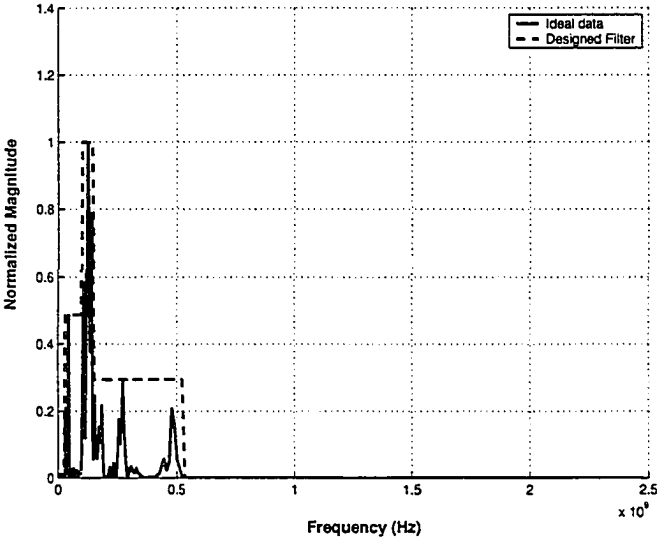

Figure 5.2: ANEXT Filter

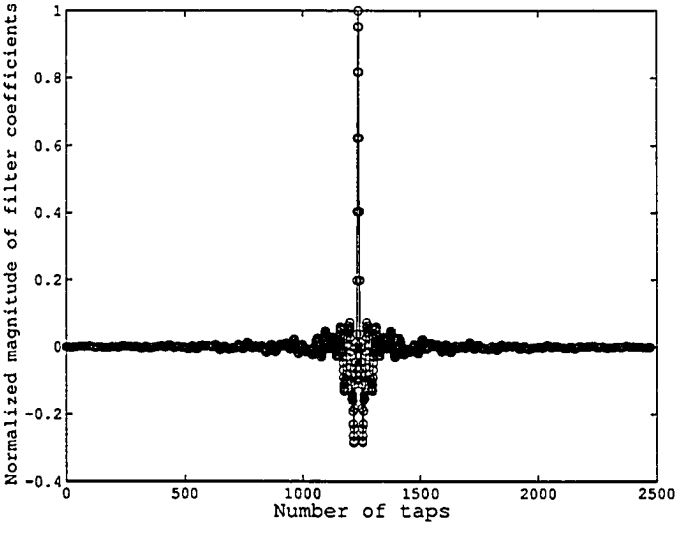

Figure 5.3: Impulse Response of ANEXT Filter

The frequency response of the filter was compared to the measurement data. It is seen from the Figure 5.4 and Figure 5.5 that the output of the designed filter follows the measurement data reasonably closely. There is a steep transition band that exactly matches that of the measurement data. ANEXT signals for another set of measurement data are shown in Figure 5.6 and Figure 5.7. ANEXT signal is the output of the ANEXT filter when the filter input is a stream of Tomlinson-Harashima Precoded (THP) Pulse Amplitude Modulation (PAM)-12 symbols. This will be discussed further in the following chapter.

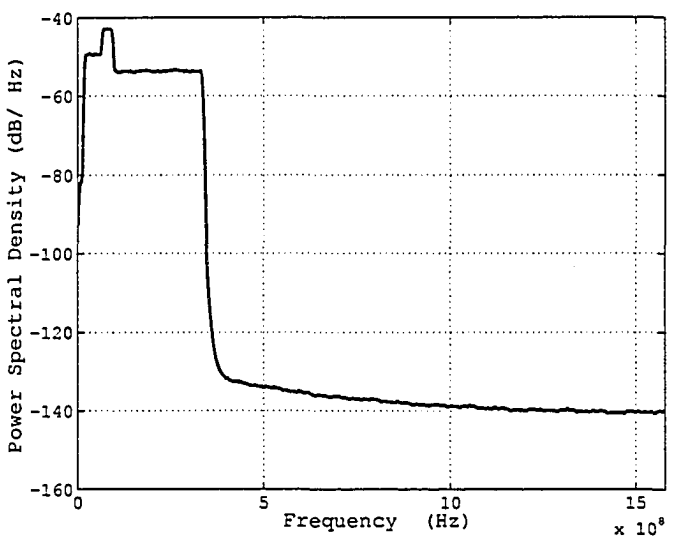

Figure 5.4: ANEXT Signal obtained using model for Data Set I

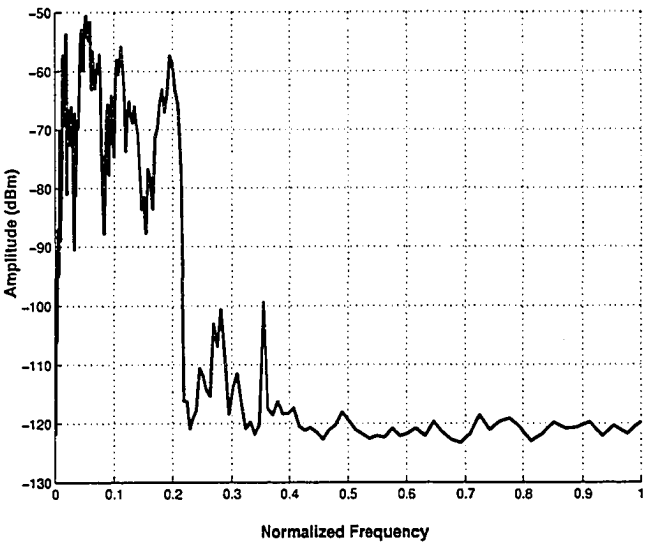

Figure 5.5: ANEXT Data Set I obtained from measurements

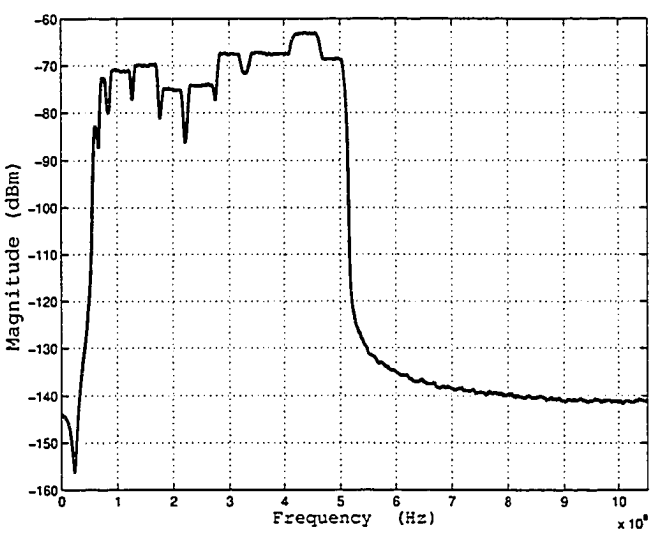

Figure 5.6: ANEXT Signal obtained using model for Data Set II

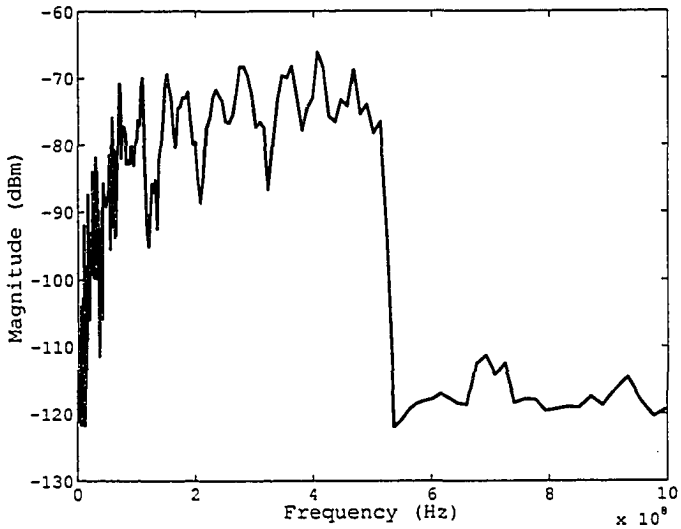

Figure 5.7: ANEXT Data Set II obtained from measurements

5.3 Conclusion

This chapter presented the design of the filter model of ANEXT. The model was generated from the measurement data by dividing it into smaller sets depending on the number of points that yielded in a filter that closely matched the measured data. A number of notch filters were designed and convolved with each other to generate the final ANEXT filter model. It is seen that the frequency response of the designed ANEXT filter model matched the measurement data reasonably well. This approach can be employed further to design filter models for any set of ANEXT measurement data.

Chapter 6

Issues Relevant to ANEXT Mitigation

In the previous chapters, we discussed the ANEXT measurement setup, results and proposed the idea of modeling of ANEXT. The current chapter investigates some aspects relevant to ANEXT mitigation.

The dependence of ANEXT on installation practices is seen from our experimental results. Moving cables farther apart helps to reduce the ANEXT power. It was also mentioned in Chapter 1 that the 10GBASE-T Task Force has suggested installation practices as possible solution to the problem of ANEXT. These include unbundling of UTP cables, using enhanced quality patch cords and foiled twisted pair [1]. However, such practices may not be feasible due to the close placing of connectors and cables in patch panels and switches.

Therefore, it is desirable to develop a mitigation technique for ANEXT that avoids dependence on installation practices. In this chapter, a digital signal processing approach is proposed to mitigate ANEXT and several aspects of its design are considered.

6.1 Cyclostationary nature of ANEXT

As it was previously discussed in Chapter 1, NEXT is a type of interference caused by signal coupling into one of the four pairs of UTP cable from the adjacent three pairs simultaneously [8]. It is measured from the near end of the transmitter and

so named as NEXT. ANEXT is also similar to NEXT since it is also unwanted interference between UTP cable pairs. The difference between the two lies in the source of this interference. In NEXT, the source is the three pairs of same UTP cable while in ANEXT, it is the pairs of the adjacent cable.

In the earlier lower data rate version of XBASE-T Ethernet i.e. 1000BASE-T systems, the "disturber" signals are synchronous to the "victim" signals. NEXT signal originates from the local transmitters and therefore, the nature of the disturbing signal is known and standard cancellation techniques can be employed [10]. In 10GBASE-T systems, ANEXT is the coupled signal originating from a transmitter of another pair of UTP cable. Therefore, it is no longer guaranteed that the signals in the "disturber" UTP cable are synchronous with the desired receive signal in the "victim" UTP cable. The frequency at which the receiver for the "victim" operates is not necessarily the same as the frequency of the "disturber" transmitter. Thus, the ANEXT signals are no longer stationary but are cyclostationary (CS) in nature. The term cyclostationary refers to signals that have time-varying statistical properties [19]. The mean and autocorrelation of such signals are periodic in time [11, 12].

As the source of the ANEXT signal is a transmitter that is the external to the system, these signals are unknown. Therefore, blind, asynchronous cancellation is necessary. This is a much more complicated task than for 1000BASE-T systems.

6.2 Modeling the 10GBASE-T System

In order to better understand the problem of ANEXT and develop mitigation techniques, a simple model of the 10GBASE-T system considering the problem of ANEXT was implemented in MATLAB to determine the transmitter and receiver characteristics. This simple model was used to study the affect of different factors in the mitigation of ANEXT at the receiver. This section presents a discussion of the simulated system and the corresponding MATLAB code is included in Appendix B.

In Ethernet systems, information is sent from transmitter to receiver over a

UTP channel using baseband modulation. In a baseband system, information is directly encoded and impressed upon the transmission medium [8]. According to the 10GBASE-T Task Force, the modulation scheme to be used is defined as Pulse Amplitude Modulation (PAM) [1]. The data bits are mapped into corresponding voltage levels that are sent over the UTP cable. The number of voltage levels is determined on the basis of the number of levels present in the PAM scheme. The proposed PAM scheme in 10GBASE-T is PAM-12, thus there are twelve voltage levels [1].

Since we want to characterize ANEXT and find a mitigation technique for it, we need to analyze the 10GBASE-T signals traveling on UTP cables, which give rise to ANEXT. The desired 10GBASE-T signal travels on the "victim" cable. ANEXT is the interfering signal from the neighboring cable i.e. the "disturber", which superimposes itself on the desired signal. It is thus noted that the source of ANEXT is also a 10GBASE-T signal. Therefore, it is necessary to study and simulate the stream of data symbols on the UTP channel.

The 10GBASE-T signal traveling along the UTP cable will suffer from several impairments as mentioned in Chapter 1. One of these impairments is Intersymbol Interference (ISI) that arises in the channel [23]. Due to the dispersive nature of the channel, the duration of each symbol transmitted extends beyond the time interval used to represent that symbol. As a result, the consecutive received symbols overlap in time and this interference is called ISI. To recover the signal correctly in presence of ISI, the receiver should have a means for compensating or reducing the ISI in the received signal. Equalization is an efficient technique to compensate the ISI introduced by the channel and the compensator is called equalizer. The following section discusses the way that ISI is eliminated in the presence of ANEXT in 10 Gigabit Ethernet systems. We need to consider this as it impacts on our ANEXT System model.

6.2.1 Tomlinson-Harashima Precoding

Generally an equalizer is used at the receiver to remove the effect of ISI. This equalizer employs feedforward and feedback filters to eliminate ISI. In the equalization technique, the feedback filter requires an infinite number of taps. If the number of taps is lower, the compensation of ISI is only approximate [13]. An alternative precoding technique for uncoded modulation to solve the problem of ISI was simultaneously but independently proposed by Tomlinson and Harashima [13].

A Tomlinson-Harashima precoder (THP) can be used at the transmitter to solve the ISI problem. The major idea of THP is that the ISI introduced in the channel is subtracted at the transmitter. THP can be used in systems where the channel does not change and the channel characteristics are known at the transmitter. Both of these conditions are satisfied in 10GBASE-T systems [1]. The impulse response of the channel, which is already known at the transmitter, is multiplied with previously transmitted data symbols and the result is subtracted from the currently transmitted data symbol to obtain the transmit signal. The precoding ensures that ISI is removed at the transmitter and therefore eliminates the use of equalizer at the receiver. A major advantage of this scheme is that it reduces the complexity of the receiver. The following section describes the 10GBASE-T system simulated in MATLAB considering Tomlinson-Harashima precoding approach.

6.2.1.1 Tomlinson-Harashima Precoding Simulation

As the proposed modulation scheme in 10GBASE-T systems is PAM-12 [1], we consider this modulation scheme for our simulation. We consider a signal set A, which consists of 12 equally spaced levels, e.g., $A = \{\pm 1, \pm 3, \pm 5, \pm 7, \pm 9, \pm 11\}$, i.e. the set of all odd integers in the interval [-11, 11].

The THP operates on the transmitted signal, x_k. Tomlinson-Harashima precoding is illustrated in Figure 6.1. The impulse response of the channel, h(D) is multiplied with the previously transmitted data symbols and subtracted from the current data symbol. A typical UTP channel is a low-pass filter and its channel response can be approximated by

$$h(z) = 1 + \frac{z^{-1}}{2}, \tag{6.1}$$

where z is a unit delay [1]. Since the subtracted part is due to previously transmitted symbols, the part of channel response that is multiplied is only h(D) - 1. The result is operated upon by a modulo (mod) operation denoted by the block mod 22. The resulting sequence is then transmitted over the channel that introduces additive white gaussian noise (AWGN) and the ISI.

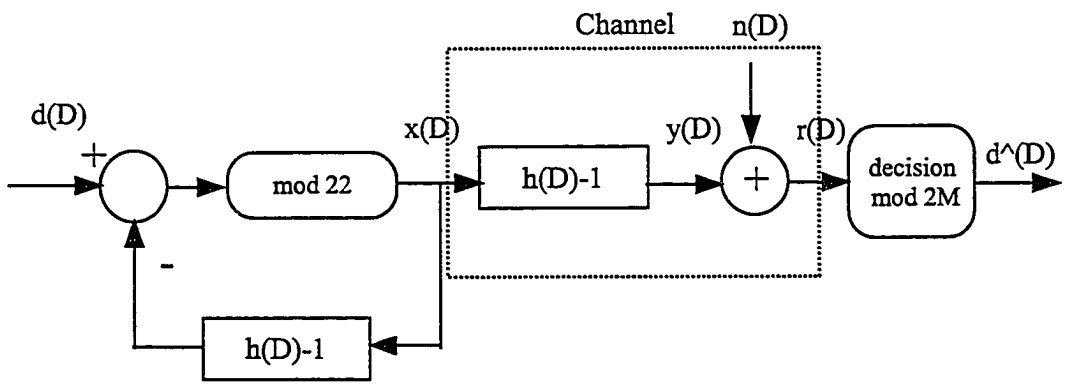

Figure 6.1: Tomlinson-Harashima Precoding [13]

As was mentioned previously, ANEXT is also a 10GBASE-T signal that originates from the "disturber" cable i.e. a neighboring 10GBASE-T transmitter. Therefore, we performed the Tomlinson Harashima precoding on the ANEXT data in our simulation. To study the effect of ANEXT, the generated symbols were then filtered through the ANEXT filter that generates the ANEXT signal.

The ANEXT signal from the neighboring cable i.e. the "disturber" is then superimposed on the received signal at the receiver. Thus, the received signal contains precoded PAM-12 signal from the transmitter filtered by UTP cable and the ANEXT from another PAM-12 signal traveling on a neighboring cable. We then attempted to recover the ANEXT signal at the receiver to compensate it. A system model illustrating the "victim" and "disturber" UTP cable systems and how the different signals are received at the "victim" receiver is given in Figure 6.2.

The received signal is sampled at precise instants at the receiver where analog-

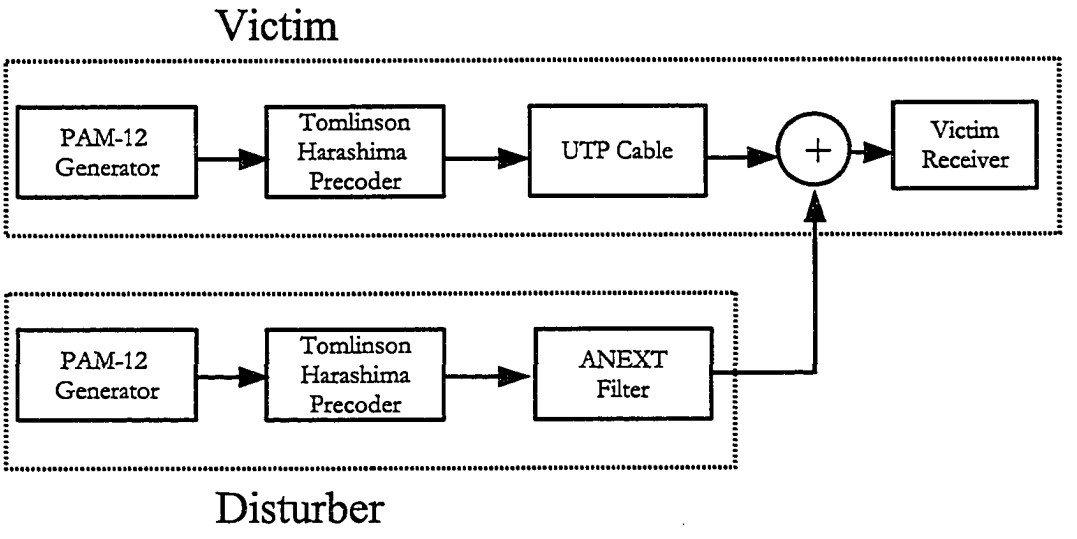

Figure 6.2: A simple model of 10GBASE-T system

to-digital (A/D) conversion takes place. Due to imperfections in the crystals at the transmitter and receiver, the A/D conversion at the receiver does not automatically take place at exactly the same frequency as the transmitter. Therefore, recovery of the transmitter clock signal is required. The process of extracting such clock signal at the receiver is usually called *symbol synchronization* or *timing recovery*. A major problem in 10GBASE-T systems is the high sampling frequency of 825 MHz. Even a slight error in the sampling rate can result in a great loss in received data. The following section discusses the problem of timing recovery in the presence of ANEXT and the impact of timing recovery jitter on our ability to mitigate ANEXT signals.

6.3 Proposed ANEXT Cancellation Circuit

In this thesis, we propose an ANEXT cancellation circuit using an adaptive scheme. The ANEXT cancellation circuit is illustrated in Figure 6.3 and employs digital signal processing techniques. In this circuit, ANEXT filter is adaptive in nature and its taps change in each iteration to minimize the error. The output of the ADC at the "victim" receiver contains the desired receive signal combined with noise from

the channel and ANEXT. ANEXT signal is cancelled from the received signal by using the adaptive ANEXT filter. As we are investigating a technique for ANEXT mitigation, we propose the scheme for canceling the ANEXT signal only. For this cancellation to produce desirable output, ANEXT timing recovery and ANEXT symbol detection need to be implemented first and are discussed in the following sections. As we are investigating an ANEXT mitigation technique, we propose the scheme for canceling the ANEXT signal alone and not the noise.

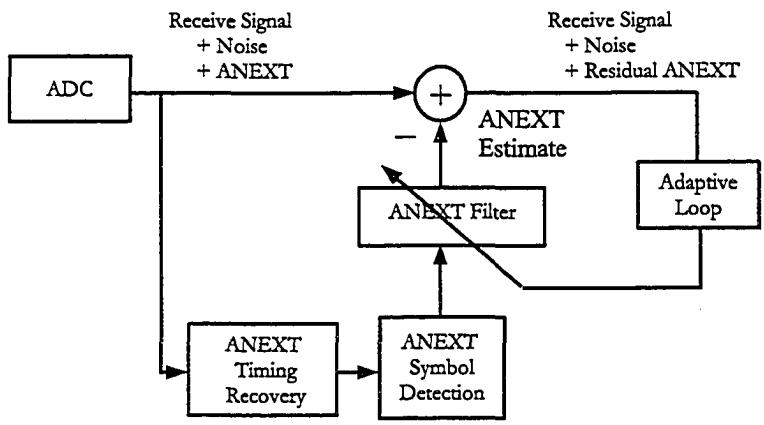

Figure 6.3: Proposed ANEXT Cancellation Circuit

6.3.1 Timing Recovery

For proper reconstruction of the transmitted signal at the receiver, one of the conditions is that the transmitter and the receiver should operate at the same frequency. This is not possible in case of ANEXT in 10GABSE-T systems since the "disturber" transmitter and "victim" receiver crystals will differ. We consider that the clock at the "victim" receiver will differ by some amount Δ, which is the frequency offset.

In order to estimate this frequency offset, the "victim" receiver would have to employ a device called *clock synchronizer*. The task of timing recovery is to extract the frequency offset i.e. the error and adaptively adjust the clock at the receiver to sample the ANEXT signal at the correct frequency.

There are several types of timing recovery techniques [16, 23]. They can be

classified as *external* or *self* synchronization. In the former, the clock signal is transmitted with the transmitted signal and used for timing recovery. Although it is a simple scheme, it is inefficient since additional bandwidth and power are used in transmitting the clock signal. In *self* synchronization, the timing signal is extracted from the received signal itself. Although it makes efficient use of resources, the receiver structure becomes complex. For PAM systems with zero mean, a popular timing synchronization technique is spectral line generating synchronizer that uses a non-linear block to generate a spectral line at the symbol rate [18, 19, 21]. External synchronization cannot be used for ANEXT timing recovery.

In order to characterize ANEXT and propose its mitigation technique, we performed an open loop simulation of the timing recovery section of the 10GBASE-T receiver in presence of ANEXT. The simulation was performed to analyze the behavior of the timing error. In our simulations, we assumed the sampling rate to be 825 MHz that has been specified by the 10GBASE-T Task Force [1].

6.3.1.1 Simulation of Timing Error Detector Characteristics

The aim of the timing error detector was to investigate if the frequency offset of the ANEXT signal can be recovered at the receiver. Simulations were conducted using a spectral line generating synchronizer with a nonlinear block followed by a phase locked loop (PLL) with multiplying timing error detector to study the timing error detector (TED) characteristics [19]. A non-linear operation i.e. squaring was performed on the the received PAM signal filtered through the UTP cable and ANEXT signal. The squared PAM signal denoted by $p(t;\varepsilon)$ and squared ANEXT signal denoted by $a(t;\varepsilon)$ are then multiplied with the reference signal $r(t;\varepsilon)$ to obtain the timing error detector output signal, $x_1(t;\varepsilon)$ and $x_2(t;\varepsilon)$ for the respective signals [19]. The results of the multiplications can be expressed as

$$x_1(t;\varepsilon) = k_1 p(t;\varepsilon) * r(t;\varepsilon), \tag{6.2}$$

$$x_2(t;\varepsilon) = k_2 a(t;\varepsilon) * r(t;\varepsilon), \tag{6.3}$$

where k_1 and k_2 are the gains of the multiplication and are not equal. These simulations were performed under open-loop conditions, which are suitable for obtaining the timing error detector characteristics [19].

The TED characteristics for the received PAM signal and for ANEXT signal were obtained from the simulations. These are also called synchronizer characteristics or S-curves and are presented in Figure 6.4.

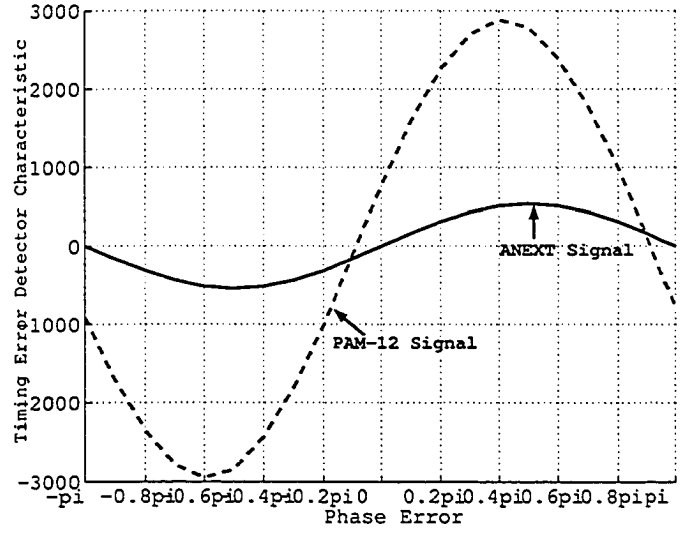

Figure 6.4: Timing Error Detector Characteristics for Received PAM Signal with ANEXT

It is seen from the simulation results that the timing information for PAM-12 signal is larger than that for the ANEXT signal. Therefore, the timing recovery signals may lock to the incorrect frequency. It can be concluded from the nature of the S-curves that it is possible to recover the timing information of the ANEXT signal at the receiver.

6.3.2 ANEXT Symbol Detection

In order to cancel ANEXT using the ANEXT cancellation scheme, ANEXT symbols should be correctly detected at the "victim" receiver. The design of the receiver when the channel is corrupted by ANEXT becomes complicated because the symbols of the corrupting signal are unknown. Therefore, any cancellation scheme for

ANEXT must be based on blind symbol recovery which is much more complicated than non-blind cancellation [9]. The area of blind symbol detection needs to be investigated. However, it is beyond the scope of this thesis and can be pursued as an independent research.

6.3.3 Impact of Clock Jitter on ANEXT Cancellation

In the previous sections we have discussed the problem of timing recovery and blind symbol detection in the recovery of ANEXT signal. The nature of the timing error detector characteristics for the desired PAM-12 signal and ANEXT signal show that clock recovery is a difficult task in 10GBASE-T systems. The other problem with recovery of ANEXT signal is blind symbol detection. However, even if both these problems are resolved and we are able to recover the ideal symbols and compensate the clock, another problem still remains. This problem is the jitter in clock sources [28, 29].

Jitter is defined by the International Telecommunications Union (ITU) as the "short-term variations of the significant instants of a digital signal from their ideal positions in time" [5]. ANEXT signal after the timing recovery block and blind symbol detection block will be sampled at precise instants at the "victim" receiver. But due to imperfections in the clock, the actual sampling instants differ from the ideal sampling instants giving rise to timing jitter.

If we consider a continuous signal $x(t)$ being sampled at discrete multiples of the period T. The samples can be expressed as

$$x_n = x(nT). \tag{6.4}$$

Due to clock jitter, these samples are not taken at exact multiples of the period, nT but at $(nT + \zeta_n)$ where ζ_n represents the error of jitter. The corresponding samples now become

$$Y_n = x(nT + \zeta_n). \tag{6.5}$$

The difference between the ideal samples and samples taken by the jittered clock introduce sampling errors.

In our simulations, we determined the root mean square (RMS) error due to random jitter introduced in the system. The results are presented in Figure 6.5. It is seen from the plot that the RMS error is zero for no jitter. It increases linearly for jitter values of 1 ps to 10 ps.

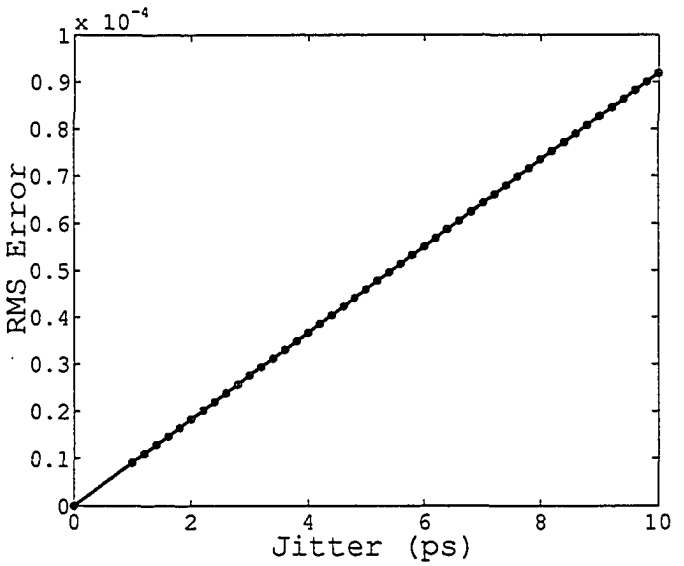

Figure 6.5: Error due to Clock jitter

6.4 Conclusion

This chapter proposed a possible cancellation scheme for ANEXT. Simulations were carried out to analyze a model of the 10GBASE-T system to investigate the aspects of PAM symbol generation, precoding using THP and timing recovery. The issues of timing recovery, blind symbol recovery and clock jitter pose a major challenge in the recovery of ANEXT signal. These problems need to be resolved for any ANEXT cancelation scheme to yield desired results. The TED results indicate that detecting the frequency offset of the ANEXT signal in the presence of the cable signal may be very difficult. This may make DSP techniques for ANEXT mitigation unimplementable.

Chapter 7

Conclusions and Future Work

7.1 Conclusions

The IEEE is working on the latest standard for Ethernet that will provide data rates of 10Gbps. This new standard is called 10GBASE-T and will be formalized as IEEE802.3an sometime in 2006. Besides the obvious advantage of higher data rate, it will run over UTP copper cable leading to cost efficiencies compared to 10 Gbps protocols that operate over optical fiber. Despite the numerous advantages, 10GBASE-T like the previous Ethernet standards, suffers from numerous impairments that must be tackled for its deployment.

Among all the impairments mentioned in Chapter 1, Alien crosstalk will be a problem unique to 10GBASE-T systems. This is because 10GBASE-T systems will involve signalling frequencies up to 500 MHz. This new type of crosstalk has been identified as one of the major impairments for the deployment of 10GBASE-T systems by the 10GBASE-T Task Force.

This thesis characterized this ANEXT independently from the 10GBASE-T Task Force. The uniqueness of the problem and lack of research in this area were the main motivating factors for conducting this research. This thesis proposed a technique to measure ANEXT in a laboratory environment. The major accomplishments included setting up a wireline testbed for conducting the experiments, measuring ANEXT using different categories of UTP cables under different scenarios and developing models of ANEXT. One of the tasks in setting up the testbed was to

create interfaces in the form of PCBs to interconnect the measurement instruments to the UTP cable. During experiments, these PCBs gave rise to electromagnetic interference. Calibration measurements were performed to determine the contribution of these interfaces to the measurement data. As was mentioned in Chapter 3, a suitable shielding technique in the form of a Faraday cage like structure made of lead was employed to get rid of this unwanted interference. Another problem of impedance matching was resolved by using components like baluns and 100 Ω termination circuits.

An interesting point in the thesis is the results of our measurements. We compared our results with the measurement data of the IEEE Task Force. Although there are obvious differences in the two setups, one being an industrial environment and ours being a laboratory environment, we notice that the our measurement results for the single "disturber" case match closely with the Task Force results.

We also proposed several characteristics of ANEXT on the basis of our measurement results. One of the most important results is that ANEXT signal coupling is most dominant at the connectors. Therefore, separating cables alone may not result in a significant amount of ANEXT reduction. ANEXT coupling reduces across the ports of a patch panel. Therefore, it can be concluded that ANEXT can be reduced by terminating cables at distant ports of the patch panel. Due to the fixed distance between the ports, ANEXT cannot be completely eliminated. The other interesting result is that ANEXT does not change with cable length. However, ANEXT coupling does reduce by unbundling the cables. The contribution of these results is important to find a suitable technique to mitigate ANEXT.

Another contribution of the thesis is the filter model of ANEXT that is obtained from the measurement results of our experiments. The modeling procedure is explained in Chapter 5. The modeling of ANEXT was necessary to characterize its nature and to develop a model to investigate techniques to mitigate it. It was mentioned in Chapter 1 that several mitigation techniques have been proposed by the IEEE Task Force. However, they are based on ways of finding suitable installation practices, better UTP cables and enhanced patch cords. The area of digital signal

processing for ANEXT compensation has not been investigated to date. One of the main challenges in this area is the recovery of the disturbing ANEXT signal. We investigated the timing recovery problem and also determined the performance of a TED for ANEXT. We proposed a possible mitigation technique for ANEXT in the form of an adaptive canceller but showed that there are major implementation issues for our proposed architecture.

7.2 Possible Future Work

This thesis has presented work on the characterization of ANEXT through experimentation, modeling and a possible mitigation technique. We propose a possible solution to the ANEXT problem using DSP approach. We show that ANEXT might be mitigated by designing a suitable cancelation filter. The implementation of this system could be undertaken as an independent research program.

The recovery of the ANEXT signal is critical for its cancellation. Estimation techniques to recover the desired PAM signal and undesired ANEXT signal at the receiver need to be investigated. The timing recovery section would form a major part of such a receiver. Our simulation results show the nature of the timing error and the difficulty of recovering the ANEXT signal at the receiver due to the energy of the ANEXT signal being a lot less than the cable signal. A major research work can be done to find a suitable timing recovery scheme and implement it.

Another problem with the recovery of ANEXT is the presence of jitter in clock sources and its impact on the cancellation. However, jitter is inherent in clock sources and good performance in presence of jitter can only be achieved by specifying acceptable amounts of jitter for the 10GBASE-T systems. This thesis can be considered the basis for further research on the problems of ISI, timing recovery technique and its implementation.

The hardware implementation of the ANEXT filter can also be undertaken as an independent future project. The low-pass FIR digital filter is physically realizable and can be implemented using ASICs and hardware description languages like Verilog HDL or VHDL.

It is seen from our measurement results that ANEXT power increases with frequency. It is approximately -120 dBm in the 1 MHz to 100 MHz range and rises to -50 dBm at 500 MHz. It is seen that at lower frequencies, another crosstalk similar to ANEXT, which is measured at the further end of the transmitter and so called Alien Far-End Crosstalk (AFEXT) gains importance. Contributions by several Task Force members like Broadcom have shown that AFEXT is dominant at lower frequencies where ANEXT is not so dominant. For reliable data transmission in 10GBASE-T systems, AFEXT cannot be neglected at lower frequencies and needs to be canceled. Characterization of AFEXT, its modeling and mitigation can also form an area of future research.

Bibliography

[1] 10GBASE-T Taskforce. *http://www.ieee.org/802/3/10GBT/.*

[2] Agilent Technologies. *http://www.agilent.com.*

[3] Ethernet Drawing. *http://www.ethermanage.com/ethernet.*

[4] Horizontal Cabling. *http://www.linktionary.com/c/cabling.html.*

[5] International Telecomuunications Union. *http://www.itu.int.*

[6] Test Balun. *http://www.bhelectronics.com/PDFs/040-0092.pdf.*

[7] ANSI/TIA/EIA-568-B.2-1-2002. Technical report, Jun 2002.

[8] *IEEE Std 802.3-2002.* The Institute of Electrical and Electronics Engineers, Inc., 2002.

[9] S. Bates. VLSI Issues for the Implementation of 10GBASE-T Ethernet. In *Proceedings of the International Conference on Signal Processing applications*, pages 382–386, 2004.

[10] S. Bates and B. Murray. Issues for the design and implementation of a 1000BASE-T Gigabit Ethernet Transceiver. In *Proceedings of the International Conference on Signal Processing applications*, 2000.

[11] J.C. Campbell, A.J. Gibbs, and B.M. Smith. The Cyclostationary Nature of Crosstalk Interference from Digital Signals in Multipair Cable - PartI : Fundamentals. *IEEE Trans. on Communications*, 31(5):629–637, May 1983.

[12] J.C. Campbell, A.J. Gibbs, and B.M. Smith. The Cyclostationary Nature of Crosstalk Interference from Digital Signals in Multipair Cable - PartII : Applications and Further Results. *IEEE Trans. on Communications*, 31(5):638–649, May 1983.

[13] Jr. G.D.Forney and M.V. Eyuboglu. Combined Equalization and Coding Using Precoding. *IEEE Communications Magazine*, pages 25–34, December 1991.

[14] Simon Haykin. *Communications Systems*. John Wiley and Sons, Inc., 2001.

[15] Paul Izzo. *Gigabit Networks*. John Wiley and Sons, Inc., 2000.

[16] E.A. Lee and D.G. Messerschmitt. *Digital Communication*. Mc Graw Hill, 1988.

[17] A. Leon-Garcia and Indra Widjaja. *Communication Networks - Fundamental Concepts and Key Architectures*. Mc Graw Hill, 2004.

[18] Louis Litwin. Matched filtering and timing recovery in digital receivers. *RF time and freqeuncy www.rfdesign.com*, pages 32–48, September 2001.

[19] H. Meyr, M. Moeneclaey, and S. A. Fechtel. *Digital Communication Receivers: Synchronization, Channel Estimation, and Signal Processing*. John Wiley & Sons, Inc., 1998.

[20] Ralph Morrison. *Grounding and Shielding Techniques in Instrumentation*. John Wiley and Sons, 1986.

[21] K.H. Mueller and M. Mueller. Timing Recovery in Digital Synchronous Data Receivers. *IEEE Transactions on Communications*, pages 517–530, May 1976.

[22] A.V. Oppenheim, R W. Schafer, and J. R. Buck. *Discrete-Time Signal Processing*. Prentice Hall, 1999.

[23] John G. Proakis. *Digital Communications*. McGraw Hill, 1992.

[24] John G. Proakis and D.G. Manolakis. *Digital Signal Processing - Principles, Algorithms and Applications*. McGraw Hill, 1990.

[25] Douglas C. Smith. *High Frequency Measurements and Noise in Electronic Circuits*. Morgan Kaufmann, 1992.

[26] William Stallings. *Data and Computer Communications*. Pearson Prentice Hall, 2004.

[27] T. Starr, J.M. Cioffi, and P.J. Silverman. *Understanding Digital Subscriber Line Technology*. Prentice Hall, 1999.

[28] Ransom Stephens. Analyzing Jitter at High Data Rates. *IEEE Optical Communications*, pages 6–10, February 2004.

[29] P.R. Trischitta and E.L. Varma. *Jitter in Digital Transmission Systems*. Artech House, 1989.

Appendix A

Experimental Configuration

A.1 Apparatus

1. Agilent E4438C ESG Vector Signal Generator (250 kHz - 3.0 GHz),
2. Agilent E4402B ESA-E Series Spectrum Analyzer (9 kHz - 3.0 GHz),
3. Category 5E/6 UTP Patch cord,
4. Category 5E/6 UTP Cable,
5. SMA connectors,
6. RG58C/U coaxial cable,
7. Balun (1MHz to 650MHz),
8. SMA Connector PCB,
9. 100 Ω Termination PCB,
10. 24-port Patch Panels,
11. Rack,
12. Cat5E/6 jacks,
13. Crimping Tool,
14. Continuity tester,

15. Punch-down tool,

16. Faraday cages made of copper and lead.

A.2 RJ45 Pin configuration

Table A.1: RJ45 Pin Configuration

Position from left	Wire Color
1	White-orange
2	Orange
3	White-green
4	Blue
5	White-blue
6	Green
7	White-brown
8	Brown

Appendix B

MATLAB Code

B.1 Code for ANEXT Filter

```
%%=========================================================================
%This program creates  a filter from the measurement data for ANEXT.
%The filters are designed using window method.
% A suitable number of notch filters are designed and convolved with each
% other to get the final ANEXT filter.
%%=========================================================================

function anext_notch = anext_filter(anext_measfile)

anext_data              = open(anext_measfile);
names                   = fieldnames(anext_data);
eval(['struct = anext_data.' names{1} ';']);

% Amplitude and Frequency obtained from the data file
amplitude               = struct.y_data;
frequency               = struct.x_data;

%%=========================================================================
% converting amplitude to linear units

amplitude               = 10.^(amplitude/10);
amplitude               = amplitude./max(amplitude);


% plot(frequency,amplitude)


% create a number of  filters and then convolve them
% fir2 function designs a frequency sampling-based finite
% impulse response filter
% Filter1
anext_frequency1        = [0 frequency(1) frequency(2) frequency(127)...
        frequency(128) frequency(130) frequency(end)]/frequency(end);
anext_amplitude1        = [0 0 amplitude(1) amplitude(1) 1 1 1];
anext_filter1           = fir2(8192,anext_frequency1,anext_amplitude1);


% figure
% plot(anext_filter1)
%
% [h,w]                 = freqz(anext_filter1,1,512);
%
% figure
```

```
% hold on;
% plot(anext_frequency1./max(anext_frequency1),anext_amplitude1,'b'); hold on;
% anext_frequency1./max(anext_frequency1)
%
% plot(w/pi,abs(h),'r--')
% legend('Ideal','fir2 Designed')
% title('Comparison of Frequency Response Magnitudes1')


%Filter2
anext_frequency2      = [0 frequency(126) frequency(127) frequency(207)...
        frequency(208) frequency(210) frequency(end)]/frequency(end);
anext_amplitude2      = [0 0 amplitude(188) amplitude(188) 1 1 1];
anext_filter2         = fir2(8192,anext_frequency2,anext_amplitude2);

figure
plot(anext_filter2)

% [h,w]               = freqz(anext_filter2,1,512);
%
% figure
% hold on;
% plot(anext_frequency2./max(anext_frequency2),anext_amplitude2,'b'); hold on;
% plot(w/pi,abs(h),'r--')
% legend('Ideal','fir2 Designed')
% title('Comparison of Frequency Response Magnitudes2')

%Filter3
anext_frequency3      = [0 frequency(206) frequency(207) frequency(262)...
        frequency(263) frequency(264) frequency(end)]/frequency(end);
anext_amplitude3      = [1 1 amplitude(227) amplitude(227) 1 1 1];
anext_filter3         = fir2(8192,anext_frequency3,anext_amplitude3);

% figure
% plot(anext_filter3)
%
% [h,w]               = freqz(anext_filter3,1,512);
%
% figure
% hold on;
% plot(anext_frequency3./max(anext_frequency3),anext_amplitude3,'b'); hold on;
% plot(w/pi,abs(h),'r--')
% legend('Ideal','fir2 Designed')
% title('Comparison of Frequency Response Magnitudes3')
%

%Filter4
anext_frequency4      = [0 frequency(255) frequency(256) frequency(278)...
        frequency(290) frequency(291) frequency(end)]/frequency(end);
anext_amplitude4      = [1 1 amplitude(272) amplitude(272) 1 1 1];
anext_filter4         = fir2(8192,anext_frequency4,anext_amplitude4);

% figure
% plot(anext_filter4)

% [h,w]               = freqz(anext_filter4,1,512);

% figure
% hold on;
% plot(anext_frequency4./max(anext_frequency4),anext_amplitude4,'b'); hold on;
% plot(w/pi,abs(h),'r--')
% legend('Ideal','fir2 Designed')
% title('Comparison of Frequency Response Magnitudes4')


%Filter5
```

```
anext_frequency5      = [0 frequency(278) frequency(279) frequency(340)...
        frequency(342) frequency(345) frequency(end)]/frequency(end);
anext_amplitude5      = [1 1 amplitude(305) amplitude(305) 1 1 1];
anext_filter5         = fir2(8192,anext_frequency5,anext_amplitude5);


% figure
% plot(anext_filter5)

% [h,w]               = freqz(anext_filter5,1,512);

% figure
% hold on;
% plot(anext_frequency5./max(anext_frequency5),anext_amplitude5,'b'); hold on;
% plot(w/pi,abs(h),'r--')
% legend('Ideal','fir2 Designed')
% title('Comparison of Frequency Response Magnitudes5')

%Filter6
anext_frequency6      = [0 frequency(333) frequency(334) frequency(390)...
        frequency(398) frequency(399) frequency(end)]/frequency(end);
anext_amplitude6      = [1 1 amplitude(335) amplitude(335) 0 0 0];
anext_filter6         = fir2(8192,anext_frequency6,anext_amplitude6);

% figure
% plot(anext_filter6)
%
% [h,w]               = freqz(anext_filter6,1,512);
%
% figure
% hold on;
% plot(anext_frequency6./max(anext_frequency6),anext_amplitude6,'b'); hold on;
% plot(w/pi,abs(h),'r--')
% legend('Ideal','fir2 Designed')
% title('Comparison of Frequency Response Magnitudes6')

%%=============================================================================
%convolving the designed filters

anext_filter_conv     = conv(anext_filter1,anext_filter2);
anext_filter_conv     = conv(anext_filter_conv,anext_filter3);
anext_filter_conv     = conv(anext_filter_conv,anext_filter4);
anext_filter_conv     = conv(anext_filter_conv,anext_filter5);
anext_filter_conv     = conv(anext_filter_conv,anext_filter6);
anext_filter          = anext_filter_conv;

%%=============================================================================


[h,f]                 = freqz(anext_filter,1,1024,2*frequency(400));
figure
hold on;grid on; zoom on
plot(frequency,amplitude, 'b');
plot(f,abs(h),'r—')
legend('Ideal','fir2 Designed')
title('Comparison of Overall Frequency Response Magnitudes');
%

% fid = fopen('anext_filter_file.dat','w');
% fwrite(fid,anext_filter,'double');
% fclose(fid);
%
% figure
% plot(anext_filter)
```

B.2 Code for 10GBASE-T System Model

```
%%=============================================================================
%%=============================================================================
%%This program generates PAM-12 symbols
%%The generated PAM symbols are precoded using Tomlinson-Harashima Precoding
%%The precoded symbols pass through the UTP channel
%%The precoded symbols are passed throught the ANXET channel filter obtained
%%from our measurement data.The PSD of output of this ANEXT filter is
%%plotted.This is compared with the actual measurement data.
%%=============================================================================
%%At the transmitter, PAM-12 symbols of length equal to nSimlen are generated
%%This is the 10GBASE-T signal in the victim cable
%%=============================================================================
clear all;
close all;

%% epsilon is used to compare the transmitted symbols and those received
epsilon                 = 0.00001;
nSimlen                 = 100000; %Simulation length
Fs                      = 825e6;   % Sampling Frequency

rand('state',0)
randn('state',0)

peSigmaNoise            = 0;

epsilon1                = rand(1,1);
epsilon2                = rand(1,1);

%%Random numbers of length equal to simulation length specified by variable
%%nSimlen are generated
peRandom                = rand(1,nSimlen);

%%Equiprobable PAM-12 symbols are generated
pnPlusEleven            = find(peRandom<1/12);
pnPlusNine              = find(peRandom>=1/12 & peRandom<2/12);
pnPlusSeven             = find(peRandom>=2/12 & peRandom<3/12);
pnPlusFive              = find(peRandom>=3/12 & peRandom<4/12);
pnPlusThree             = find(peRandom>=4/12 & peRandom<5/12);
pnPlusOne               = find(peRandom>=5/12 & peRandom<6/12);
pnMinusOne              = find(peRandom>=6/12 & peRandom<7/12);
pnMinusThree            = find(peRandom>=7/12 & peRandom<8/12);
pnMinusFive             = find(peRandom>=8/12 & peRandom<9/12);
pnMinusSeven            = find(peRandom>=9/12 & peRandom<10/12);
pnMinusNine             = find(peRandom>=10/12 & peRandom<11/12);
pnMinusEleven           = find(peRandom>=11/12 & peRandom<1.0);

%%Bit to symbol mapping where all symbols are equi-probable
%% with probablility = 1/12
pnSymbols               = zeros(1,nSimlen);
pnSymbols(pnPlusEleven) =  11;
pnSymbols(pnPlusNine)   =  9;
pnSymbols(pnPlusSeven)  =  7;
pnSymbols(pnPlusFive)   =  5;
pnSymbols(pnPlusThree)  =  3;
pnSymbols(pnPlusOne)    =  1;
pnSymbols(pnMinusOne)   = -1;
pnSymbols(pnMinusThree) = -3;
pnSymbols(pnMinusFive)  = -5;
pnSymbols(pnMinusSeven) = -7;
pnSymbols(pnMinusNine)  = -9;
pnSymbols(pnMinusEleven)= -11;

pamLevels               = [-11,-9,-7,-5,-3,-1,1,3,5,7,9,11];
```

```
% figure(1)
% [n,x]                          = hist(pnSymbols,100);
% bar(x,n/nSimlen);

% title('Input Symbols Waveform','Fontsize',12);
% xlabel('Pam Levels','Fontsize',12);
% ylabel('Probability','Fontsize',12);

%% Amal Ekbal definition of M
M                          = pamLevels(end) + 1;
d                          = 2;

%=============================================================
%This is the 10GBASE-T signal in the adjacent cable
%i.e. the "disturber" cable ANEXT symbols are generated
%due to signal coupling i.e when the signal in
%disturber is passed through our ANEXT filter
%Random numbers of length equal to simulation length
%specified by variable nSimlen are generated same as for
%"victim" cable
%=============================================================

peAnextRandom                  = rand(1,nSimlen);

%%Equiprobable PAM-12 symbols are generated
pnAnextPlusEleven          = find(peAnextRandom<1/12);
pnAnextPlusNine            = find(peAnextRandom>=1/12 & peAnextRandom<2/12);
pnAnextPlusSeven           = find(peAnextRandom>=2/12 & peAnextRandom<3/12);
pnAnextPlusFive            = find(peAnextRandom>=3/12 & peAnextRandom<4/12);
pnAnextPlusThree           = find(peAnextRandom>=4/12 & peAnextRandom<5/12);
pnAnextPlusOne             = find(peAnextRandom>=5/12 & peAnextRandom<6/12);
pnAnextMinusOne            = find(peAnextRandom>=6/12 & peAnextRandom<7/12);
pnAnextMinusThree          = find(peAnextRandom>=7/12 & peAnextRandom<8/12);
pnAnextMinusFive           = find(peAnextRandom>=8/12 & peAnextRandom<9/12);
pnAnextMinusSeven          = find(peAnextRandom>=9/12 & peAnextRandom<10/12);
pnAnextMinusNine           = find(peAnextRandom>=10/12 & peAnextRandom<11/12);
pnAnextMinusEleven         = find(peAnextRandom>=11/12 & peAnextRandom<1.0);

%Bit to symbol mapping where all symbols are equi-probable
%i.e probablility = 1/12
pnAnextSymbols                     = zeros(1,nSimlen);
pnAnextSymbols(pnAnextPlusEleven)  =  11;
pnAnextSymbols(pnAnextPlusNine)    =  9;
pnAnextSymbols(pnAnextPlusSeven)   =  7;
pnAnextSymbols(pnAnextPlusFive)    =  5;
pnAnextSymbols(pnAnextPlusThree)   =  3;
pnAnextSymbols(pnAnextPlusOne)     =  1;
pnAnextSymbols(pnAnextMinusOne)    = -1;
pnAnextSymbols(pnAnextMinusThree)  = -3;
pnAnextSymbols(pnAnextMinusFive)   = -5;
pnAnextSymbols(pnAnextMinusSeven)  = -7;
pnAnextSymbols(pnAnextMinusNine)   = -9;
pnAnextSymbols(pnAnextMinusEleven)= -11;

pamLevels                  = [-11,-9,-7,-5,-3,-1,1,3,5,7,9,11];

%%=============================================================================
%%=============================================================================

% UTP channel
% Given Channel response
%h = 1 + 1/2*(z^-1);
%h = 1 + 1/2*(z^-1) -1/4*z^-2
%
peUtpChannel               = [1  0.5];
% peUtpChannel              = [1  0.5  -0.25];
```

```
%=====================================================================
%            Our filter obtained from ANEXT measurement data
%============================== ANEXT Channel=========================
%This comes from the matlab program and ANEXT measurement file
%anext_notch('c:/anext_measurements/anext_setup1_cat5e.mat')
% Complete ANEXT channel
fid                          = fopen('anext_filter_file.dat','r');
peCompAnextChannel           = fread(fid,inf,'double');
fclose(fid);


%% ANEXT channel coefficients where power >99.9%
pePower                      = [];
nStepSize                    = 10;
nPowerLimit                  = 0.9999;

for nCrop = 0:nStepSize:length(peCompAnextChannel)/2
    pePower = [ pePower  sum(peCompAnextChannel(1+nCrop:end-nCrop).^2) ];
end

%% figure
%% plot(pePower);
%% plot(pePower./pePower(1));
%% grid;
%% title('Anext Coeff. Power');

peAnextChannelCoeff          = [];
peNormPower                  = pePower./pePower(1);
nCropThreshPreCor            = min(find(peNormPower <= nPowerLimit));
nCropThresh                  = nCropThreshPreCor*nStepSize;

peAnextChannel               = peCompAnextChannel...
(1+nCropThresh:end-nCropThresh);
peScaledAnextChannel         = max(peUtpChannel)...
    /max(peAnextChannel)*peAnextChannel;
peAnextChannel   = 0.03*peScaledAnextChannel;

% figure;
% hold on ; grid on ; zoom on
% plot(peCompAnextChannel,'+')
% plot([1+nCropThresh:length...
%(peCompAnextChannel)-nCropThresh],peAnextChannel,'ro')
% legend('Original Filter','New Filter');
% xlabel('Tap Id');
%
disp(['INFO: We removed ',num2str(2*nCropThresh),' of ',num2str(length...
   (peCompAnextChannel)),...
    ' taps (',num2str(100*2*nCropThresh/length(peCompAnextChannel)),'%)...
     which contained ',num2str(100*...
     (1-peNormPower(nCropThreshPreCor))),'% of the total energy.']);

% peAnextChannel               = peAnextChannel./max(peAnextChannel);
%
%  figure
% plot(peAnextChannel,'o-');
%
% figure
% plot(peScaledAnextChannel,'ko-');
%=====================================================================
% Tomlinson-Harashima Precoding according to the following expression
%           x(k) = pnSymbols(n) - conv(h(D),pnCodedSymbols(n-1))
% It assumes that the channel characteristics are known at the
% transmitter
%=====================================================================
%
```

```
% Stored precoded symbols (sent to the channel)
% Most recent (k-1) on the left side to the oldest (k-2) to the right side
peStoredCodedSymbols          = zeros(1,length(peUtpChannel));

%% Vector that contains all the transmitted symbols
peCodedSymbols                = zeros(1,nSimlen);

%% Initializatin of the algorithm (Amal Ekbal)
peStoredCodedSymbols(1)       = pnSymbols(1);
peCodedSymbols(1)             = pnSymbols(1);

for ii=2:nSimlen
    % original expression
    % temp = pnSymbols(ii) - (peUtpChannel * peStoredCodedSymbols.');
    % Stanford's Amal Ekbal

    % For a channel such as [1 0.5]
    temp = pnSymbols(ii) - peUtpChannel(2) * peStoredCodedSymbols(1);


    % Amal Ekbal modulo operator (seems not to work for temp = 12.5??)
    % peCodedSymbols(ii)          = temp - d*M*floor((temp+M*d/2)/(M*d));
    if ( temp > M )
        peCodedSymbols(ii)        = temp - 2*M* (floor((temp-M)/(2*M))+1);
    elseif (temp <= -M )
        peCodedSymbols(ii)        = temp + 2*M* (floor((abs(temp)-M)/(2*M))+1);
    else
        peCodedSymbols(ii)        = temp;
    end

    peStoredCodedSymbols(2:end) = peStoredCodedSymbols(1:end-1);
    peStoredCodedSymbols(1)       = peCodedSymbols(ii);
end

disp(['INFO: Power of TX signal is ',num2str(std(peCodedSymbols).^2),' ...
    (',num2str(10*log10(std(peCodedSymbols).^2)),') in dB.'])

[psdCodedSymbols,wp]              = PSD(peCodedSymbols,1024);
% plot(10*log10(abs(Pxx)))

% figure
% psdplot(psdCodedSymbols,wp,'','DB','Power Spectral Density of Coded symbols')

%%Upsampling the data symbols i.e. the coded symbols by 6 to make the
%%symbol rate and sampling rate same 825*6 = 4950MHz
peUpsampledCodedSymbols           = upsample(peCodedSymbols,12);

% peMeanPAMSignal = mean(peCodedSymbols);
% disp(['Mean of PAM signal is (',num2str(peMeanPAMSignal),')']);
%
% peRMSPAMSignal = mean(peCodedSymbols.^2);
% peRMSPAMSignal = sqrt(peRMSPAMSignal);
% disp(['RMS of PAM signal is (',num2str(peRMSPAMSignal),')']);
%==========================================================================
%==========================================================================
%Tomlinson-Harashima precoder for ANEXT symbols i.e. symbols from the
%disturber cable adjacent to the victim cable
%%
%% Stored precoded symbols (sent to the channel)
%% Most recent (k-1) on the left side to the oldest (k-2) to the right side
peAnextStoredCodedSymbols         = zeros(1,length(peUtpChannel));

%% Vector that contains all the transmitted symbols
peAnextCodedSymbols               = zeros(1,nSimlen);

%% Initializatin of the algorithm (Amal Ekbal)
```

```
peAnextStoredCodedSymbols(1)     = pnAnextSymbols(1);
peAnextCodedSymbols(1)           = pnAnextSymbols(1);

for ii=2:nSimlen
    % Stanford 's Amal Ekbal

    % For a channel such as [1 0.5]
    anexttemp = pnAnextSymbols(ii) - peUtpChannel(2) * ...
        peAnextStoredCodedSymbols(1);

    % peCodedSymbols(ii)          = temp - d*M*floor((temp+M*d/2)/(M*d));
    if ( anexttemp > M )
        peAnextCodedSymbols(ii)      = anexttemp - 2*M* ...
            (floor((anexttemp-M)/(2*M))+1);
    elseif (anexttemp <= -M )
        peAnextCodedSymbols(ii)      = anexttemp + 2*M* ...
            (floor((abs(anexttemp)-M)/(2*M))+1);
    else
        peAnextCodedSymbols(ii)      = anexttemp;
    end

    peAnextStoredCodedSymbols(2:end) = ...
        peAnextStoredCodedSymbols(1:end-1);
    peAnextStoredCodedSymbols(1)     = ...
        peAnextCodedSymbols(ii);
end

%disp(['INFO: Power of TX signal is ',...
%num2str(std(peCodedSymbols).^2),' ...
%(',num2str(10*log10(std(peCodedSymbols).^2)),') in dB.'])

[psdAnextCodedSymbols,wp]          = ...
    PSD(peAnextCodedSymbols,1024);
% plot(10*log10(abs(Pxx)))
% figure
% psdplot(psdCodedSymmbols,wp,'','DB',...
%'Power Spectral Density of Coded symbols')

%%Upsampling the data symbols i.e. the coded symbols by 6 to make the
%%symbol rate and sampling rate same 825*6 = 4950MHz
peAnextUpsampledCodedSymbols       = upsample(peAnextCodedSymbols,12);
% peAnextSignal                      = filter(peScaledAnextChannel,1,...
peAnextUpsampledCodedSymbols);

% peAnextChannel = *peAnextChannel;
peAnextSignal                      = filter(peAnextChannel,1,...
    peAnextUpsampledCodedSymbols);
%
% figure
% hold on ; grid on ; zoom on
% NumberofAnextSymbols          = length(peAnextSignal);
% NumberofAnextSymbols
% plot(peAnextSignal);
% [n,x]                      = hist(peAnextSignal,100);
% bar(x,n/nSimlen);
% title('ANEXT Signal','Fontsize',12);

% xlabel('Value','Fontsize',12);
% ylabel('Probability','Fontsize',12);

% figure(2)
% [n,x]                          = hist(peCodedSymbols,100);
% bar(x,n/nSimlen);
% title('Transmit Waveform','Fontsize',12);
% xlabel('Value','Fontsize',12);
% ylabel('Probability','Fontsize',12);
```

```
[Pxx,f]                          = PSD(peAnextSignal,1024,12*826e6);
%The psdplot plots the Power Density Spectrum
%of the ANEXT signal
%Dividing by sqrt(825MHz) so that the frequency
%and power spectrum in same scale

% figure
% psdplot(Pxx./sqrt(825e6),f,'','DB',...
%'Power Spectral Density of ANEXT signal') ·

psdplot(Pxx./sqrt(825e6),f,'','DB')

% %%=============================================================
% %%% Mean and RMS of the output ANEXT signal
% %%=============================================================
% % peMeanAnextSignal = mean(peAnextSignal);
% % disp(['Mean of ANEXT signal is (',num2str...
%(peMeanAnextSignal),')']);
% %
% % peRMSAnextSignal = mean(peAnextSignal.^2);
% % peRMSAnextSignal = sqrt(peRMSAnextSignal);
% % disp(['RMS of ANEXT signal is (',num2str...
%(peRMSAnextSignal),')']);


% %%=============================================================
% %%% After transmission through the channel
% %%=============================================================
% peReceivedSymbols                = filter(peUtpChannel,1,...
%peUpsampledCodedSymbols);
%
% %
% % peReceivedSymbols                = zeros(1,length...
%(peUpsampledCodedSymbols));
% %%% figure
% %%% stem(pnSymbols)
% %%% title('Ideal Symbols','Fontsize',12);
% %%% xlabel('Time','Fontsize',12);
% %%% ylabel('Level','Fontsize',12);
% %
%
% % figure
% % stem(peReceivedSymbols)
% % title('Channel Output Symbols (should look like ideal symbols)'...
%,'Fontsize',12);
% % xlabel('Time','Fontsize',12);
% % ylabel('Level','Fontsize',12);
% %
% %%% Generate Noise
% peNoise                          = peSigmaNoise*randn(1,length...
%(peUpsampledCodedSymbols));
%
% % Received Waveform in presence of normally distributed noise
% peReceivedSymbols                = peReceivedSymbols + peNoise;
%
% %Received waveforms in presence of ANEXT also contain ANEXT signal
% peActualReceivedSymbols          = peNoise +  + peReceivedSymbols...
%+ peAnextSignal;
%
% % figure
% % plot(peActualReceivedSymbols);
% %%% pamLevels                      = [-11,-9,-7,-5,-3,-1,1,3,5,7,9,11];
% %%% n                              = histc(peChannelFilterOutput,pamLevels);
%
% % [n,x]                          = hist(peReceivedSymbols,100);
```

```
% % stem(peChannelFilterOutput);
% % bar(x,n/nSimlen);
% % title('Received Symbols','Fontsize',12);
% % xlabel('Pam Levels','Fontsize',12);
% % ylabel('Probability','Fontsize',12);
%
% %%=========================================================================
% %%% Feedforward filter at the receiver
% %%=========================================================================
 for j = 1:nSimlen
%     % This does not do the modulo operation correctly
     peFFEReceivedSymbols(j) = round(peReceivedSymbols(j) - ...
    M*d*floor((peReceivedSymbols(j)+M*d/2)/(M*d)));
   peFFEReceivedSymbols(j) = peReceivedSymbols(j) - ...
       M*d*floor((peReceivedSymbols(j)+M*d/2)/(M*d));
     if ( peActualReceivedSymbols(j) > M )
         peFFEReceivedSymbols(j) = peActualReceivedSymbols(j) - ...
             2*M* (floor((peActualReceivedSymbols(j)-M)/(2*M))+1);
     elseif (peReceivedSymbols(j) <= -M )
         peFFEReceivedSymbols(j) = peActualReceivedSymbols(j) + ...
             2*M* (floor((abs(peActualReceivedSymbols(j))-M)/(2*M)) + 1);
     else
         peFFEReceivedSymbols(j) = peActualReceivedSymbols(j);
     end
 end
 % figure
 % stem(peFFEReceivedSymbols)
 % title('Channel Output Symbols (should look like ideal symbols)'...
 %,'Fontsize',12);
 % xlabel('Time','Fontsize',12);
 % ylabel('Level','Fontsize',12);
 %
 %
 % figure
 % pamLevels                          = [-11,-9,-7,-5,-3,-1,1,3,5,7,9,11];
 %%  n                                = histc(peChannelFilterOutput,pamLevels);
 % n                                   = histc(peFFEReceivedSymbols,pamLevels);
 % bar(pamLevels,n/nSimlen);
 % title('Received Symbols','Fontsize',12);
 % xlabel('Pam Levels','Fontsize',12);
 % ylabel('Probability','Fontsize',12);

 % error = 0;
 % for n=1:nSimlen
 %     if ( pnSymbols(n) - peFFEReceivedSymbols(n) > epsilon )
 %         error= error + 1;
 %     end
 % end

%==========================================================================
% Feedforward filter at the receiver for ANEXT
%==========================================================================
% for j = 1:nSimlen
%     % This does not do the modulo operation correctly
%     % peFFEReceivedSymbols(j) = round(peReceivedSymbols(j) - ...
                %M*d*floor((peReceivedSymbols(j)+M*d/2)/(M*d)));
%     % peFFEReceivedSymbols(j) = peReceivedSymbols(j) - ...
                %M*d*floor((peReceivedSymbols(j)+M*d/2)/(M*d));
%     if ( peAnextSignal(j) > M )
%         peANEXTFFEReceivedSymbols(j) = peAnextSignal(j) - ...
                %2*M* (floor((peAnextSignal(j)-M)/(2*M))+1);
%     elseif (peReceivedSymbols(j) <= -M )
%         peANEXTFFEReceivedSymbols(j) = peAnextSignal(j) + ...
                    %2*M* (floor((abs(peAnextSignal(j))-M)/(2*M)) + 1);
%     else
%         peANEXTFFEReceivedSymbols(j) = peAnextSignal(j);
```

```
%     end
% end
% figure
% stem(peFFEReceivedSymbols)
 %% title('Channel Output Symbols (should look like ideal symbols)'...
 %,'Fontsize',12);
% xlabel('Time','Fontsize',12);
% ylabel('Level','Fontsize',12);
%
%
% figure
% pamLevels                          = [-11,-9,-7,-5,-3,-1,1,3,5,7,9,11];
%%  n                                = histc(peChannelFilterOutput,pamLevels);
% n                                   = histc(peFFEReceivedSymbols,pamLevels);
% bar(pamLevels,n/nSimlen);
% title('Received Symbols','Fontsize',12);
% xlabel('Pam Levels','Fontsize',12);
% ylabel('Probability','Fontsize',12);

% error = 0;
% for n=1:nSimlen
%     if ( pnSymbols(n) - peFFEReceivedSymbols(n) > epsilon )
%         error= error + 1;
%     end
% end

%=========================================================================
% Sampling of received signals at the receiver at 825 + epsilon! MHz
% ADC
% Timing Error Detector Characteristics
%%=========================================================================

%eEpsilon                           = 1043.78/1e6*825e6;  % for PAM + ANEXT
% crossing at 0
% eEpsilon                          = 1067.7/1e6*825e6;
% AdcFreq                           = 2*(825e6 + eEpsilon);
% peTemp = [];
% peTempIdeal = [];
% figure
% plot(pnSymbols,'o')

% figure
% hold on; grid on
% for eThisPhase =[-1:0.1:1]
%
%     SignalTime                    = ([0:length(peTxSignal)-1]./825e6);
%     AnextSignalTime               = ([0:length(peFFEReceivedSymbols)-1]./825e6);
%     InputTime                     = [eThisPhase/AdcFreq:1/AdcFreq:...
% AnextSignalTime(end)];
%
%     % figure
%     % hold on ; grid on
%     % plot(SignalTime(1:6:end).*AdcFreq,'o')
%     % plot(InputTime.*AdcFreq,'r*')
%     % %[b,a]= butter(5,0.5);
%
%    Signal                        = upsample(peTxSignal,12);
%     ADCSamplesIdeal                 = spline(SignalTime,peTxSignal,InputTime);
%     ADCSamples                      = spline(AnextSignalTime,...
%peFFEReceivedSymbols,InputTime);
%
%     % figure
%     % plot(ADCSamples,'o-')
%
%      SqADCSamples                 = ADCSamples.^2;
%      ProductSequenceIdeal           = SqADCSamples.*(ADCSamplesIdeal(1:end-1))';
```

```
%      DiffADCSamplesIdeal       = diff(SqADCSamplesIdeal);
%      ProductSequenceIdeal      = DiffADCSamplesIdeal.*ADCSamplesIdeal(1:end-1);
%
%      DiffADCSamples            = diff(ADCSamples);
%      ProductSequence           = DiffADCSamples.*ADCSamples(1:end-1);
%
%      pSequence                 = zeros(size(DiffADCSamples));
%      pSequence(1:2:end)        = +1;
%      pSequence(2:2:end)        = -1;
%
%      FinalSequenceIdeal        = pSequence.*ProductSequenceIdeal;
%      peTempIdeal               = [peTempIdeal sum(FinalSequenceIdeal)];
%
%      FinalSequence             = pSequence.*ProductSequence;
%      peTemp                    = [peTemp sum(FinalSequence)];
% end
%
% % plot([-1:0.1:1],peTemp);
% % figure
% % hold on;zoom on;grid on;
% % plot([-1:0.1:1],peTemp);
% % % plot([-1:0.1:1],peTempIdeal);
% %
% % plot([-1:0.1:1],peTemp,[-1:0.1:1],peTempIdeal,'r-');
%
%
% % figure
% % hold on ; grid on;
% % plot(AnextTime,AnextSignal,'o-');
% % plot(InputTime,ADCSamples,'r*-');
% % hold off;

%%=====================================================================
% Error introduced by jitter 1ps to 10 ps
% jitter value from takatori_1_1104 jitter = 2 ps
%=====================================================================
% peTempJitter                      = [];
% AnextChannelTime                  = ([0:length(peAnextChannel)-1]./825e6);
% %
% % for eNoiseVariance = [0:.1:10]
%      eNoiseVariance = 10;
%
%      [M,N]           = size(AnextChannelTime);
%      ClockNoise      = randn(M,N)*1*(10^-12);
% %      ClockNoise      = 0;
% %    ClockNoise      = 2*10^-12;
%      randn('state',0)
%
%      ClockTime                 = AnextChannelTime + ...
%        eNoiseVariance*ClockNoise;
%      AnextClockSample          = spline(AnextChannelTime,...
%      peAnextChannel,ClockTime);
%      JitterError               = sqrt(mean(...
%      (AnextClockSample' - peAnextChannel).^2));
%      JitterError             = (AnextClockSample' - peAnextChannel).^2;
%      peTempJitter              = [peTempJitter JitterError];
%  end

% peTempJitter
% figure
% hold on;grid on;
% stem(peAnextChannel);
% stem(AnextClockSample,'r');
% figure
% plot([0:.1:10],peTempJitter,'-*');
%=====================================================================
```